MONOGRAFIAS
DE LA

ACADEMIA DE CIENCIAS

Exactas
Físicas
Químicas y
Naturales

DE
ZARAGOZA

Comunicaciones presentadas en el
INSTITUTO DE ESTUDIOS AVANZADOS DE LA OTAN
sobre "Computación de Curvas y Superficies".
Puerto de la Cruz (Tenerife, España), 1989.

N.º 2

1990

Depósito legal: Z. 1.667 - 1990

Impreso en:
Sdad. Coop. Art. Gráf. Ltda.
LIBRERIA GENERAL
Pedro Cerbuna, 23
50009-Zaragoza

Contributions to the Computation of Curves and Surfaces

edited by

Wolfgang Dahmen
Institut für Mathematik I
Freie Universität, Berlin, FRG

Mariano Gasca
Department of Applied Mathematics
University of Zaragoza, Spain

and

Charles A. Micchelli
IBM T.J. Watson Research Center
Yorktown Heights, N.Y., USA

A selection of the contributed papers to the NATO Advanced Study Institute on Computation of Curves and Surfaces, Puerto de la Cruz, Tenerife, Spain, July 10-21, 1989.

PROLOGO

Este número especial de la nueva colección de *Monografías de la Academia de Ciencias de Zaragoza* contiene una selección de las comunicaciones cortas presentadas en el Instituto de Estudios Avanzados de la OTAN sobre Computación de Curvas y Superficies, que tuvo lugar en Puerto de la Cruz, Tenerife, España, del 10 al 21 de julio de 1989.

La parte fundamental del Instituto consistió en las conferencias que con estilo tutorial impartieron dieciseis prominentes investigadores, representando a nueve países de la OTAN. Sus conferencias constituirán un voluminoso libro que con el título de *Computation of Curves and Surfaces* será publicado por Kluwer Academic Pub. en el presente año. Además de esto, otros participantes presentaron comunicaciones cuyo interés y novedad también las hacen merecedoras de ser publicadas. Esta fue la razón por la que se pensó en este número de *Monografías de la Academia de Ciencias de Zaragoza* para ellas.

Se presentan aquí varios artículos que cubren amplias zonas del diseño geométrico de curvas y superficies por ordenador. Es esta una nueva disciplina que se basa en varias ramas de las matemáticas, entre las que destacan la Teoría de Aproximación, el Análisis Numérico y las Geometrías Diferencial y Algebraica. Como nueva área de investigación, ofrece una amplia colección de cuestiones matemáticas abiertas, pero además posee un fuerte potencial de aplicaciones científicas y tecnológicas. Los artículos aquí contenidos representan los esfuerzos de una serie de investigadores al mejor conocimiento de esta área.

Nuestra mayor deuda de gratitud es con la División de Asuntos Científicos de la OTAN, sin cuya generosa ayuda económica, así como asistencia técnica en las tareas organizativas, hubiera sido imposible alcanzar las cotas de éxito logradas en el congreso. Deseamos agradecer también fervientemente la ayuda económica de la Armada de los EEUU de América, a través de la Oficina de Investigación Naval de Londres, y al Ministerio de Educación y Ciencia de España.

Las Universidades de La Laguna y Zaragoza, especialmente sus Departamentos de Análisis Matemático y Matemática Aplicada respectivamente, nos prestaron inapreciable ayuda en la resolución de problemas logísticos y organizativos, tanto personales como materiales. A este respecto queremos destacar muy vivamente nuestro agradecimiento a la importante labor realizada por el Dr. Nacere Hayek, Profesor Emérito de la Universidad de La Laguna. Indudablemente, todos los participantes estarán de acuerdo también en que la amistosa y generosa hospitalidad del Cabildo de Tenerife y del Ayuntamiento de Puerto de la Cruz, puestas de manifiesto especialmente en los actos sociales con que nos obsequiaron en los Lagos Martiánez, Parador Nacional del Teide y Casino del Puerto de la Cruz, aumentaron

muy significativamente el agradabilísimo ambiente del congreso.

También queremos mencionar aquí la ayuda indirecta que supuso para nosotros el hecho de que el Dr. C.A. Micchelli estuvo disfrutando de una estancia sabática en España subvencionada por la DGICYT del Ministerio de Educación y Ciencia, en los meses de mayo a octubre de 1989. Ello nos permitió una mejor coordinación y nos simplificó las labores organizativas, tanto del congreso como de las posteriores publicaciones, como la presente.

Finalmente, agradecemos a la Academia de Ciencias de Zaragoza su buena disposición para la publicación de esta Monografía y a la Universidad de Zaragoza su ayuda económica para ella.

Wolfgang Dahmen
Mariano Gasca *
Charles A. Micchelli

*Proyecto de Investigación CICYT PS87 0060.

PREFACE

This special issue of *Monografías de la Academia de Ciencias de Zaragoza* contains papers presented at the NATO Advanced Study Institute on *Computation of Curves and Surfaces* held in Puerto de la Cruz, Tenerife, Spain, during the period of July 10th to July 21st, 1989.

The conference was organized around sixteen prominent speakers representing nine NATO countries. Their lectures will be published elsewhere by Kluwer Academic Pub. in the book *Computation of Curves and Surfaces.* In addition to the main lectures we were fortunate to have numerous novel and interesting contributed talks also deserving of publication. For this reason the idea of a special issue of *Monografías de la Academia de Ciencias de Zaragoza* was conceived.

We have here several articles which address broad issues pertaining to the design of curves and surfaces. This is a new emerging discipline which draws upon a variety of mathematical subjects including Approximation Theory, Numerical Analysis and Differential and Algebraic Geometry. This area of investigation offers both a rich collection of mathematical questions as well as provides a strong potential for scientific and technological applications.

The articles contained here represent the efforts of researchers to further our understanding of this challenging and important new field of curve and surface design.

Obviously, we owe our major debt of gratitude to the NATO Scientific Affairs Division whose generous financial support, helpful organizational guidelines, assistance and encouragement made it possible for us to organize a successful meeting. We would also like to gratefully acknowledge additional financial support of the U.S. Navy, Office of Naval Research, London, and the Ministerio de Educación y Ciencia of Spain.

The Universities of La Laguna and Zaragoza, especially their respective departments, Analisis Matemático and Matemática Aplicada, provided us with valuable assistance in solving logistical and organizational problems, as well as making their facilities available to us. In this regard, we single out for special thanks Professor Nacere Hayek, emeritus professor of the University of La Laguna, for his efforts. No doubt, each participant would agree that the friendly and generous hospitality of Cabildo de Tenerife and Ayuntamiento de Puerto de la Cruz, as expressed by the social events they organized at Lagos Martianez, Parador Nacional del Teide and the Casino de Puerto de la Cruz, added significantly to the pleasant ambiance of the meeting.

We would like to mention the timely financial support of the Ministerio de Educación y Ciencia of Spain under the DGICYT program for a sabbatical visit of

Dr. C.A. Micchelli. This allowed us to coordinate and simplify many of the tasks we faced in organizing the meeting and preparing these conference proceedings.

Finally, special thanks are given to the Academy of Sciences of Zaragoza for the publication of this issue and to the University of Zaragoza for the financial support provided to it.

Wolfgang Dahmen
Mariano Gasca
Charles A. Micchelli

INDICE (CONTENTS)

LIST OF ATTENDANTS

S. ACAR; D.A.C.A.M., Cranfield Institute of Technology, Cranfield, Bedford MK 43 OAL, England.

J.L. BABEAU; Institut für Mathematik I, Freie Universität Berlin, Arnimallee 2-6, D-1000 Berlin, Federal Republic of Germany.

B. BARSKY; Computer Sciences Division , Electrical Engineering & Computer Sciences Department, University of California , Berkeley, CA 94720, U.S.A.

G. BASZENSKI; Ruhr Universität, Computer Center, P.O.Box 102148. D-4630 Bochum 1, Federal Republic of Germany.

V. BENÍTEZ; Departamento de Matemática Aplicada, Facultad de Ciencias del Mar, Universidad Politécnica de Las Palmas, Las Palmas de Gran Canaria, Spain.

L. BOS; Department of Mathematics, University of Calgary, Calgary, Alberta, T2N IN4, Canada.

W. BÖHM; Institut für Angewandte Geometrie, Technische Universität Braunschweig, Braunschweig D-3300, Federal Republic of Germany.

C. BREZINSKI; U.E.R d'I.E.E.A., M-3, Université des Sciences et Techniques de Lille 1, 59655 Villeneuve d'Ascq CEDEX, France.

M.D. BUHMAN; Department of Applied Mathematics, University of Cambridge, Silver St., Cambridge CB3 9EW, England.

A. BULUT; Dokuz Eylul Universitesi, Mühendislik Mimarlik Fakultesi, Makina Bolümü, Bornova, Izmir, Turkey.

M. CALVO; Departamento de Matemática Aplicada, Facultad Ciencias (Matemáticas), Universidad de Zaragoza, 50009 Zaragoza, Spain.

R. CARLSON: Lawrence Livermore National Laboratory, P.O.Box 808, L-61, Livermore, CA 94550, U.S.A.

J.M. CARNICER; Departamento de Matemática Aplicada, Facultad Ciencias (Matemáticas), Universidad de Zaragoza, 50009 Zaragoza, Spain.

A.S. CAVARETTA; Department of Mathematical Sciences, Kent State University, Kent, OH 44240, U.S.A.

C.K. CHUI; Center for Approximation Theory, Texas A & M University, College Station, TX 77843, U.S.A.

J.A. CORDÓN; Departamento de Análisis Matemático, Facultad de Ciencias, Av. Castros s/n., 39005 Santander. Spain.

W. DAHMEN; Institut für Mathematik I, Freie Universität Berlin, Arnimallee 2-6, D-1000 Berlin, Federal Republic of Germany.

C. DE BOOR; Center for Mathematical Research, 610 Walnut St., University of Wisconsin. Madison, WI 53705 U.S.A.

R. DEVORE; Department of Mathematics, University of South Carolina, Columbia, S.C.29208, U.S.A.

N. DYN; School of Mathematical Sciences, Tel-Aviv University, Ramat Aviv, Tel Aviv 69978, Israel.

F. FONTANELLA; Dipartimento di Energetica, Universita degli Studi de Firenze, Via S. Marta 3, I 50139 Firenze, Italia.

M. GASCA; Departamento de Matemática Aplicada, Facultad Ciencias (Matemáticas), Universidad de Zaragoza, 50009 Zaragoza, Spain.

R. GOLDMAN; Department of Computer Sciences, University of Waterloo, Waterloo, Ontario N2L 3G1, Canada.

J. GONG; Department of Mathematics, University of South Florida, Tampa, FL 33620, U.S.A.

P. GONZÁLEZ; Departamento de Análisis Matemático, Universidad de La Laguna, Tenerife, Canary Islands, Spain.

T.N.T. GOODMAN; Department of Mathematics & Computer Sciences, University of Dundee, Dundee DD1 4HN Scotland, Great Britain.

J. GREGORY; Mathematics & Statistics Deptartment, Brunel University, Uxbridge, Middlesex, UB8 3PH, Great Britain.

S. GÜNAY; Department of Statistics, Hacettepe University, Faculty of Sciences, 06532 Beytepe-Ankara, Turkey.

N. HAYEK; Departamento de Análisis Matemático, Universidad de La Laguna, Tenerife, Canary Islands, Spain.

C. HOFFMANN; Department of Computer Sciences, Purdue University, West Lafayette, IN 47907, U.S.A.

J. HOSCHECK; Fachbereich Mathematik, Technische Hochschule Darmstadt, D-6100 Darmstadt, Federal Republic of Germany.

A. LE MÉHAUTÉ; Université de Lille, Laboratoire d'Analyse Numérique et Optimization, 59655 Villeneuve d'Ascq Cédex, France.

L. LENARDUZZI; Istituto per le Applicazzioni della Matematica e dell'Informatica, C.N.R.,Via Ampere 56, Milano, Italy.

D. LEVIATAN; School of Mathematical Sciences, Tel-Aviv University, Ramat Aviv, Tel Aviv 69978, Israel.

D. LEVIN; School of Mathematical Sciences, Tel-Aviv University, Ramat Aviv, Tel Aviv 69978, Israel.

X. LIU; Department of Mathematics, University of South Florida, Tampa, FL 33620, U.S.A.

C. LOOP; Department of Computer Sciences, FR-35, University of Washington, Seattle WA 98195. U.S.A.

M.C. LÓPEZ DE SILANES; Departamento de Matemática Aplicada, E. T. S. I. I., María de Luna 3, 50015 Zaragoza, Spain.

T. LYCHE; Universitetet i Oslo, Institut for Informatikk, P.O.Box 1080, Blindern, 0316 Oslo 3, Norway.

J.I. MAEZTU; Departamento de Matemática Aplicada, Facultad Ciencias, Apartado 644, 48080 Bilbao, Spain.

C. MANNI; Istituto Matematico U. Dini, Viale Morgagni 67/A, 50134 Firenze, Italy.

J. MARTÍNEZ-AROZA; Departamento de Matemática Aplicada, Facultad Ciencias, Av. Fuentenueva s/n, Granada, Spain.

J.J. MARTÍNEZ; Departamento de Matemática Aplicada, Facultad Ciencias (Matemáticas), Universidad de Zaragoza, 50009 Zaragoza, Spain.

J. MEIER; Universität Oldenburg, Fachbereich Mathematik, PF 2503, D-2900, Federal Republic of Germany.

C.A. MICCHELLI; I.B.M. T.J.Watson Research Center, P.O.Box 218, Yorktown Heights, NY 10598 U.S.A.

M. MORANDI CECCHI; Dipartamento Matematica Pura ed Applicata, Universita di Padova, Via Belzoni 7, 35131 Padova, Italy.

G. MÜHLBACH; Institut fur Angewandte Mathematik, Universität Hannover, Welfengarten 1, D-3000 Hannover 1, Federal Republic of Germany.

J. MUÑOZ; Departamento de Matemática Aplicada, Facultad Ciencias, Av. Fuentenueva s/n, Granada, Spain.

E. NADLER; Department of Mathematics, Wayne State University, Detroit, MI 48202, U.S.A.

C. OLMSTED; Geophysical Institute, University of Alaska, Fairbanks, Alaska 99775-0800, U.S.A.

G. PALASSOPOULOS; Military Academy of Greece, 41 Blessa Street, Papagos, Athens 15669, Greece.

F. PÉREZ-ACOSTA; Departamento de Análisis Matemático, Universidad de La Laguna, Tenerife, Canary Islands, Spain.

M. PETERS; Tektronix Inc., P.O.Box 500, Mail Station 50-321, Beaverton, Oregon 97077. U.S.A.

B. PIPER; Department of Mathematical Sciences, Rensselaer Polytechnical Institute, Troy, NY 12180-3590, U.S.A.

E. QUAK; Fachbereich Mathematik, Universität Dortmund, Postfach 500 500,. D-4600 Dortmund 50, Federal Republic of Germany.

C. RABUT; Department of Mathematics, I.N.S.A., Toulouse Cedex, France.

V. RAMÍREZ; Departamento de Matemática Aplicada, Facultad Ciencias, Av. Fuentenueva s/n, Granada, Spain.

M. REDIVO-ZAGLIA; Dipartamento Matematica Pura ed Applicata, Universita di Padova, Via Belzoni 7, 35131 Padova, Italy.

J. RODRÍGUEZ; Departamento de Análisis Matemático, Universidad de La Laguna, Tenerife, Canary Islands, Spain.

N. ROTHMAN; Mathematics Department, I.U.-P.U., 1125 East 38th St., Indianapolis, IN 46205, U.S.A.

P. SABLONNIERE; L.A.N.S., I. N. S. A., 20 Av. Buttes de Coesmes, 35043 Rennes, France.

H. SADOK; U.E.R. d'I.E.E.A., M-3, Université des Sciences et Techniques de Lille 1, 59655 Villeneuve d'Ascq CEDEX, France.

E. SAINZ DE LA MAZA; Departamento de Matemática Aplicada, Facultad Ciencias, Aptdo. 644, 48080 Bilbao, Spain.

G. SCENNA; Dipartamento Matematica Pura ed Applicata, Universita di Padova, Via Belzoni 7, 35131 Padova, Italy.

K. SCHERER; Institut für Angewandte Mathematik, Universität Bonn, Wegelerstrasse 6, D-5300 Bonn, Federal Republic of Germany.

J. SCHICK; Institut für Systemdynamik, Facultät für Luft- und Raumfahrttechnik, Universität der Bundeswehr München, Werner-Heisenberg Weg 39, D-8014, Neubiberg, Federal Republic of Germany.

E. SCHMITT; Institut für Numerische und Angewandte Mathematik, Lotzestrasse 16-18, D-3400 Göttingen, Federal Republic of Germany.

L. L. SCHUMAKER; Department of Mathematics, Vanderbilt University, Nashville, TN 37235, U.S.A.

H.P. SEIDEL; Wilhelm-Schickard Institut für Informatik, Auf der Morgenstelle 10, C9, D-7400 Tübingen, Federal Republic of Germany.

J.J. SILVESTRE MADEIRA; Departamento Matematica, Universidade de Coimbra. Aptdo. 3008, 3000 Coimbra, Portugal.

J.J. TORRENS; Departamento de Matemática Aplicada, E.T.S.I.I., María de Luna 3, 50015 Zaragoza, Spain.

C. TRAAS; Department of Mathematics, University Twente, P.O.Box 217, 7500 AE Enschede, Holland.

L. TRAVERSONI; Departamento de Ingeniería de Procesos, Ingeniería Hidrológica, Aptdo. 55-534, Universidad Autónoma Metropolitana Iztapalapa, 09340 Mexico D.F., Mexico.

R. VAN DAMME; Department of Mathematics, University Twente, P.O.Box 217, 7500 AE Enschede, Holland.

G. VANECEK; Department of Computer Sciences, Purdue University, West Lafayette, IN 47907, U.S.A.

E. VAN VLECK; Department of Mathematics, Georgia School of Technology, Atlanta, Georgia, U.S.A.

J. WARREN; Department of Computer Sciences, Rice University, P.O.B. 1892, Houston, TX 77251, U.S.A.

O. WOHLRAB; S.F.B. 256, Institut für Angewandte Mathematik, Universität Bonn, Wegelerstrasse 6. D-5300 Bonn 1, Federal Republic of Germany.

FINITE ELEMENT INTERPOLATION WITH WEIGHTED SMOOTHING

L. BOS, J. E. GRABENSTETTER, K. SALKAUSKAS
DEPARTMENT OF MATHEMATICS AND STATISTICS
UNIVERSITY OF CALGARY
CALGARY, ALBERTA
CANADA T2N 1N4

Abstract. In this note we consider finite element type interpolants which minimize a semi–norm simlilar to the bending energy semi–norm of thin plate splines. We weight the semi–norm in a data dependent manner in order to control the curvature of the resulting interpolant.

1. Introduction

Suppose that we are given a set $X:=\{x_i\}_{i=1}^m \subset \mathbb{R}^2$ of non–collinear points and function values $\{z_i\}_{i=1}^m \subset \mathbb{R}$. We consider the problem of constructing a (simple) function $f:\mathbb{R}^2 \to \mathbb{R}$ which interpolates this data; i.e., $f(x_i)=z_i$, $1 \le i \le m$. One common solution to this problem is to interpolate by elements from some finite element space. Typically, one forms a triangulation, $\mathcal{T}$, of the convex hull of X, $\mathcal{H}(X)$, with vertex set exactly X. The Delauney triangulation is the usual choice. Generally speaking, the interpolant is a function of a fixed smoothness which, when restricted to $T \in \mathcal{T}$, is a polynomial of low degree. In this work we will consider two specific finite element spaces:

a) $S_3^1 := \{f \in C^1(\mathcal{H}(X)) : f|_T$ is a cubic polynomial, $\forall T \in \mathcal{T}\}$; i.e., C^1 piecewise cubics.

b) $CT := \{f \in C^1(\mathcal{H}(X)) :$ f is piecewise cubic on $\mathcal{T}_1\}$ where $\mathcal{T}_1$ is the subtriangulation which results when each $T \in \mathcal{T}$ is split into the three triangles formed by connecting the vertices to the centroid; i.e., the Clough–Tocher space.

An immediate difficulty with using these spaces for function interpolation is that the dimensions of these spaces are significantly larger than the number of interpolation conditions. In fact, if we let B denote the number of points in X on the boundary of $\mathcal{H}(X)$ and I the number in the interior, then from Alfeld[1]

$$\dim(S_3^1) \ge 3B + 2I + 1 > 2 \times \mathrm{card}(X).$$

Since the Clough–Tocher split is obtained by adding one vertex at the centroid of each triangle in $\mathcal{T}$,

$$\dim(CT) \ge 3B + 2(I+T) + 1$$

where T is the number of triangles in $\mathcal{T}$. But using Euler's formula, it is easy to see that $T=B+2I-2$, so that

$$\dim(CT) \ge 5B + 6I - 3 \ge 5 \times \mathrm{card}(X).$$

Often, additional gradient values are specified in order to obtain as many conditions as degrees of freedom. Indeed, this is the manner in which Clough–Tocher finite elements are usually applied. More recently, the success of thin plate splines has induced some authors (see e.g. [3] and [6]) to suggest that the extra degrees of freedom be eliminated by a smoothing procedure. More specifically, define the semi–inner product,

$$(f,g) := \int_\Omega \sum_{|\alpha|=2} D^\alpha f D^\alpha g \, ,$$

where we have used standard multinomial notation for partial derivatives. Here $\Omega := \mathcal{H}(X)$. To this semi–inner product is associated the semi–norm

$$|f|^2 := (f,f).$$

Then the $s \in S$ which interpolates the given data for which $|s|$ is a minimum is known as the smoothed interpolant. Here S denotes the appropriate finite element space.

As the spaces which we consider, S_3^1 and CT, are only spaces of $C^1(\Omega)$ functions and the inner product used involves second derivatives we pause to give an interpretation of the semi–inner product for C^1 piecewise cubics.

Theorem 1: If $s_1, s_2 \in S_3^1$ then the distributional derivatives $D^\alpha s_1, D^\alpha s_2 \in L_2(\Omega)$ for $|\alpha|=2$,

$$D^\alpha s_i = \sum_{T \in \mathcal{T}} D^\alpha [s_i|_T] \chi_T,$$

and consequently

$$(s_1,s_2) = \sum_{T \in \mathcal{T}} \int_T \sum_{|\alpha|=2} D^\alpha s_1 D^\alpha s_2.$$

Similarly, if $s_1, s_2 \in CT$ then the distributional derivatives $D^\alpha s_1, D^\alpha s_2 \in L_2(\Omega)$ for $|\alpha|=2$,

$$D^\alpha s_i = \sum_{T \in \mathcal{T}_1} D^\alpha [s_i|_T] \chi_T,$$

and consequently

$$(s_1,s_2) = \sum_{T \in \mathcal{T}_1} \int_T \sum_{|\alpha|=2} D^\alpha s_1 D^\alpha s_2.$$

Proof: This is essentially the content of Theorem 2.1.2 of Ciarlet[2].□

Unfortunately, this smoothing procedure does not yield interpolants which are as visually pleasing as might be hoped for. In Figures 3 and 4, below, we show the smoothed interpolants from S_3^1 and CT, respectively, to the data set of Figure 2. Compared with the thin plate spline shown in Figure 5, these interpolants are excessively oscillatory. Notice, however, that the Clough–Tocher interpolant is distinctly less oscillatory than the S_3^1 interpolant. Perhaps this is due to the fact that $\dim(CT) \approx 3 \times \dim(S_3^1)$. Other authors have also noticed the oscillatory nature of such smoothed interpolants. See for instance Quak and Schumaker[5] whose response to this problem is to replace the Delauney triangulation with an "optimal" data–dependent triangulation. In this work we consider the effect not of adjusting the triangulation but rather of using a (possibly) data–dependent semi–norm in the smoothing procedure. More specifically, define the weighted semi–inner product

$$(f,g)_w := \int_\Omega \{ \sum_{|\alpha|=2} D^\alpha f \, D^\alpha g \} \, w$$

where $w : \Omega \to \mathbb{R}^+$ is a suitable weight function. To this semi–inner product associate the semi–norm

$$|f|_w^2 := (f,f)_w.$$

Although more general weight functions may be used, in this work we will restrict ourselves to the case when w is piecewise constant on the triangulation $\mathcal{T}$; i.e., when there are real $w_T>0$, such that

$$w(x)|_T := w_T \ \forall T \in \mathcal{T}. \tag{1}$$

Because of the derivative formula given in Theorem 1, it is not hard to see that, for this choice of weight function,

$$(s_1,s_2)_w = \sum_{T\in\mathcal{T}} w_T \int_T \sum_{|\alpha|=2} D^\alpha s_1 D^\alpha s_2$$

for $s_1,s_2 \in S_3^1$, and

$$(s_1,s_2)_w = \sum_{T\in\mathcal{T}_1} w_T \int_T \sum_{|\alpha|=2} D^\alpha s_1 D^\alpha s_2$$

for $s_1,s_2 \in CT$.

2. Interpolation with Weighted Smoothing

Suppose that S is either S_3^1 or CT and assume that w is piecewise constant as in (1). We first show that weighted smoothed interpolants exist and are unique provided interpolation at the given data points by elements of S is possible. Let N=dim(S).

Lemma 2: Suppose that $\Phi = \{\varphi_j\}_{j=1}^N \subset S$ is a basis such that the first m functions of Φ are cardinal for function evaluation at x_i, i=1,···,m, so that $\varphi_j(x_i) = \delta_{ij}$, i,j=1,···,m. As we can subtract from each φ_j, j=m+1,···,N its interpolant at the x_i, $\sum_{k=1}^m \varphi_j(x_k)\varphi_k(x)$, without altering the linear independence of Φ, we may assume that, in addition, $\varphi_j(x_i)=0$, i=1,···,m and j=m+1,···,N. Let the N×N matrix V be defined by $v_{ij}:=(\varphi_i,\varphi_j)_w$ and be partitioned as

$$V = \left[\begin{array}{c|c} V_{11} & V_{12} \\ \hline V_{21} & V_{22} \end{array}\right] \begin{array}{l} m \\ N-m \end{array} \tag{2}$$

(m columns; N–m columns)

Then V_{22} is strictly positive definite.

Proof: As V_{22} is a matrix of semi–inner products, it is non–negative definite. We need only show that is is also non–singular. Hence suppose that there is a non–zero $d:=[d_{m+1},\cdots,d_N]^t \in \ker(V_{22})$. Then setting $s:=\sum_{i=m+1}^N d_i\varphi_i$ we have $(s,s)_w=0$ so that s is actually a (global) linear polynomial. But by the additional assumption on the basis Φ, $s(x_i)=0$, i=1,···,m contradicting the fact that X is not collinear.□

Theorem 3: Suppose that Φ is as in the hypothesis of Lemma 2, and that $z\in\mathbb{R}^m$. Then there exists a unique $c^t=[c_1^t|c_2^t]$, $c_1\in\mathbb{R}^m$, $c_2\in\mathbb{R}^{N-m}$, such that $s := c^t\varphi$

interpolates z and for which $|s|_w$ is a minimum. Here $\varphi:=[\varphi_1,\cdots,\varphi_N]^t$, $c_1 = [z_1,\cdots,z_m]^t$, and c_2 is the unique solution of

$$V_{22}c_2 = -V_{12}c_1. \tag{3}$$

Proof: By Lemma 1, V_{22} is strictly positive definite and in particular, non–singular. Hence there is a unique solution c_2 to (3). Let $0\neq\delta:=[0|\delta_2]\in\mathbb{R}^N$; then $|(c+\delta)^t\varphi|_w^2 = (c+\delta)^tV(c+\delta) = c^tVc + 2c^tV\delta + \delta_2^tV_{22}\delta_2$; but $c^tV\delta = c_1^tV_{12}\delta_2 + c_2^tV_{22}\delta_2 = 0$ from (3). Thus $|(c+\delta)^t\varphi|_w > |s|_w$ and so s is the unique minimizing interpolant in $sp(\Phi)$.□

For Clough–Tocher interpolants it is easy to construct such a cardinal basis. In fact Φ may be taken to consist of functions of local support. See Grabenstetter[4] for these details. Thus the computation of CT smoothed interpolants reduces to linear least squares with sparse matrix. Because the Gram matrix V_{22} is constructed from the inner products of locally supported functions (and is sparse), it might be expected that the conditioning of this least squares problem does not depend too strongly on the number of data points. Thus it may very well be possible to effectively compute smoothed CT interpolants of very large data sets. Although we have not yet experimented with such large systems and make no definite claim, we mention this possibility because, as is well known, thin–plate spline interpolants of more than several hundred points are numerically difficult to compute.

On the other hand, it does not seem to be known whether interpolants from S_3^1 always exist. We suspect that they do as we have not yet encountered any numerical,or other, difficulty in computing smoothed interpolants. Because of the lack of structure of S_3^1, we compute this smoothed interpolant in a rather straight–forward manner. We consider all functions piecewise cubic on $\mathcal{T}$, constrain the coefficients of the resulting collection of cubics so that the global function is C^1, and then minimize. This results in a linear least squares problem with linear constraints. Again we refer the reader to Grabenstetter[4] for the details of this computation. A similar computation is done in Quak and Schumaker[5].

3. Computational Examples

Only one class of weight functions is examined in this work, namely those that are piecewise constant over the triangles T of $\mathcal{T}$. For CT interpolants we will again not be as general as possible and consider only weight functions which are piecewise constant on the macro–triangles. Our choice of weights is analogous to the piecewise constant weight functions used to determine weighted univariate C^1 cubic splines of [7,8]. Specifically, we consider weight functions, w, given by

$$w(x,y)|_T := (1+\|\nabla g_T\|^2)^{-p}, \tag{4}$$

where $z=g_T(x,y)$ is the plane passing through the interpolated surface at the vertices of T. Explicitly, if the vertices of T are (x_1,y_1), (x_2,y_2), and (x_3,y_3), with $f(x_1,y_1)=z_1$, etc., then

$$\nabla g_T(x,y) = -\frac{1}{\gamma}(\alpha,\beta),$$

where

$$\left.\begin{aligned}\alpha&=(y_2-y_1)(z_3-z_1)-(z_2-z_1)(y_3-y_1)\\ \beta&=(z_2-z_1)(x_3-x_1)-(x_2-x_1)(z_3-z_1)\\ \gamma&=(x_2-x_1)(y_3-y_1)-(y_2-y_1)(x_3-x_1)\end{aligned}\right\}. \tag{5}$$

As γ is just twice the (signed) area of T, w is well defined for non–degenerate triangulations.

The rationale for this form of weight function is that

$$\int_\Omega \frac{(\frac{\partial^2 f}{\partial x^2})^2+(\frac{\partial^2 f}{\partial y^2})^2+2(\frac{\partial^2 f}{\partial x\partial y})^2}{(1+(\frac{\partial f}{\partial x})^2+(\frac{\partial f}{\partial y})^2)^{5/2}}\,dxdy$$

is roughly the potential energy of bending of a thin elastic plate (with appropriately chosen modulus of elasticity and Poisson's ratio) constrained to have displacement f(x,y) for all $(x,y)\in\Omega$. However, we have found that an exponent p=1.25 in (4) has the visually most pleasing effect. In one variable it is known precisely how the weights control the curvature of the resulting spline, (see [7] or [8]) but we know of no satisfactory analogue of this in several variables. However, as is seen in the examples below, this choice of weighting does seem to have an effect similar to the one variable effect. It should also be remarked that the weights may also be regarded as a collection of "shape" parameters. Generally speaking, a region with relatively large weights will be forced to have "low" curvature and conversely, a region with relatively small weights is allowed to have "large" curvature. Thus the weights may be adjusted to affect the surface in a desired manner. However, we consider the main purpose of weighted splines to be the interpolation of rapidly changing data and leave other applications to the interested reader.

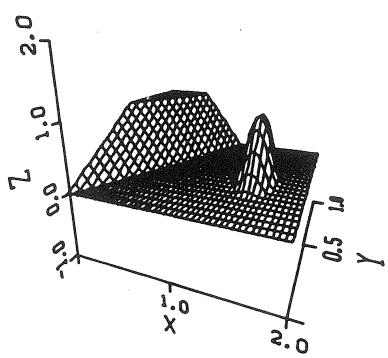

Figure 1
Ramp and Mountain Function

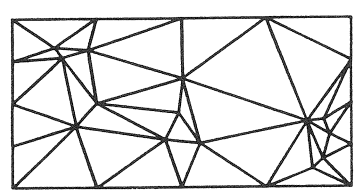

Figure 2
A set of 30 data points and its triangulation

Our data is taken from the function shown in Figure 1. Clearly any C^1 interpolant will have difficulty coping with the steep "ramp" and the non–smooth junction with the "mountain". The actual set of 30 data points used is displayed pictorially in Figure 2.

We first show the non–weighted smoothed interpolants to this data.

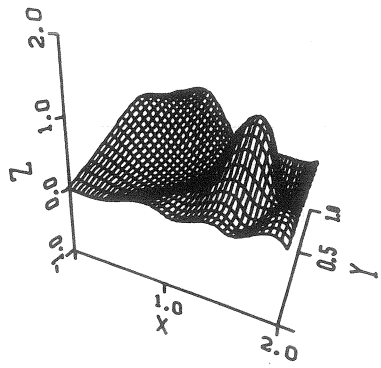

Figure 3
Smoothed S_3^1 interpolant

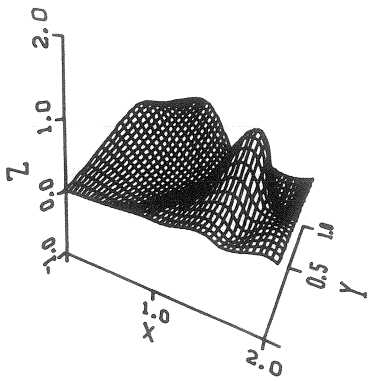

Figure 4
Smoothed Clough–Tocher interpolant

Notice that the Clough–Tocher interpolant is somewhat less oscillatory than the S_3^1 interpolant. Perhaps this is to be expected as S_3^1 is a reasonably small subspace of CT. These smoothed interpolants should be compared with the thin–plate spline, shown in Figure 5. As remarked in the introduction, this latter interpolant is much less oscillatory.

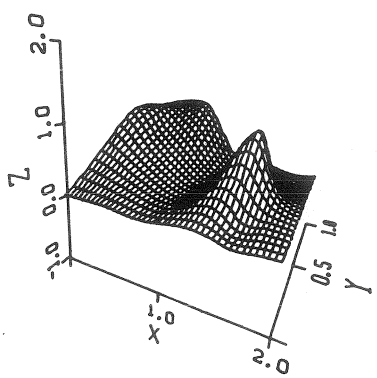

Figure 5
Thin–plate spline interpolant

We now give the weighted smoothed interpolants with piecewise weight function as in (4).

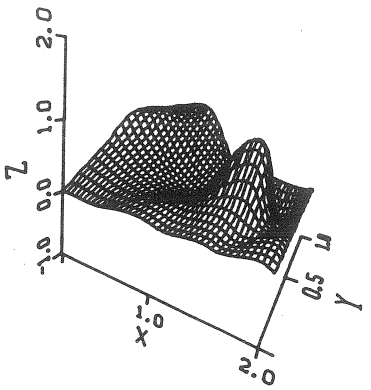

Figure 6
Weighted smoothed S_3^1 interpolant

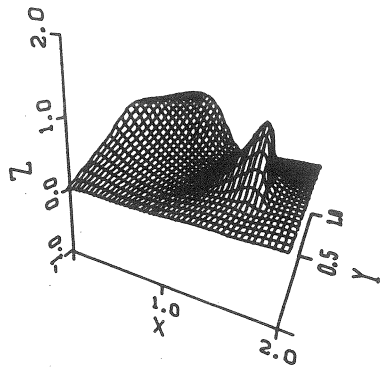

Figure 7
Weighted smoothed CT interpolant

Notice that a significant portion of the over– and undershoot has been eliminated.

References

1. Alfeld, P. (1986) 'On the dimension of multivariate piecewise polynomials', in D.F. Griffiths and G.A. Watson, (eds.), Numerical Analysis, Longman Scientific and Technical, Essex U.K., 1986, pp. 1–23.
2. Ciarlet, P.G. (1978) The Finite Element Method for Elliptic Problems, North Holland, Amsterdam.
3. Gmelig Meyling, R.H.J. (1987) 'Approximation by cubic C^1 splines on arbitrary triangulations', Numer. Math. 51, 65–85.
4. Grabenstetter, J.E. (1988) Aspects of Finite Element Interpolation with Smoothing, M.Sc. Thesis, University of Calgary.
5. Quak, E. and Schumaker, L. (1989) 'Algorithms for smoothest spline interpolation'.
6. Renka, R.J. (1981) Triangulation and bivariate interpolation for irregularly distributed data points, Ph.D. Thesis, Univ. Texas at Austin.
7. Salkauskas, K. (1984) 'C^1 splines for interpolation of rapidly varying data', Rocky Mtn. J. Math 14, 239–250.
8. Salkauskas, K. and Bos, L. 'Weighted splines as optimal interpolants', to appear in Rocky Mtn. J. Math.

SHAPE PRESERVING BICUBIC INTERPOLATION: A PROGRESS REPORT

R. E. Carlson
Lawrence Livermore National Laboratory
P. O. Box 808; L-61
Livermore, CA 94550
USA

ABSTRACT Cubic and bicubic Hermite interpolation methods have been used quite effectively to solve univariate and bivariate shape preserving interpolation problems. Methods are currently being devised to solve two new shape preserving problems. The first problem involves data which are monotone in only one variable, and monotonicity in this variable must be preserved in the interpolant. The second problem involves data which is piecewise monotonic in both variables. For this problem a nontrivial question is determining regions where monotonicity should be preserved. This paper discusses general bicubic Hermite interpolation methods, the inequalities that must be satisfied by the Hermite coordinates to solve these problems, and recent progress towards achieving practical solutions.

1. Introduction

Cubic and bicubic Hermite functions have proven to be extremely useful in solving shape preserving interpolation problems. In 1980 Fritsch and Carlson [7] established a set of necessary and sufficient conditions for a cubic polynomial to be monotone over a closed interval. These conditions led to the development of a monotone cubic Hermite interpolation algorithm. In 1984 Fritsch and Butland [6] simplified and significantly improved the original algorithm for computing the Hermite derivatives. In 1985 Carlson and Fritsch [2] derived a set of necessary and sufficient conditions for a bicubic polynomial to be monotone over a rectangle. These conditions led to the development of a monotone bicubic Hermite interpolation

algorithm. The original algorithm was quite complicated, and in 1989 it was improved and simplified [3].

Two problems have recently been encountered in which bicubic Hermite interpolation methods appear to offer excellent possibilities for solution. The first problem involves bivariate data which is monotone in only one variable, and the intended application requires the interpolant to preserve the monotonicity present in the underlying data. Attempts to use the monotone bivariate algorithm described in [3] (enforcing the monotonicity constraints in only one variable) have failed in that an interpolant can be produced that is nonmonotonic in both variables. Therefore, to solve this problem, a new algorithm is needed.

The second problem involves piecewise monotonic data. Currently, problems of this type are frequently solved using bicubic spline interpolation. Unfortunately, bicubic splines do not work well with data sets that have ridges and very steep slopes adjacent to regions in which the data are comparatively flat. Bicubic splines tend to produce significant "overshoots" and undesirable oscillations which are not present in the data.

The purpose of this paper is to describe bicubic Hermite interpolation techniques, to show the inequalities which must be satisfied to preserve monotonicity, and to describe recent progress in solving both of the problems described above.

2. Preliminary Results

The basic concepts for monotonicity preserving bicubic interpolation methods depend heavily on the univariate results described below.

Let $p(x)$ be a cubic polynomial defined on the closed interval $[a,b]$. Then $p(x)$ is uniquely determined by $\{p(a), p(b), p'(a), p'(b)\}$. Assuming $p(a)$ and $p(b)$ are given, then the monotonicity (or lack thereof) for $p(x)$ depends only on the values for $p'(a)$ and $p'(b)$. Setting both of these derivatives to zero guarantees monotonicity, but the resulting function is neither interesting nor useful for most applications. The parameter $\Delta = [p(b) - p(a)]/(b - a)$, which is the slope of the line segment joining $(a,p(a))$ and $(b,p(b))$, is crucial in determining acceptable values for $p'(a)$ and $p'(b)$ such that $p(x)$ is monotone. Note that if $\Delta = 0$, $p(x)$ is monotone if and only if $p'(a) = p'(b) = 0$, in which case $p(x)$ is constant. For $\Delta \neq 0$, if $\text{sign}(p'(a)) = \text{sign}(p'(b)) = \text{sign}(\Delta)$, $p(x)$ is nonmonotonic if and only if one or both of the ratios $\alpha = p'(a)/\Delta$ and $\beta = p'(b)/\Delta$ is too large. In 1980 Fritsch and Carlson [7] proved the following:

Theorem 1: The cubic polynomial p(x) is monotone on [a,b] if and only if

$$p'(a) = p'(b) = 0 \text{ whenever } \Delta = 0, \text{ or}$$
$$(\alpha,\beta) \in \mathfrak{R} \text{ whenever } \Delta \neq 0$$

where $\mathfrak{R}$ is shown in Figure 1.

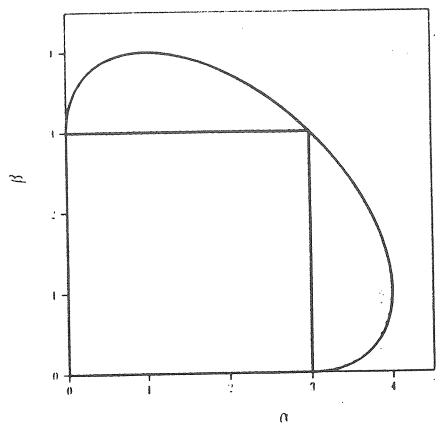

Figure 1: Monotonicity region $\mathfrak{R}$ for univariate cubic interpolation.

Remark: Note the square subregion $0 \leq \alpha, \beta \leq [0,3]$ of $\mathfrak{R}$ highlighted in Figure 1. This subregion plays an important role in extending univariate monotonicity results to bivariate functions. Also, in solving univariate problems, it is important for the interpolant to be "visually pleasing". Usually, the most visually pleasing curves occur when (α,β) is near the circle of radius 3 centered at the origin.

A typical univariate interpolation problem involves a mesh $x_1 < x_2 < \ldots < x_n$ together with values $f_i = f(x_i)$ of a function f which is to be approximated by the interpolant. A cubic Hermite interpolant to f is a function $p(x) \in C^1[x_1,x_n]$ which is cubic in each subinterval $[x_1,x_{i+1}]$ and which satisfies

$$p_i = p(x_i) = f_i , \quad i = 1,2, \ldots, n.$$

The function p(x) is uniquely determined by its Hermite coordinates $\{p(x_i), p'(x_i): i = 1,2, \ldots, n\}$. Because $\{p(x_i)\}$ are determined by the interpolation conditions, a cubic Hermite interpolation algorithm is simply a procedure for computing the set of Hermite derivatives $\{p'(x_i)\}$. Because the first derivatives match up at the polynomial break points, $p(x) \in C^1[x_1,x_n]$.

To preserve monotonicity the set $\{p'(x_i)\}$ must be chosen such that $p'(x_i) = 0$ when Δ_i or $\Delta_{i-1} = 0$, or $(\alpha_i,\beta_i) \in \mathcal{R}$ otherwise. What makes this problem interesting is the interaction of the Hermite derivatives in adjacent intervals. As noted above, a useful algorithm not only produces Hermite derivatives which satisfy the monotonicity requirements, but one in which the interpolant is visusally pleasing as well.

For bivariate functions the basic domain element is a rectangle. A bicubic polynomial defined on a rectangle $[a,b]x[c,d]$ is uniquely determined by sixteen Hermite coordinates, p, p_x, p_y, and p_{xy} at each corner. The following result, proven in [2], is the bivariate analog to Theorem 1.

Theorem 2: Let $p(x,y)$ be a bicubic polynomial defined on the rectangle $R = [a,b]x[c,d]$ where

(1) $\text{sign}\{p(b,c) - p(a,c)\} = \text{sign}\{p(b,d) - p(a,d)\}$

and

(2) $\text{sign}\{p(a,d) - p(a,c)\} = \text{sign}\{p(b,d) - p(b,c)\}$. Then

$p(x,y)$ is monotone in y if and only if

(a) $\Delta_1(x)$ does not change sign for $x \in [a,b]$;
(b) $p_y(x,c) = p_y(x,d) = 0$ whenever $\Delta_1(x) = 0$;
(c) $(\alpha_1(x),\beta_1(x)) \in \mathcal{R}$ whenever $\Delta_1(x) \neq 0$.

$p(x,y)$ is monotone in x if and only if

(d) $\Delta_2(y)$ does not change sign for $y \in [c,d]$;
(e) $p_x(a,y) = p_x(b,y) = 0$ whenever $\Delta_2(y) = 0$;
(f) $(\alpha_2(y),\beta_2(y)) \in \mathcal{R}$ whenever $\Delta_2(y) \neq 0$

where $\Delta_1(x) = [p(x,d) - p(x,c)]/(d - c)$, $\alpha_1(x) = p_y(x,c)/\Delta_1(x)$, and $\beta_1(x) = p_y(x,d)/\Delta_1(x)$ whenever $\Delta_1(x) \neq 0$. (Similarly for $\Delta_2(y)$, $\alpha_2(y)$, and $\beta_2(y)$.)

A typical bivariate interpolation problem involves a rectangular grid $x_1 < x_2 < \ldots < x_{nx}$; $y_1 < y_2 < \ldots < y_{ny}$ together with given values $f_{i,j} = f(x_i,y_j)$ of an unknown function f which is to be approximated. A bicubic Hermite interpolant to f is a function $p(x,y) \in C^{1,1}[R]$ where $R = [x_1,x_{nx}]x[y_1,y_{ny}]$ such that $p(x,y)$ is a bicubic polynomial in each rectangular element $[x_i,x_{i+1}]x[y_j,y_{j+1}]$ and

$$p_{i,j} = f_{i,j}, \text{ all } i,j.$$

The function p(x,y) is uniquely determined by its Hermite coordinates {$p_{i,j}$, $px_{i,j}$, $py_{i,j}$, and $pxy_{i,j}$}. Because the function values $p_{i,j}$ are specified by the interpolation conditions, a bicubic Hermite interpolation algorithm is a procedure for computing the Hermite derivatives at each grid point. The interpolant is monotone in R if the conditions of Theorem 2 are satisfied in each rectangular element. Preserving monotonicity in the bivariate case is significantly more complicated than in the univariate case because interactions occur in both coordinate directions. Monotonicity along grid lines does not guarantee monotonicity on the interior of an element.

In 1985 Carlson and Fritsch [2] developed a monotone bicubic Hermite interpolation algorithm. The key to this algorithm was replacing the necessary and sufficient conditions in Theorem 2 by a set of sufficient conditions which allowed some decoupling of the Hermite coordinates between adjacent grid points. The first sufficient condition is given below.

Theorem 3: Let p(a) and p(b) be of the same sign. Then the cubic polynomial p(x) does not change sign on [a,b] if

(3) $-3*\text{sign}(p(a))/(b-a) \le \text{sign}(p(a))*p'(a)$

and

(4) $\text{sign}(p(b))*p'(b) \le 3*\text{sign}(p(b))*p(b)/(b - a)$.

The second set of sufficient conditions involves shrinking the monotonicity region for α and β from all of $\mathcal{R}$ to the subregion [0,3]x[0,3] shown in Figure 1. This shrinkage makes very little difference in the ability to select reasonable values for the first partial derivatives, but it further decouples bounds on the Hermite coordinates from those at neighboring points.

Applying the sufficient conditions to the Hermite coordinates at each grid point leads to the following system of linear inequalities. If (5)-(8) are satisfied, then the resulting interpolant is monotone on R (provided the underlying data are montone).

(5y) $0 \le s_y*py_{i,k} \le s_y*3*\Delta_{1,j}(x_i)$ $\quad k = j,j+1,\ i = 1,2,\ ...,\ nx$

(5x) $0 \le s_x*px_{k,j} \le s_y*3*\Delta_{1,j}(x_i)$ $\quad k = i,i+1,\ j = 1,2,\ ...,\ ny$

(6y) $[-a_{i,j}/h_i] \le s_y*[px_{i,j+1} - px_{i,j}] \le [a_{i,j}/h_{i-1}]$

(6x) $[-b_{i,j}/k_j] \le s_x*[py_{i+1,j} - py_{i,j}] \le [b_{i,j}/k_{j-1}]$

$$
\begin{array}{lccc}
(7y) & -3p_{yi,j}^{+} & & 3p_{yi,j}^{-} \\
& 3[A_{i,j} + p_{yi,j}^{-}] & \le s_y * p_{xyi,j} \le & 3[B_{i,j} - p_{yi,j}^{+}] \\
& 3[A_{i,j-1} + p_{yi,j}^{-}] & & 3[B_{i,j-1} - p_{yi,j}^{+}]
\end{array}
$$

$$
\begin{array}{lccc}
(7x) & -3p_{xi,j}^{+} & & 3p_{xi,j}^{-} \\
& 3[C_{i,j} + p_{xi,j}^{-}] & \le s_x * p_{xyi,j} \le & 3[D_{i,j} - p_{xi,j}^{+}] \\
& 3[C_{i-1,j} + p_{xi,j}^{-}] & & 3[D_{i,j} - p_{xi,j}^{+}]
\end{array}
$$

where s_x and s_y denote the monotonicity in x and y respectively (i,e, $+1 \Rightarrow$ monotone increasing, $-1 \Rightarrow$ monotone decreasing),

$h_i = x_{i+1} - x_i$, $k_j = y_{j+1} - y_j$,

$p_{xi,j}^{+} = s_x * p_{xi,j}/k_j$, $p_{xi,j}^{-} = s_x * p_{xi,j}/k_{j-1}$,

$a_{i,j} = 3s_y*(p_{i,j+1} - p_{i,j}) \ge 0$, $b_{i,j} = 3s_x*(p_{i+1,j} - p_{i,j}) \ge 0$,

$A_{i,j} = s_y*\{[p_{xi,j+1} - p_{xi,j}]/k_j - [3/h_{i-1}]*[p_{i,j+1} - p_{i,j}]/k_j\}$,

$B_{i,j} = s_y*\{[p_{xi,j+1} - p_{xi,j}]/k_j - [3/h_i]*[p_{i,j+1} + p_{i,j}]/k_j\}$,

$C_{i,j} = s_x*\{[p_{yi+1,j} - p_{yi,j}]/h_i - [3/k_{j-1}]*[p_{i+1,j} - p_{i,j}]/h_i\}$, and

$D_{i,j} = s_x*\{[p_{yi+1,j} - p_{yi,j}]/h_i + [3/k_j]*[p_{i+1,j} - p_{i,j}]/h_i\}$.

As shown above the inequalities in (7) may not be solvable because (7y) and (7x) may have an empty intersection. The algorithm described in [2] checked this possibility and modified other Hermite coordinates if necessary. However, compatibility between (7y) and (7x) is guaranteed if 0 is forced to be an acceptable value of $p_{xy_{i,j}}$. This condition produces the following additional restrictions on $(p_{xi,j+1} - p_{xi,j})$ and $(p_{yi+1,j} - p_{yi,j})$:

$$
\begin{array}{ll}
(8y) & [-3s_x*(p_{i,j+1} - p_{i,j}) - k_j \max\{s_y*p_{yi,j+1}, s_y*p_{yi,j}\}]/h_i \\
& \le s_y*[p_{xi,j+1} - p_{xi,j}] \le \\
& [3s_x*(p_{i,j+1} - p_{i,j}) + k_j \max\{s_y*p_{yi,j+1}, s_y*p_{yi,j}\}]/h_{i-1}
\end{array}
$$

$$
\begin{array}{ll}
(8x) & [-3s_y*(p_{i+1,j} - p_{i,j}) - h_i \max\{s_x*p_{xi+1,j}, s_x*p_{xi,j}\}]/k_j \\
& \le s_x*[p_{yi+1,j} - p_{yi,j}] \le \\
& [3s_y*(p_{i+1,j} - p_{i,j}) + h_i \max\{s_x*p_{xi+1,j}, s_x*p_{xi,j}\}]/k_{j-1}.
\end{array}
$$

Note that if (8) is satisfied, so is (6).

Algorithms for computing the Hermite derivatives satisfying (5)-(8) consist of the basic steps shown below.

Step 1. Determine the monotonicity of the data.

Step 2. Compute initial values for $px_{i,j}$ and $py_{i,j}$.

Step 3. Check inequalities (8x) and (8y), changing Hermite coordinates as needed to correct violations.

Step 4. Construct an interval of acceptable values (containing 0) for $pxy_{i,j}$, changing partial derivative values as necessary to satisfy (7).

Step 5. Compute values for $pxy_{i,j}$.

Step 2 is accomplished using the univariate cubic Hermite interpolation algorithms contained in the software package PCHIP [5]. The key to implementing Steps 3 and 4 is the algorithm for modifying the Hermite coordinates computed in Step 3. These changes must be such that once an inequality is satisfied in Step 3, subsequent changes to the Hermite derivatives will not violate the Step 3 inequalities which have already been satisfied. Care must abe taken because of the interaction of the Hermite derivatives at neighboring grid points In all cases, changes made in the Hermite derivatives involve reductions in magnitude but not changes in sign.

For the special case in which the data are monotone in x but not monotone in y, it would seem reasonable to enforce only (8x) and ignore (8y). Unfortunately, the solution is not that simple. If the data are monotone in both x and y, but the monotonicity constraints are not enforced in the y direction, this approach works. However, if the data are **not** monotone in y, an interpolant can be produced which is not monotone in x in the interior of one or more elements. This predicament arises because the sign of $py_{i,j}$ may vary from point to point.

To avoid this complication we observe that inequalities (6x) and (8x) are of the form

(9) $-\text{lhs} \le (d_2 - d_1) \le \text{rhs}$

where lhs and rhs ≥ 0.

The dimension of bivariate spline spaces over special partitions.

Carla Manni
Istituto Matematico Ulisse Dini
Universita' di Firenze
Viale Morgagni 67/A
50134 Firenze, Italy

Abstract. The dimension of the space of piecewise polynomials of smoothness k and degree $n \geq 3k$, defined over a rectilinear partition which is a generalization of quasi cross-cut partition is determined. As an important application we obtain the dimension of cubic C^1 splines over these partitions.

1. Introduction.

We are interested in the space of bivariate splines of degree n and smoothness k, $n > k \geq 0$. associated with a given partition Δ of a simply connected domain $\Omega \subset \mathbb{R}^2$:

$$S_n^k(\Omega,\Delta) = \{ s : s \in C^k(\Omega),\ s_{|\Omega_i} \in \mathbb{P}_n,\ \forall\ \Omega_i \in \Delta \}\ ,$$

where $\mathbb{P}_n$ is the $(n+1)(n+2)/2$ dimensional linear space of polynomials of total degree n.

Here and throughout, we shall assume Ω is polygonal domain and $\Delta = \{\Omega_i, i=1,..,\omega\}$ a rectilinear partition of Ω, i.e. for each i, Ω_i is a polygon.
In recent years there has been considerable work on identifying the dimension of the spline spaces $S_n^k(\Omega,\Delta)$ (Schumaker (1984a), Dahmen and Micchelli (1983), Alfeld and Schumaker (1989) and references therein).

For general values of n and k and for arbitrary partitions both lower and upper bounds on the dimension are known (Schumaker (1984a)). If Δ is a triangulation, dimension formulae have been established in the cases $n \geq 3k+2$ (Dong (1988), Ibrahim and Schumaker (1988)), and, for non-degenerate triangulations, $n=3k+1$ (Alfeld and Schumaker (1989)).

Concerning partitions which are not necessarly triangulations the dimension of the space presents a more subtle geometric dependence even if n is arbitrary large w.r.t. k (Diener 1988a)). Then in order to find the value of the dimension it is necessary to require that Δ satisfies some additional properties. Formulae for the dimensions have been given for quasi-cross-cut partitions (Chui and Wang (1983b)) and for general rectilinear partitions if $n \leq k+(k+1)/D$, where $D+1$ is the maximum number of edges with different slopes emanating from an interior vertex Δ (Manni (1988)).

In this paper we investigate the dimension problem for the spline space defined over a partition wich is a generalization of a quasi-cross-cut partition (Chui and Wang (1983b)). In particular we prove that the dimension agrees with the lower bound given in Schumaker (1984a) if $n \geq 3k$, therefore we include the important case of cubic C^1 splines.

To establish these results we shall consider the usual cartesian coordinates, indeed the barycentric coordinates which are a basic tool for studing multivariate piecewise polynomials over triangulations are of no use if Δ is a general rectilinear partitions.

Due to page limitation, proofs of the results and some generalizations will be published elsewhere.

2. Notations and Background.

Let us introduce some notations. Let $P_i=(x_i,y_i)$, $i=1,...,V$ be the vertices of Δ and $P_i=(x_i,y_i)$, $i=1,...,v < V$, the interior vertices. Two vertices, P_i and P_j, are called adjacent if there is an edge of Δ joining P_i to P_j. For $i = 1,..., v$, let us put :

I_i = $\{j : P_j$ is adjacent to P_i , $1 \leq j \leq V\}$,

l_{is} = edge joining P_i to P_s,

ϵ_i = number of edges of Δ emanating from P_i,

e_i = number of edges of Δ emanating from P_i with different slopes,

E = number of edges of Δ not belonging to $\partial\Omega$,

E_d = number of edges of Δ joining two interior vertices,

β = $(n\text{-}k)(n\text{-}k+1)\frac{1}{2}$,

α = $(n+1)(n+2)\frac{1}{2}$.

It is well known (Chui and Wang (1983a)) that an element of $S_n^k(\Omega,\Delta)$ is determined by one polynomial of total degree n and by $2E$ polynomials, $q_{ij} \in \mathbb{P}_{n-k-1}$, which must satisfy the following conformality conditions (Chui and Wang (1983a)):

$$\sum_{j \in I_i} [l_{ij}(x,y)]^{k+1} q_{ij}(x,y) \equiv 0 \quad , \quad i=1,\ldots\ldots,v, \tag{2.1}$$

$$q_{ij} \equiv -q_{ji} \quad , \tag{2.2}$$

where :

$$l_{ij}(x,y)=l_{ji}(x,y)=a_{ij}x+b_{ij}y-(a_{ij}x_i+b_{ij}y_i)=0 \quad , \quad (a_{ij})^2+(b_{ij})^2 > 0,$$

is the equation of the line containing the edge l_{ij} .

In order to determine the dimension of $S_n^k(\Omega,\Delta)$ we have to compute the rank of the matrix of the linear system (2.1)-(2.2). Then it is convenient to rewrite it in a different form. Let us consider the translation :

$$\begin{cases} \xi = x - x_i \ , \\ \sigma = y - y_i \ . \end{cases} \tag{2.3}$$

From the Taylor expansion it immediately follows that if $q(x,y) \in \mathbb{P}_d$, and $p(\xi,\sigma) = q(x(\xi),y(\sigma))$, then

$$p(\xi,\sigma) = \sum_{j=0}^{d} \frac{1}{j!} D_{j,i}\, q(\xi,\sigma), \tag{2.4}$$

where

$$D_{0,i} = I, \quad D_{1,i} = x_i \frac{\partial}{\partial \xi} + y_i \frac{\partial}{\partial \sigma},$$

$$D_{j,i} = D_{1,i} D_{j-1,\,i}, \quad j=2,\,3,\ldots\ldots \ , \tag{2.5}$$

and I denotes the identity operator.

Let us consider the isomorphism $L_i : \mathbb{P}_{n-k-1} \rightarrow \mathbb{P}_{n-k-1}$, given by

$$L_i = I + D_{1,i} + \frac{1}{2!} D_{2,i} + \ldots + \frac{1}{(n-k-1)!} D_{n-k-1,i} \ .$$

Considering at each interior vertex of Δ a translation as (2.3) and observing that $L_i\, L_j = L_j\, L_i$ (indeed the derivatives commute in $\mathbb{P}_{n-k-1}$) conditions (2.1), (2.2) become respectively

$$\sum_{j\in I_i}[a_{ij}x+b_{ij}y]^{k+1}p_{ij}(x,y)\equiv 0 \quad , \quad i=1,\ldots\ldots,v. \tag{2.6}$$

$$L_j\ p_{ij}(x,y) + L_i\ p_{ji}(x,y) \equiv 0, \tag{2.7}$$

where

$$p_{ij}(x,y)= L_i\ q_{ij}(x,y).$$

System (2.6) -(2.7) involves $2E\beta$ unknowns, but $\beta(E\text{-}E_d)$ of them, associated with the edges emanating from boundary vertices, appear in (2.7) only, so they are determined by the others explicitly.

Hence

$$\dim S_n^k(\Omega,\Delta) = \alpha+\beta(E+E_d) - \text{rank } \mathcal{M}_b, \tag{2.8}$$

where, putting

$$p_{ij}(x,y) = \sum_{r=0}^{n-k-1} p_{ij}^{(r)}(x,y) = \sum_{r=0}^{n-k-1}\ \sum_{t=0}^{r} \alpha_{rt}\ x^t y^{r-t},$$

$$\mathcal{M}_b = \begin{bmatrix} M^1 & 0 & \ldots & 0 \\ \vdots & M^2 & & \vdots \\ 0 & & \ldots & M^v \\ & & L & \end{bmatrix}.$$

Each M^i, $i = 1,\ldots, v$, is the diagonal block matrix of the equations (2.6) related to the vertex P_i and it captures the influence of the edges emanating from this vertex. More precisely

$$M^i = \begin{bmatrix} M^i_{n-k} & & & \ldots & 0 \\ & M^i_{n-k-1} & & & \\ \vdots & & & & \\ 0 & & \ldots & & M^i_1 \end{bmatrix}.$$

where M^i_r is the $(r+k+1)$ by $r\epsilon_i$ matrix containing the equations (2.6) involving $p_{ij}^{(r-1)}(x,y)$, for all $j \in I_i$. In particular, $M^i_r=[M^i_{r,1}|\ldots|\ M^i_{r,\epsilon_i}]$ where $M^i_{r,j}=(h_{ut})$ is a $(r+k+1)$ by r matrix, and, denoting by i_j the j-th element of I_i, one has

$$h_{ut} = \begin{cases} 0, & \text{if } t>u,\ u>t+k+1, \\ \binom{k+1}{u-t} a_{ii_j}^{u-t}\, b_{ii_j}^{k+1-u+t}, & \text{otherwise.} \end{cases} \qquad 1\le u\le k+1+r,\ 1\le t\le r.$$

Then to each couple of collinear edges crossing P_i corresponds a couple of equal submatrices $M^i_{r,j}$, $M^i_{r,t}$ in M^i_r. In addition (Schumaker 1984b):

$$\text{rank } M^i_r = min\,(k+1+r,\ re_i)\ .$$

The matrix L contains the equations (2.7), so it controls the interaction of interior vertices. In order to investigate its structure we recall that the set

$$\{ y^{n-k-1}, y^{n-k-2}x, \ldots, x^{n-k-1}, \ldots, y, x, 1\},$$

forms a basis of $\mathbb{P}_{n-k-1}$.

If L_i denotes the matrix of L_i with respect to this basis, then L_i is a lower triangular block matrix :

$$L_i = \begin{bmatrix} I & & & \\ B_i^{1,n-k-1} & I & & \\ \vdots & & \ddots & \\ B_i^{n-k-1,n-k-1} & \cdots & B_i^{1,1} & I \end{bmatrix},$$

where $B_i^{r,s}$ is the $(s+1-r)$ by $(s+1)$ matrix representing the operator

$$\frac{1}{r!} D_{r,i} : \langle y^s, \ldots, x^s \rangle \to \langle y^{s-r}, \ldots, x^{s-r} \rangle\ .$$

Then

$$L = \begin{bmatrix} \Lambda_1 \\ \vdots \\ \Lambda_{E_d} \end{bmatrix},$$

where each Λ_s is a matrix with β rows and it contains the equations (2.7) for two polynomials p_{ir}, p_{ri} associated with an edge joining two interior vertices. More precisely, the only non zero columns in Λ_s are those corresponding to the columns of M^i (M^r) related to p_{ir} (p_{ri}): the first $(n\text{-}k)$ columns of L_r are aligned with the $(n\text{-}k)$ columns of M^i_{n-k} associated to $p^{(n-k-1)}_{ir}(x,y)$ and so on.

The following lemma holds (Manni 1989):

LEMMA 2.1 *Let* t_i, $t_r \in \mathbb{N}$ *be such that* $t_i + t_r = n\text{-}k$ *and* $B_{ir}=(B_i|B_r)$ *the submatrix of* $(L_i \mid L_r)$, *where* :

$$B_i = \begin{bmatrix} I & \dots & 0 \\ B_i^{1,d} & & \vdots \\ \vdots & \ddots & 0 \\ B_i^{t_i-1,d} & \dots & I \\ \vdots & & \vdots \\ B_i^{t_i+t_r-1,d} & \dots & B_i^{t_r,d+1-t_i} \end{bmatrix},$$

and B_r *is defined analogously by interchanging* i *with* r. *Then, if* $(x_i,y_i)\neq(x_r,y_r)$ *rank* $B_{ir}=\beta$.

3. The Dimension.

Recalling that a cross-cut is a line joining two boundary vertices of Δ, a ray is a line connecting a interior vertex of Δ to a boundary vertex and that Δ is quasi-cross-cut partition if it involves only cross-cuts and rays (Chui and Wang (1983b)), we consider the following

DEFINITION 3.1: Δ *is called generalized quasi-cross-cut partition provided that each interior vertex is crossed at least by two cross-cuts or rays.*

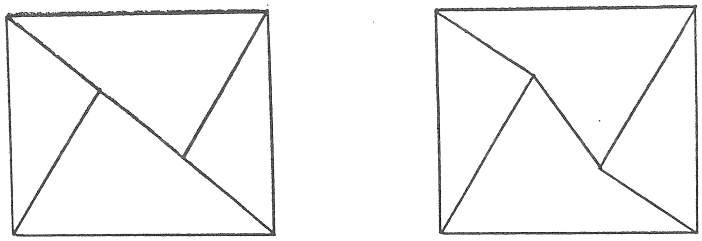

Fig. 1 A quasi-cross-cut partition and a generalized quasi-cross-cut partion.

It is well known (Schumaker (1984a)), that a lower bound for the dimension of $S_n^k(\Omega,\Delta)$ is

$$dim\ S_n^k(\Omega,\Delta) \geq \alpha + \beta E - \gamma\ , \qquad (3.1)$$

where

$$\gamma = \sum_{j=1}^{n-k} \sum_{i=1}^{v} min(k+1+j, je_i)\ .$$

In order to prove that (3.1) holds with the equality sign from (2.8) we have to establish that, for generalized quasi-cross-cut partitions, and for $n \geq 3k$:

$$\text{rank}\ \mathcal{M}_b \geq \beta E_d + \gamma\ .$$

At this point some remarks are in order.

REMARK (3.1)

Because Δ is a generalized quasi-cross-cut partition each interior vertex, P_i, is crossed at least by two cross-cuts or rays. Then we can construct a submatrix of maximum rank of M_r^i, $r \geq k+1$, considering only those submatrices $M_{r,j}^i$ which correspond to the edges lying on cross-cuts or rays.

REMARK (3.2)

If one edge of Δ, l_{is}, lies on a cross-cut or a ray it has a collinear edge in P_i and/or in P_s. On the other hand if l_{is} does not lie on a cross-cut or a ray it is possible that there are no edges collinear with it neither in P_i nor in P_s. But, in view of the previous remark, for each pair of edges, l_{is} and l_{si}, not lying on cross-cuts or rays we have a number $T = 2\sum_{j=k+1}^{n-k} j$ of columns which are not necessary to construct submatrices of maximum rank either in M_r^i, or in M_r^s, $r=k+1,\ldots,n-k$. In addition, if $n \geq 3k$, $T \geq \beta$.

The structure of $\mathcal{M}$, the previous remarks and the lemma (2.1) are the main tools to prove the following result:

THEOREM 3.1 *Let Δ be a generalized quasi-cross-cut partition of a simply connected domain $\Omega \subset \mathbb{R}^2$, then*

$$dim\ S_n^k(\Omega,\Delta) = \alpha + \beta E - \gamma\ ,\ \forall\ \ n \geq 3k\ .$$

We refer to (Manni 1989) for the complete details of the proof.

4. Final Remarks and Examples.

We end with some remarks and examples.

REMARK (4.1)

The boundary of Ω has no effect in determining the dimension of $S_n^k(\Omega,\Delta)$. That is theorem (3.1) applies to any simply connected domain Ω with a rectilinear partition.

REMARK (4.2)

Definition (3.1) gives in some sense the weaker useful generalization of the concept of quasi-cross-cut partition. Actually if we consider partitions such that each interior vertex is crossed at least by one cross-cut or one ray we do not have any chance to prove a result similar to theorem (3.1). Indeed the partition Δ_4 in Fig. 2 has the previous property but $dim\ S_n^k(\Omega,\Delta_4) > \alpha + \beta E - \gamma$, for all $n \geq 4k+1$ (Diener 1988a).

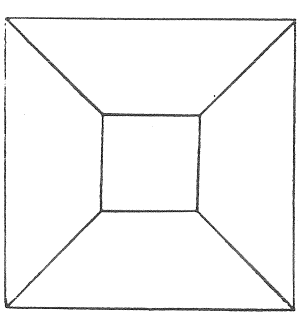

Fig. 2. The partition Δ_4

REMARK (4.3)

The lower bound for the degree obtained in theorem (3.1) is sharp if we do not require any additional property on Δ. Indeed we can consider the famous Morgan Scott example. From theorem (3.1) $dim\ S_n^k(\Omega,\Delta) = \alpha + \beta E - \gamma$, for all $n \geq 3k$ while $dim\ S_{2k}^k(\Omega,\Delta) > \alpha + \beta E - \gamma$, (Diener 1989b).

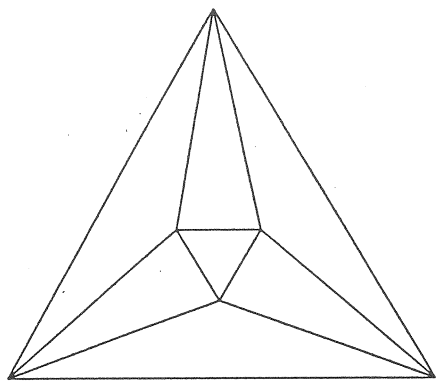

Fig. 3 The Morgan Scott example.

EXAMPLE (4.1) (Gmelig and Pfluger (1988))

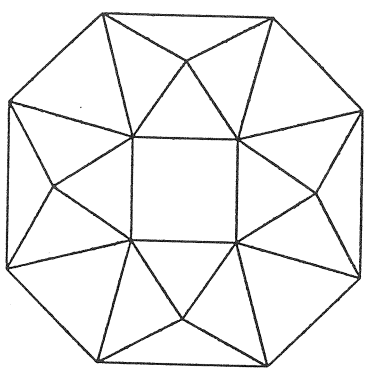

Fig. 4 v=8, E=28, $dim\ S_n^k(\Omega,\Delta) = \alpha + \beta E - \gamma \quad \forall\ n \geq 3k$.

P. ALFELD AND L.L. SCHUMAKER (1989), *On the dimension of bivariate spline spaces of smoothness r and degree* $d = 3\ r + 1$, Preprint.

C.K. CHUI AND R.H. WANG (1983), *On smooth multivariate spline functions*, Math. Comp., 41, pp. 131-142.

C.K. CHUI AND R.H. WANG (1983), *Multivariate spline spaces*, J. Math. Anal. Appl., 34, pp. 197-221.

W. DAHMEN AND C.A. MICCHELLI (1983), *Recent progress on multivariate splines*, in: Approximation Theory IV, C.K. Chui, et al. eds., New York, Academic Press, pp. 27-121.

D. DIENER (1988), *Geomerty dependence of the dimension of space of piecewise polynomials on rectilinear partitions*, submitted for pubblication.

D. DIENER (1988), *Instability in the dimension of spaces of bivariate piecewise polynomials of degree* $2r$ *and smoothness order* r, submitted for pubblication.

H. DONG (1988), *Space of multivariate spline functions over triangulations*, Master Thesis, Zheziang Univ.

R.H.J. GMELIG AND P.R. PFLUGER (1988), *On the dimension of the space of quadratic* C^1*-splines in two variables*, Approx. Theory & its Appl., 4, pp. 37-54.

A. KH. IBRAHIM AND L.L. SCHUMAKER (1988), *Superspline spaces of smoothness r and degree* $d \geq 3r+2$, Constructive Approximation, to appear.

C. MANNI (1988), *On the dimension of bivariate spline spaces over rectilinear partitions*, submitted for pubblication.

C. MANNI (1989), *On the dimension of bivariate spline spaces over generalized quasi-cross-cut partitions*, submitted for pubblication.

L.L. SCHUMAKER (1984), *Bounds on the dimension of space of multivariate piecewise polynomials*, Rocky Mountain J. Math., 14, pp. 251-264.

L.L. SCHUMAKER (1984), *On spaces of piecewise polynomials in two variables*, in: Splines and Approximation Theory (Singh et al. eds) Dordrecht, Reidel, pp. 151-197.

UN MÉTODO DE TRIANGULACIÓN DE FIGURAS PLANAS NO CONVEXAS

J. MARTINEZ-AROZA
V. RAMIREZ-GONZALEZ
Departamento de Matemática Aplicada
Facultad de Ciencias - Universidad de Granada
18071 GRANADA (ESPAÑA)

RESUMEN. Los problemas de triangulación de figuras aparecen con frecuencia en diversas áreas de actividad. En este trabajo se presenta y describe un algoritmo sencillo de triangulación de figuras planas no necesariamente convexas, con las ventajas de no ser destructivo, y de requerir un tiempo óptimo. Para figuras convexas la triangulación obtenida es una triangulación de Delaunay, y para figuras no convexas es cuasi-Delaunay.

1. Introducción

1.1. DEFINICION

Sea $\mathcal{A}$ un conjunto de n puntos del plano P_i $(i=1,2,\ldots,n)$, de los que m de ellos, dados en un cierto orden, son considerados como *puntos frontera*, es decir, la poligonal cuyos vértices son $P_1,P_2,\ldots,P_m$ (por este mismo orden, u otro cíclicamente equivalente) es una curva cerrada y simple $\mathcal{C}$, recorrida en sentido antihorario (el sentido creciente de los ángulos), y todos los demás puntos $P_{m+1},P_{m+2},\ldots,P_n$ son estrictamente interiores a dicha curva. Por 'curva simple' queremos decir que $\mathcal{C}$ no se corta ni se toca a sí misma, o sea, no forma lazos. Una *Triangulación* de $\mathcal{A}$ es una partición del área $\mathcal{S}$ encerrada por $\mathcal{C}$, constituída exclusivamente por triángulos T_j $(j=1,2,\ldots,t)$ que tengan por vértices los puntos de $\mathcal{A}$, de modo que todo punto de $\mathcal{A}$ es vértice de al menos un triángulo de la partición, y además se cumpla:

$$\text{i) } \mathcal{S} = \bigcup_{j=1}^{t} T_j \; ; \qquad \text{ii) } T_j \cap T_k = \begin{cases} \emptyset \\ \text{Un vértice común} \\ \text{Un lado común} \end{cases}$$

1.2. CONSIDERACIONES PREVIAS

La existencia de una triangulación para una figura convexa queda elegantemente demostrada usando el *diagrama de Voronoi*, cuyo dual es la *triangulación de Delaunay* [2]. Para figuras no convexas puede servir el argumento constructivo que muestra el propio algoritmo objeto de este trabajo.

Es evidente que un problema de triangulación no admite solución única, puesto que una figura tan simple como un cuadrilátero convexo cualquiera admite exactamente dos triangulaciones diferentes. Pero lo que sí es un invariante, que sólo depende de la figura, es el número total de triángulos que componen cualquier triangulación de aquella. Dicho número t sólo depende del número de puntos frontera y del de puntos interiores de la figura, y no de la forma que ésta tenga.

Proposición: *En una figura con* n *puntos en total, de los que* m *de ellos constituyen la frontera, el número de triángulos* t *de cualquier triangulación posible es constante e igual a* $2\cdot(n-1)-m+1$.

Demostración: Reconstruyamos la triangulación partiendo de un triángulo cualquiera, y añadiendo un nuevo triángulo cada vez, adyacente a los anteriores. Si el nuevo triángulo sólo tiene un lado común con los anteriores, entonces aumentan n y m a la vez. Si tiene dos lados comunes, se mantiene n y disminuye m. En todo caso, el número 2n-m aumenta en una unidad. Como para n=m=3 tenemos t=1, esto nos lleva a la expresión $t = 2\cdot(n-1)-m+1$. ■

En teoría de algoritmos se demuestra que existe un algoritmo para obtener la triangulación de Delaunay en un tiempo del orden de $n\cdot\log(n)$. La demostración más usual se basa en que el problema de triangulación es transformable en un problema de *sorting* u ordenación, y el tiempo de transformación es lineal, o al menos no sobrepasa el orden citado. Como el tiempo óptimo de un algoritmo de ordenación es del orden de $n\cdot\log(n)$, la transformación no aumenta la complejidad. Se han desarrollado algoritmos que requieren tiempo óptimo [1],[2],[3],[4], pero todos ellos exigen la convexidad de la figura como hipótesis básica. Nuestro algoritmo posee en su primera forma una complejidad del orden de n^2, es muy sencillo de poner a punto y su ejecución es sumamente rápida, sin necesitar tiempo de preproceso alguno ni memoria adicional importante, y conservando el conjunto inicial de datos. Posteriormente veremos algunas formas de disminuir este tiempo efectuando un preproceso de los datos y utilizando alguna memoria de trabajo, que puede ser útil en grandes nubes de puntos. Empleando técnicas de numeración rápidas, como son los árboles de inserción, se consigue que la complejidad de la forma mejorada de nuestro algoritmo sea óptima, esto es, del orden de $n\cdot\log(n)$.

Una ventaja adicional está en que, salvo esporádicos saltos producidos por el paso 5 del algoritmo, la sucesión de triángulos generada es conexa, es decir, cada triángulo es adyacente al anterior y al siguiente construidos. En ciertas aplicaciones esto es muy útil. Piénsese, por ejemplo, en trabajos de topografía donde los operarios deban recorrer el terreno una vez triangulado. O, simplemente, en que una triangulación debe ser trazada por un plotter, y si cada triángulo está cerca del siguiente, la máquina reducirá considerablemente el tiempo de trazado.

2. El Algoritmo Básico

2.1. FORMULACION INICIAL

La idea primaria de nuestro algoritmo consiste en ir construyendo triángulos con al menos un lado en la frontera de la figura. Cuando se construye un triángulo tal, se rehace la frontera de forma que éste quede fuera de ella, con lo que se logra una reducción de la figura (que no necesariamente una reducción de la frontera). El algoritmo parte del conocimiento de los puntos frontera en orden antihorario de recorrido, y de los puntos interiores en cualquier orden. Es así:

ALGORITMO DE REDUCCION EN FRONTERA:

1: Elegir un segmento de la frontera.
2: Sean J y K los extremos del segmento considerado.
3: Encontrar el punto R más cercano por la izquierda del segmento, según el sentido antihorario de recorrido de la curva.
4: Si R no está en la frontera, ir al paso 6.
5: Si R no es consecutivo con J y K, ir al paso 1 (para evitar la desconexión en dos regiones). En caso contrario, ir al paso 7.
6: Si algún segmento RJ, RK corta a la frontera, ir al paso 9.
7: Construir un nuevo triángulo con vértices R, J y K.
8: Reordenar la frontera.
9: Si quedan más de dos puntos en la frontera, ir al paso 1.
10: Fin del algoritmo.

Hay una serie de cuestiones relativas a este algoritmo que pueden ser resueltas de diversas maneras, con resultados ciertamente diferentes. En primer lugar hay que dotar de significado riguroso al calificativo 'más cercano' del paso 3. Este problema es tratado en la sección 2.2. Otros problemas relacionados con la rapidez de ejecución del algoritmo son tratados en las secciones 2.3 Y 2.4. Posteriormente se presenta y describe una técnica matricial que permite rebajar el tiempo al óptimo (sección 3).

2.2. DISTANCIA DE UN PUNTO A UN SEGMENTO

Esta cuestión no es trivial. En principio parece que podría servir la distancia euclídea de un punto a un segmento, es decir, la menor distancia entre el punto dado y cualquiera de los del segmento. Más sencilla de calcular sería la distancia al punto medio del segmento, pero tal medida no sirve para el algoritmo, puesto que en el interior de un triángulo RJK podría haber puntos más alejados del segmento JK que el propio R.

Con la distancia euclídea este problema no existe. Buscando otras alternativas, casi inmediatamente podemos pensar en la suma de distancias euclídeas entre el punto R y cada uno de los extremos del segmento, que llamaremos *distancia suma*. No sirven tampoco ni la distancia mínima (menor de las distancias a los extremos), ni la distancia máxima (mayor de las distancias a los extremos), porque ambas adolecen del mismo inconveniente que la distancia al punto medio.

Con objeto de buscar una distancia que evite en la medida de lo posible la aparición de triángulos 'forzados' (demasiado obtusángulos), se puede sugerir la longitud del arco de circunferencia que va desde J a K pasando por R. Así, puntos situados en posición muy oblícua respecto al segmento definirán arcos muy amplios, con una gran longitud. A efectos de buscar el punto que la minimiza, esta medida es equivalente a la altura del arco sobre el segmento JK, y también al coseno del ángulo JRK, dado que todos los ángulos inscritos en una circunferencia sobre la misma cuerda son iguales. McLain [4] utiliza esta misma distancia (medida por él como la distancia con signo desde el segmento JK al centro del círculo JKR). Es, además, inversamente equivalente al propio ángulo JRK. Para su computación, la medida adecuada es

$$\cos^{[2]}\alpha = \frac{(\overline{RJ}\cdot\overline{RK})^{[2]}}{\overline{RJ}^2\cdot\overline{RK}^2}$$

Donde $x^{[2]}$ es la función x^2 con signo, esto es, $x^{[2]} = x\cdot|x|$. Pero como $\overline{JK}^2 = \overline{RK}^2+\overline{RK}^2-2\cdot\overline{RJ}\cdot\overline{RK} \Rightarrow 2\cdot\overline{RJ}\cdot\overline{RK} = \overline{RK}^2+\overline{RK}^2-\overline{JK}^2$, entonces tendremos

$$4 \cdot \cos^{[2]}\alpha = \frac{(\overline{RJ}^2 + \overline{RK}^2 - \overline{JK}^2)^{[2]}}{\overline{RJ}^2 \cdot \overline{RK}^2}$$

Esta parece ser la forma más eficiente de calcular la distancia. El intervalo de variación es [-4,4], lo cual aporta algunas ventajas adicionales, y para su computación se necesitan 8 sumas, 8 multiplicaciones y 1 división para cada punto R, más 3 sumas y 2 multiplicaciones previas, dependientes sólo del segmento JK. Si R no está en el lado correcto del segmento, el cálculo se reduce a 2 multiplicaciones.

Tales hechos nos permiten equiparar en sencillez de cálculo a esta distancia (en adelante, *distancia angular*) con las anteriores, y las triangulaciones obtenidas con ella suelen tener mejor aspecto que con otras. Mas aún, es la mejor posible, según se desprende del siguiente resultado:

Proposición: *La triangulación obtenida por el algoritmo de reducción en frontera usando la distancia angular sobre una figura convexa es una triangulación de Delaunay.*

Demostración: Basta probar que dados dos triángulos adyacentes cualesquiera de la triangulación producida formando un cuadrilátero convexo, y trazado el círculo que circunscribe a uno de ellos, el restante vértice no puede estar en su interior. La validez de esta demostración está refrendada por el análisis de Lawson [3] sobre el *criterio del círculo* (véase la figura 1).

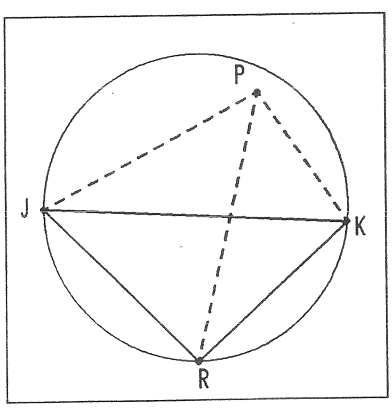

FIGURA 1: El Criterio del Círculo

Sea JKR el triángulo al cual se le circunscribe un círculo, y sea P el cuarto vértice, que delimita el segundo triángulo con el segmento JK. Supongamos que P está en el interior del círculo JKR. No sabemos en qué orden se construyó el fragmento de triangulación que nos ocupa, pero podemos analizar cualquiera de los cuatro casos posibles. Por ejemplo, si el primer segmento que se analizó fué JR, vemos que P tiene una distancia angular a JR inferior a la de K, y por tanto nunca se hubiera producido la situación actual. El mismo razonamiento vale si partimos de KR, JP, ó PK. Como es obvio, no pudo ser JK el primer segmento analizado. Por tanto esta situación es imposible con la distancia angular. ■

2.3. ELECCION OPTIMA DEL SEGMENTO

Un aspecto de mucha importancia, según veremos, es la estrategia de elección de cada nuevo segmento JK como posible base de un nuevo triángulo. Lógicamente, si al considerar un cierto segmento nos vemos en el caso del paso 5 del algoritmo (R frontera no consecutivo), no se puede construir triángulo y lo que procede es escoger otro segmento. Si no tenemos *a priori* más información, es irrelevante escoger uno determinado, así que podemos recorrer la frontera en sentido antihorario, visitando uno por uno los segmentos hasta encontrar uno que permita la construcción

de un nuevo triángulo. Cuando se construye un triángulo sobre el segmento en curso, a la hora de decidir cuál va a ser el segmento siguiente, hay dos casos a considerar: (véase la figura 2)

a) El tercer vértice R es interior: Ahora ha dejado de serlo, y la frontera posee los nuevos segmentos JR y RK. Elecciones lógicas para el nuevo segmento pueden ser: **a1)** el anterior a JR; **a2)** el mismo JR; **a3)** el RK; y **a4)** el siguiente a RK.

b) El tercer vértice R es consecutivo: en este caso, uno de los puntos J ó K es eliminado de la frontera, y ésta se reduce. Un nuevo segmento en la frontera ha aparecido en sustitución de otros dos. Hay, pues, tres elecciones lógicas posibles: **b1)** el anterior; **b2)** el nuevo; y **b3)** el siguiente.

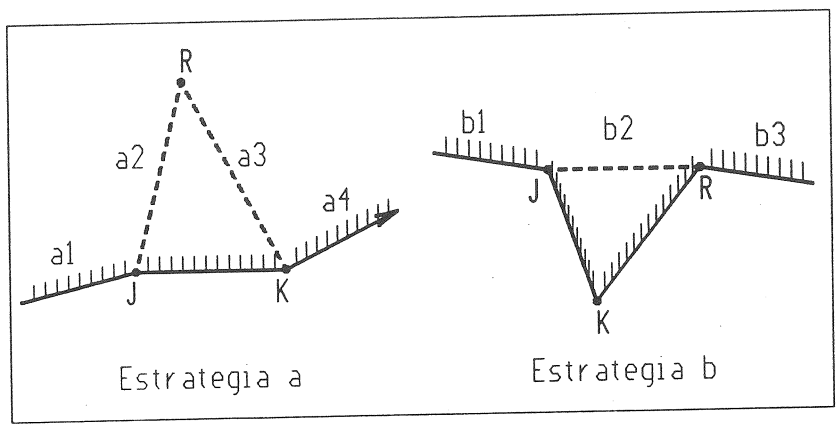

FIGURA 2: Las dos clases de estrategias de elección de segmento

En total tenemos, cruzando posibilidades, doce estrategias a estudiar. Todas ellas han sido ampliamente experimentadas, y algunas fases intermedias de triangulaciones se muestran en la figura 3. La mejor de todas resultó ser a3b1, seguida de cerca por a3b2 y las tres con a4.

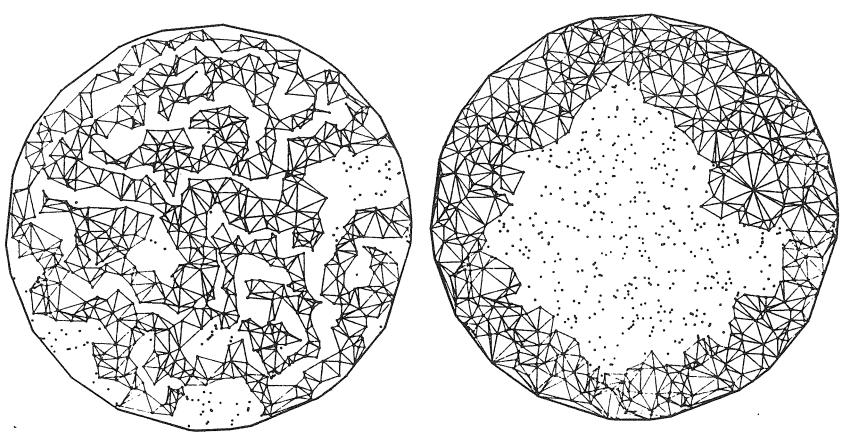

FIGURA 3: Fases intermedias de triangulaciones con las estrategias a2b3 (izda.) y a3b1 (dcha.)

Es de notar el consumo espectacular de tiempo en a2b3, más de 8 veces superior al de a3b1, que se debe a los numerosos vaivenes que el algoritmo debe dar a todo lo largo de la enorme frontera producida por un crecimiento espiral de la triangulación.

Resumiendo, podemos decir que, dado que un el paso 5 del algoritmo supone un estudio completo de un segmento desperdiciado, es aconsejable evitar esto en lo posible , y las estrategias a3b1 y a3b2 parecen hacerlo, mientras que a2b3 se comporta de manera opuesta. Por otro lado, si la frontera crece demasiado (como sucede en los casos de expansión espiral de la zona triangulada), la renumeración de puntos que hay que hacer tras cada nuevo triángulo para rehacer la figura puede alcanzar un orden de complejidad cercano a n, si se emplea una representación de datos inadecuada, lo que afectaría sensiblemente al tiempo total. Por ello, las estrategias que reducen de forma suave la frontera tienen que ser preferidas, y habrá que emplear estructuras de datos para el registro de la frontera de modo que las operaciones de inserción y borrado no superen el orden O(logn).

2.4. CORTES CON LA FRONTERA

El paso 6 del algoritmo requiere analizar si alguno de los segmentos RJ o RK cortan a la frontera de la figura, en cuyo caso sería imposible construir el triángulo RJK. Por un lado, sólo es necesario efectuar dicha comprobación con uno sólo de los segmentos, bien RJ o bien RK, porque no puede haber puntos interiores al triángulo RJK, y la frontera no hace lazos. Por la misma razón, si el punto R más cercano al segmento JK es consecutivo con los puntos J y K, entonces no es necesaria ninguna comprobación. Además, el siguiente resultado nos va a permitir eliminar completamente el test de corte con la frontera en ciertos casos.

Proposición: *Si la figura inicial es convexa, el algoritmo de reducción en frontera nunca provoca situación de corte con la frontera.*

Demostración: En una figura convexa no existen situaciones de corte con la frontera en los primeros pasos del proceso de triangulación. Conforme dicho proceso avanza, la única manera de provocar esto es, como ilustra la figura 4, mediante la construcción de un triángulo ABC sobre el segmento BC de tal modo que el punto R más cercano al segmento JK se encuentre al otro lado del triángulo. Esta situación obliga a que J, K y R tengan que estar fuera del círculo ABC, y, al mismo tiempo, a que A, B y C tengan que estar fuera del cículo JKR. La imposibilidad de esta construcción queda patente en cuanto que obliga a ambos círculos a tener cuatro puntos de intersección. Salvo el caso trivial de que todos los puntos estén en el mismo círculo, no se pueden generar situaciones de corte si se parte de una figura convexa. ■

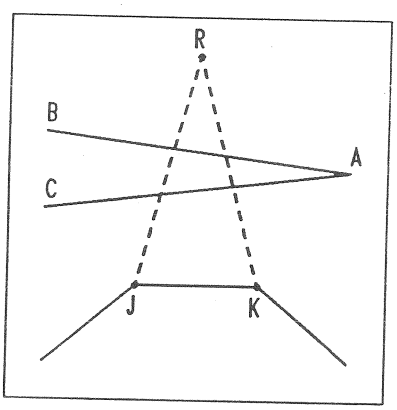

FIGURA 4: Corte con la frontera

2.5. OTRAS OBSERVACIONES

Hay un detalle sencillo para contribuir a acelerar el algoritmo. En ocasiones, el punto R más cercano al segmento JK está en la frontera y no es consecutivo, pero sólo hay un cuarto punto S entre R y los otros dos. Diremos entonces que R es *casi-consecutivo* con los puntos J y K. Normalmente esta situación puede ser resuelta con la construcción de dos nuevos triángulos a la vez, en vez de dejar que se produzca el paso 5 del algoritmo, y esto ayuda a bajar el tiempo total. La implementación de este detalle no es complicada, y hemos podido comprobar en la práctica que la reducción de tiempo así obtenida es de algo más del 12%.

El problema de figuras con agujeros, e incluso el de figuras disconexas, no requiere un tratamiento mucho más complejo que el mostrado aquí. Para el primer caso, una solución simple consiste en fracturar manualmente la figura de forma que los agujeros queden "fuera" de la misma. Esto está hecho en la figura en forma de diskette de computadora de la figura 5, donde dos agujeros han sido eliminados. Esta operación incorpora los agujeros a la frontera general (única) de la figura, y no hay ningún inconveniente en el hecho de que un punto forme parte de la frontera dos o más veces, como sucede en tales casos. En el caso de figuras disconexas existen varias fronteras disjuntas, y se puede tratar cada frontera como un problema separado. Si los puntos interiores están clasificados, tanto mejor. Pero si están desordenados y no hay forma rápida de localizar los puntos interiores a una parte concreta de la figura, en algoritmo sigue funcionando perfectamente, aunque en detrimento de su rapidez. Como veremos más adelante, esta pega no existe en el algoritmo mejorado.

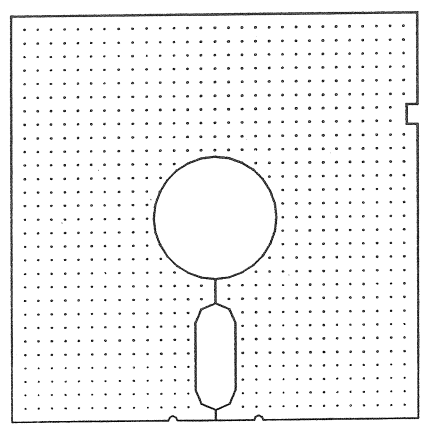

FIGURA 5: Eliminación de agujeros

3. Reducción del Tiempo: Método Matricial

3.1. PREPROCESO DE DATOS

Para muy grandes valores de n, la complejidad del algoritmo (en su versión básica es $O(n^2)$) puede resultar demasiado costosa en relación al tiempo óptimo teórico, $O(n \cdot \log n)$. Con objeto de rebajar en lo posible el coste en tiempo del algoritmo, se ha introducido un preproceso de los datos, con un consumo de memoria adicional, de manera que para encontrar el punto R más cercano al segmento JK no sea necesario estudiar sistemáticamente todos los puntos que en ese momento forman parte de la figura. Hemos tenido en cuenta para ello que, en condiciones ordinarias, no va a haber problema con el coste en memoria, y lo que importa es optimizar el tiempo. El preproceso consiste en asignar cada punto de la figura a una casilla de una cuadrícula preestablecida que cubre la figura en su totalidad, operación que puede hacerse en el momento de entrada de las coordenadas del punto. La asignación debe hacerse de forma que, dada una casilla, todos los puntos que están dentro sean rápidamente localizables sin tener que mirar todos y cada uno de los que componen la figura. De este modo, para buscar el punto más cercano a un segmento sólo hay que ir visitando las casillas vecinas a las que contienen el segmento, hasta encontrarlo. El algoritmo de preproceso, en principio, puede ser así:

ALGORITMO DE PREPROCESO

1: Cuadricular la zona de encuadre de la figura en una malla rectangular de Ch × Cv casillas iguales, con Ch y Cv prefijados de antemano.
2: Preparar una matriz M de orden Ch x Cv, inicialmente con ceros.
3: Preparar un vector G con n entradas, siendo n el número total de puntos. No necesita inicializarse.
3: Para $i=1,2,\ldots,n$ hacer:
4: Entrar las coordenadas del punto P_i.
5: Calcular la casilla (h,v) a la que pertenece el punto.
6: Si $M_{h,v}=0$, hacer $M_{h,v}=i$, $G_i=i$, y continuar en el paso 9. De lo contrario, hacer:
7: Sea $p=M_{h,v}$. Desplazar G un lugar adelante desde la posición indicada por p hasta la posición i. Hacer $G_p=i$.
8: Aumentar una unidad todas las entradas de M cuyo valor sea mayor que i.
9: Regresar al paso 3, si procede. Si no, fin del algoritmo.

Ejecutado este preproceso, el grupo de puntos contenidos en una casilla se localiza mirando el valor de la entrada correspondiente en la matriz M. Si dicha entrada es cero, no hay puntos en la casilla; de lo contrario, el valor de la entrada es el ordinal de la entrada en G que señala el índice del primer punto en la casilla. La siguiente entrada de G señala al índice del siguiente punto en la casilla, y así sucesivamente, hasta encontrar el final de G o un punto que esté fuera de la casilla:

Casilla (h,v):
- Si $M_{h,v}=0$: no hay puntos.
- Si $M_{h,v}\neq 0$: sea $p=M_{h,v}$; entonces $G_p, G_{p+1}, \ldots$ son los índices de los puntos.

Este algoritmo de preproceso tiene una complejidad del orden de $n \cdot Ch \cdot Cv$, y si, como los experimentos han mostrado ser una buena elección, tomamos Ch y Cv para que haya aproximadamente tantas casillas como puntos, la complejidad es del orden de n^2. Sin embargo, su ejecución es tan sumamente rápida que sólo para figuras con centenares de miles de puntos el tiempo de preproceso llega a superar al de la triangulación misma. Además, dado que normalmente la entrada de datos se efectúa desde un dispositivo más lento que la computadora, se puede aprovechar este tiempo para efectuar el preproceso. Esta complejidad puede rebajarse a un tiempo del orden $O(n \cdot \log n)$ si se emplean métodos eficientes de numeración con inserción y borrado, como pueden ser árboles de inserción.

Una vez introducido el preproceso en el programa, el proceso de triangulación debe ser alterado, en el modo de buscar el punto más cercano al segmento de la frontera en curso. Lo lógico es buscarlo en las casillas próximas, alejándose progresivamente en caso de encontrarlas vacías, hasta finalmente localizarlo. Este proceso de búsqueda de cerca a lejos será claramente más económico que un recorrido exhaustivo y desordenado de todos los puntos que quedan en la figura en ese momento.

3.2. LOCALIZACION DEL PUNTO MAS CERCANO

Hay que decidir una táctica de recorrido de casillas cercanas al segmento JK, y no sirve cualquiera. Una manera válida de visitar las casillas de forma que se tenga la seguridad de haber encontrado el punto más cercano consiste en visitar inicialmente todas las casillas por las que pasa el segmento JK, considerar la frontera de la región de casillas

visitadas en la búsqueda del punto R, y ampliar dicha región por el punto de su borde más cercano al JK. Entenderemos por distancia de un segmento UV al segmento JK como la mínima distancia angular de cualquier punto de UV al segmento JK. Puede ser que el punto de UV más cercano sea uno de los extremos U ó V, o también que sea un punto estrictamente interior al segmento. El método consiste en analizar todo el borde de la región visitada, y ampliarla allá donde esté el segmento UV más cercano a JK. Esto requiere llevar una lista ordenada de segmentos del borde de la región y de distancias respectivas. En el momento en que se localice el primer punto R cuya distanca a JK sea inferior a la mínima del borde, la búsqueda concluye. Esta idea ha mostrado en la práctica ha mostrado ser muy rápida, y se puede arreglar para que no necesite más que sumas, multiplicaciones y una raíz cuadrada por cada segmento UV analizado, además del cálculo final de la distancia de un punto al segmento JK.

3.3. PREPROCESO MEJORADO

Comoquiera que los tiempos de preproceso pueden ser importantes en grandes nubes de puntos, se puede modificar éste para reducir su complejidad a un tiempo lineal, suponiendo que se dispone de suficiente capacidad de almacenamiento.

El preproceso, tal como se ha descrito antes, emplea mucho tiempo en los desplazamientos que tiene que realizar en la variable G cada vez que entra un nuevo punto. La idea consiste ahora en disponer de un cierto número de capas en la matriz M en donde se vayan almacenando los índices de los puntos, dejando el vector G para cuando se completen todas las capas de M en una celdilla. Desde luego, una de las capas de M (por ejemplo la primera) seguirá conteniendo apuntadores al vector G, como antes. Sin embargo ahora el número de desplazamientos de G va a ser nulo o despreciable. Concretanto, el algoritmo puede quedar como sigue:

ALGORITMO DE PREPROCESO MEJORADO

1: Cuadricular la zona de encuadre de la figura en una malla rectangular de Ch × Cv casillas iguales, con Ch y Cv prefijados de antemano.
2: Preparar una supermatriz M de orden (nh+1) × Ch × Cv, inicialmente a cero. nh (número de capas) se ha prefijado antes.
3: Preparar un vector G con n entradas. Sin inicialización.
4: Para $i=1,2,\ldots,n$ hacer:
5: Entrar las coordenadas del punto P_i.
6: Calcular la casilla (h,v) a que pertenece.
7: Para $j=1,2,\ldots,nh$ hacer:
8: Si $M_{j,h,v}=0$, hacer $M_{j,h,v}=i$ e ir al paso 12.
9: Si $M_{nh+1,h,v}=0$, hacer $M_{nh+1,h,v}=i$, $G_i=i$ e ir al paso 12. De lo contrario hacer:
10: Sea $p=M_{nh+1,h,v}$. Desplazar G un lugar adelante desde p hasta i.Hacer $G_p=i$.
11: Aumentar una unidad todas las entradas de la capa nh+1 de M cuyo valor sea mayor que i.
12: Regresar al paso 4 si procede. Si no, fin del algoritmo.

El grupo de puntos contenidos en una casilla se localiza mirando las entradas $M_{1,h,v}$, $M_{2,h,v}$, ... , $M_{nh,h,v}$, que contienen índices de puntos. Si alguna entrada es cero, el grupo acaba ahí. En caso contrario procede mirar en el vector G desde la posición $M_{nh+1,h,v}$ en adelante, siempre que dicha posición no sea cero.

Se ha comprobado experimentalmente que un valor de nh similar al promedio de puntos por casilla, es decir, n/(Ch·Cv) es aceptable para cualquier número de puntos, y que en este caso el vector G no recibe más que algunos puntos sueltos procedentes de casillas muy pobladas. En todos los casos el preproceso tiene una complejidad lineal. Los tiempos de triangulación no se ven afectados por el cambio, ya que la localización de puntos en una casilla sigue siendo directa.

Con respecto a la triangulación, el proceso es también lineal, salvo en el único detalle de la renumeración de puntos frontera tras cada nuevo triángulo. Esta operación sólo requiere manipulación de enteros, y apenas nada de operaciones aritméticas. Si se emplea un árbol de inserción, la complejidad teórica se reduce a O(logm), donde m es el número de puntos frontera. Salvo para figuras con millones de puntos, la renumeración de la frontera consume una parte insignificante del tiempo total, por lo que el algoritmo descrito tiene un comportamiento práctico casi lineal.

4. Conclusión

En el presente trabajo se ha descrito un método de triangulación, válido para figuras planas no necesariamente convexas, ni conexas. Obviamente, para dar una figura no convexa se requiere enumerar ordenadamente los puntos que componen su frontera. La forma final del algoritmo descrito posee un tiempo óptimo teórica y prácticamente, es sencillo de implementar, y su consumo de memoria puede ser flexible y ajustable a las disponibilidades del hardware: a más memoria disponible, más eficiencia. Prestaciones adicionales del algoritmo son la orientación de los triángulos y el orden espacialmente apropiado en que se generan.

5. Referencias

[1] AKIMA,H. "A method of bivariate interpolation and smooth surface fitting for values given at irregularly distributed points", U.S. Depart. of Commerce OT Report, 1975, 75-70.

[2] CORREC,I., CHAPUIS,E. "Fast computation of Delaunay triangulations", Note of the Centre d'Electronique de l'Armement à Bruz.

[3] LAWSON,C.L. "Software for C^1 surface interpolation", in Mathematical Software III, New York: Academic Press, 1977, 161-193.

[4] McLAIN,D.H. "Two dimensional interpolation from random data", Comput. J. 19 (1976), 2, 178-181.

[5] RAMIREZ-GONZALEZ,V., MARTINEZ-AROZA,J. "Triangulation of Planar Regions Via an Algorithm of Reduction on the Boundary", Proc. of the 12th IMACS World Congress, IMACS'88, Paris 1988, 4, 468-470.

HERMITE INTERPOLATION BY C^1 BIVARIATE SPLINES

Edmond NADLER
Department of Mathematics
Wayne State University
Detroit, Michigan 48202
U.S.A.

ABSTRACT. Interpolation by C^1 bivariate piecewise polynomials of lowest degree to function value and gradient data at the vertices of a triangulation is considered. It is proven that such a piecewise quartic interpolant exists for all but a very special case of triangulation. The approach is constructive, using the Bernstein-Bézier form of a piecewise polynomial. A further approach is outlined to prove the conjecture that such interpolation can be accomplished with quartics on *any* triangulation.

1. Introduction

Let Δ be a triangulation of a connected polygonal domain in $\mathbb{R}^2$. It is desired to find a C^1 interpolant which is a low degree polynomial on each triangle, to prescribed function value and gradient data at the vertices of Δ.

This problem is one of a family of interpolation problems involving the bivariate spline spaces $S_d^r(\Delta)$ of C^r piecewise polynomials defined on the triangulation Δ, whose restriction to each triangle is a polynomial of total degree d. The basic problem is whether for given integers q, r and d, $q \leq r$, and any triangulation Δ, it is possible to interpolate with $S_d^r(\Delta)$ to prescribed function values and derivatives up to order q at the vertices of Δ. For a given q and r, naturally one would like to interpolate with the lowest possible degree d, which, as the interpolation values can be independently specified, is the smallest integer such that the dimension of $S_d^r(\Delta)$—on which at least a lower bound is known—exceeds the number of interpolation constraints. A more specific problem is then: For given integers q and r, $q \leq r$, determine whether for this minimum possible d suggested by dimensions of bivariate spline spaces, interpolation as described can be achieved with $S_d^r(\Delta)$ on *any* triangulation Δ.

For $(q,r) = (0,0)$ one has the trivial problem of interpolation to function values only by C^0 splines, where, of course, the piecewise linear ($d = 1$) functions work. The next in this family of problems is that for $(q,r) = (0,1)$, interpolation to function values by C^1 splines, and here it is known that $d = 4$ works (e.g. [3]), and conjectured that $d = 3$ works. In contrast to the first trivial problem of the family, this and all other such problems are extremely difficult. Then we come to the problem of present concern, $(q,r) = (1,1)$, interpolation to function values and gradients by C^1 splines, which shall simply be referred to henceforth as the *interpolation problem*. Here it is known that $d = 5$ works (e.g. [12]), and conjectured that $d = 4$ works, i.e.,

CONJECTURE. *For any triangulation Δ, there exists an interpolant in $S_4^1(\Delta)$ to function values and gradients at the vertices of Δ.*

In this paper we discuss this conjecture, and construct a piecewise quartic interpolant for a large class of triangulations, and give indications for how this can be done for *any* triangulation. In the next section, considerations of the dimension of spaces of C^1 splines are used to show that

piecewise quartic functions are likely to solve the interpolation problem, and the Bernstein-Bézier form of a bivariate piecewise polynomial is summarized. In Section 3, we summarize our previous work on the interpolation problem from [11],[12], developing techniques to solve the large system of linear equations which arises from the interpolation and smoothness conditions, and proving that the interpolation can be accomplished on nearly all triangulations. In Section 4, we prove that establishing interpolation on the as yet unsolved special case of triangulations amounts to a geometry problem for these triangulations, and give some ideas for solving this geometry problem.

In addition to the strong intuition we have developed for the favorable answer to the geometry problem, a further source of confidence in the Conjecture is that such an interpolant has been shown to exist for any particular triangulation so far examined.

2. Preliminaries

The most fundamental consideration of a spline space is its dimension. Let V, E, and F denote the number of vertices, edges, and faces (triangles) of the triangulation Δ. As previously indicated, the dimension must be at least as large as the number of interpolation constraints, $3V$ in the present case ($\frac{1}{2}(q+1)(q+2)V$ in general). This is, of course, only a *necessary* condition for the existence of the interpolant. It is surprising that a formula for $dim\ S_d^r(\Delta)$ in terms of V, E, and F, is not known for all r and d.

This dimension problem is an interesting and difficult one in its own right, actually involving the *geometry* of the triangulations, not just their topology. Some background on the results that have been achieved for this problem is in order. Strang [15] gave conjectures on $dim\ S_d^r(\Delta)$, which were shown by Schumaker [13], to actually be lower bounds. Morgan and Scott [10], established the dimension for the case $r = 1, d \geq 5$, and actually constructed a basis. They also constructed important examples of triangulations for which the dimension is geometry dependent. Schumaker [14], established upper bounds, which, taken with his lower bounds, establish the exact answer in some cases. Subsequently, exact dimensions for various cases have been established by Alfeld and Schumaker [2] ($d \geq 4r+1$), Alfeld, Piper, and Schumaker [3] ($d = 1, r = 4$), and Hong [8] ($d \geq 3r+2$), and Billera [5] showed that the *generic dimension* of the spline space S_d^1 always equals Schumaker's lower bound.

Proceeding, then, with the present problem, we first note that S_3^1 does not have high enough dimension to solve our interpolation problem, since for certain simple triangulations (cf. [12]), $dim\ S_3^1$, as obtained from Schumaker's formulas, is less than $3V$. S_4^1, on the other hand, has more than enough freedom for the interpolation. Schumaker's lower bound for S_4^1, expressed in the equivalent form of Alfeld [1], state that

$$dim\ S_4^1(\Delta) \geq 6V - 3 + \sigma \ , \tag{1}$$

with σ the number of **singular vertices**. A singular vertex [10] is defined to be a vertex with incident edges of only two different slopes, i.e,, one with exactly 4 incident edges with opposite edges colinear. This is the simplest example of a **geometric degeneracy**, i.e an instance where special geometry has an effect on the dimension.

This quantity is always strictly larger than the number of data $3V$, there being $3(V-1)+\sigma$ extra degrees of freedom. Recently, in fact, Alfeld, Piper and Schumaker [3] have shown that the lower bound of (1) actually *equals* the dimension for all triangulations. By elementary identities for graphs of the type being considered, i.e., triangulations, the number of extra degrees of freedom possessed by piecewise quartics for Hermite interpolation equals, equivalently

$$E + V_B + \sigma \ , \tag{2}$$

where V_B is the number of boundary vertices, an expression which actually gives an indication of how the problem is solved: *there is one free parameter to be chosen for each edge, each boundary vertex, and each singular vertex.*

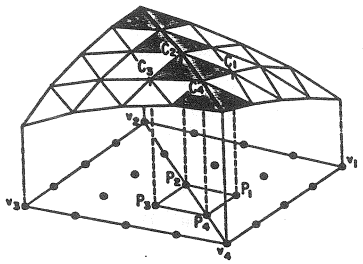

FIGURE 1. C^1 conditions between a pair of adjacent triangles.

The bivariate splines will be expressed with the Bernstein-Bézier form, popularized primarily by Farin (e.g. [9]), and by this time, in very common use. Briefly, a polynomial of degree d on a triangle is expressed as a linear combination of the **Bernstein basis polynomials**

$$B^d_{ijk}(\mathbf{x}) := \frac{d!}{i!j!k!}\beta_1^i(\mathbf{x})\beta_2^j(\mathbf{x})\beta_3^k(\mathbf{x}) \ , \ i+j+k=d \ , \tag{3}$$

in the barycentric coordinates $\beta_i(\mathbf{x})$ of the triangle. These polynomials are a basis for the space of polynomials of degree d, and the coefficients c_{ijk} in this representation of a polynomial are called **Bézier ordinates**. These Bézier ordinates can be associated with the **domain points** $P_{ijk} := (\frac{i}{d}, \frac{j}{d}, \frac{k}{d})$, $i+j+k=d$, expressed here in barycentric coordinates. Thus, to specify a polynomial of degree d on a triangle, one specifies the $\binom{d+2}{2}$ Bézier ordinates on the regular barycentric grid $\{P_{ijk}\}$. The **control points** $C_{ijk} := (P_{ijk}, c_{ijk}) \in \mathbb{R}^3$, the set of which being known as the **Bézier net**, give a more geometric aspect of this representation. The piecewise linear function which interpolates the control points gives a rough approximation of the polynomial; in particular, it agrees with the polynomial in value and gradient at the three vertices of the triangle.

To represent a *piecewise* polynomial on a triangulation, one naturally enough uses a Bézier net on each triangle. Adjacent triangles share domain points on their common edge. If the corresponding pairs of control points are identified, then continuity obtains across the edge [9]. Thus, one has a representation of *continuous* piecewise polynomials.

For the continuous piecewise polynomial to actually be C^1, there are easily stated conditions across each interior edge, namely that each of the d sets of four control points which straddle the edge, such as C_1, C_2, C_3, C_4 in Figure 1, be coplanar [9]. This can be expressed algebraically as homogeneous linear equations involving the corresponding Bézier ordinates c_i: *the scalars c_i satisfy the same homogeneous linear equation as the vertex vectors v_i*, and there are d such equations.

3. The interpolation scheme

In this section, we summarize our previous work on the interpolation problem, from [11],[12]. To solve the interpolation problem, one must specify values for all Bézier ordinates in the Bézier net for piecewise quartics on the triangulation. It must be done subject to the interpolation requirements and the C^1 requirements. We shall see that the large system of linear equations in the Bézier ordinates which results can be separated into local systems, which must, however, in some cases, be strung together in *trees*. With this approach, we succeed in showing that S^1_4 will interpolate as desired for nearly all triangulations.

The interpolation requirements are easily satisfied. The Bézier ordinates at the vertices are simply equal to the prescribed function values there. On each edge incident at a vertex, the Bézier ordinates at the domain point closest to the vertex is also determined: The corresponding control

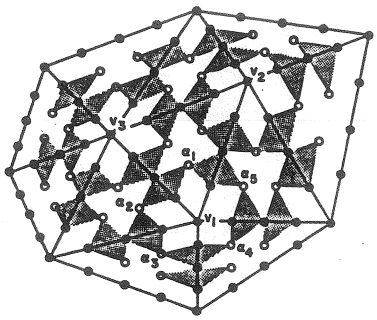

FIGURE 2. Global system of linear equations for the Hermite interpolation problem.

points lie in the tangent plane at the vertex, as determined by the interpolation data (cf. e.g. [4]). Thus, the interpolation data determines the Bézier ordinates at the domain points in a "disk of radius 1" around each vertex. This set of domain points is referred to as the **1-disk** D_1 at a vertex, following [3]. **2-disks**, disks of domain points of "radius" 2 around a vertex, will also prove useful. Also, let the terms **interior ordinates**, **edge ordinates**, and **midpoint ordinates** denote Bézier ordinates whose corresponding domain points are in the interior, on an edge, and at the midpoint of an edge of a triangle, respectively.

There are four C^1 conditions across each interior edge. With the interpolation conditions having determined the Bézier ordinates at the 1-disks of domain points in the manner just described, the two "end" C^1 conditions are automatically satisfied. Now select arbitrarily a value for the midpoint ordinate of each edge, as suggested by the *first term of the expression* (2) for the number of extra degrees of freedom possessed by S_4^1 to solve the interpolation problem. (One way this could be done is to make the quartics actually *cubic* along the edges.) Later it will turn out that for most triangulations, some of these midpoint ordinates will *not* be able to be independently specified, and their degrees of freedom will be shifted elsewhere. For the time being, though, with all midpoint ordinates, and hence all edge ordinates assumed to be fixed, we are left with the problem of determining the three interior ordinates of each triangle, subject to the two "middle" C^1 conditions across each edge, a situation illustrated in Figure 2.

With all midpoint ordinates fixed, the linear system separates into systems of equations for the interior ordinates around each vertex. For example, around vertex v_1, there is a linear system for the interior ordinates $\alpha_1, \ldots, \alpha_5$. Thus, the problem has been isolated to the 2-disks around each vertex, illustrated in Figure 3 for both interior and boundary vertices. In both cases, the edge ordinates have been specified, and the interior ordinates remain to be determined.

The set of all domain points in the Bézier net for piecewise quartics is equal to the union of the 2-disks around all vertices of the triangulation. Thus to completely specify the piecewise quartic interpolant, one must **solve each 2-disk**, i.e., determine all Bézier ordinates in the disk.

The boundary 2-disks are easily dealt with: Pick one of the interior ordinates arbitrarily, and the rest are determined by the C^1 conditions. This accounts for the *second term of the expression* (2) for the number of extra degrees of freedom possesed by S_4^1.

Consider, then, the linear system for the interior ordinates $\alpha_1, \ldots, \alpha_n$ around an *interior* vertex v_0 of degree n, with adjacent vertices $v_1, \ldots, v_n$, as depicted in Figure 4. Here the triangle T_i containing the interior ordinate α_i has edges e_{i-1} and e_i, where the indices minus 1 are taken *modulo* n, so that the indices have values in $\{1, \ldots, n\}$. a_i and b_i denote the edge ordinates adjacent to v_0, and the midpoint ordinates, respectively, on e_i. Express the geometric relationship

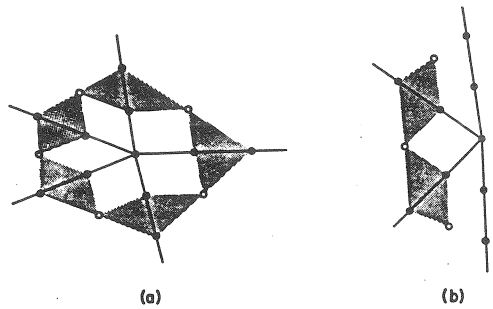

FIGURE 3. 2-disks of domain points around a vertex, with C^1 conditions: (a) interior vertex, (b) boundary vertex.

of the vertices of adjacent triangles $\Delta v_0 v_{i-1} v_i$ and $\Delta v_0 v_i v_{i+1}$ as follows:

$$\lambda_i v_{i-1} + \overline{\lambda}_i v_{i+1} = \mu_i v_i + \overline{\mu}_i v_0 \,, \quad i = 1, \ldots, n \tag{4}$$

where $\overline{\lambda}_i := 1 - \lambda_i$, $\overline{\mu}_i := 1 - \mu_i$. (Thus, $\overline{v_0 v_i}$ cuts $\overline{v_{i-1} v_{i+1}}$ in the ratio $\overline{\lambda}_i : \lambda_i$, and $\overline{v_{i-1} v_{i+1}}$ cuts $\overline{v_0 v_i}$ in the ratio $\mu_i : \overline{\mu}_i$.) Note that $\lambda_i, \overline{\lambda}_i > 0$ since v_{i-1} and v_{i+1} lie on opposite sides of $\overline{v_0 v_i}$. The C^1 conditions then imply that the α_i satisfy the following equations.

$$\lambda_i \alpha_i + \overline{\lambda}_i \alpha_{i+1} = \mu_i b_i + \overline{\mu}_i a_i \,, \quad i = 1, \ldots, n \,. \tag{5}$$

Expressing them in matrix form, we have

$$\mathbf{A}\vec{\alpha} = \mathbf{r}, \quad \text{where } \mathbf{A} := \begin{pmatrix} \lambda_1 & \overline{\lambda}_1 & 0 & \cdots & 0 \\ 0 & \lambda_2 & \overline{\lambda}_2 & \ddots & \vdots \\ \vdots & \ddots & \ddots & \ddots & 0 \\ 0 & \ddots & \ddots & \lambda_{n-1} & \overline{\lambda}_{n-1} \\ \overline{\lambda}_n & 0 & \cdots & 0 & \lambda_n \end{pmatrix}, \; r_i := \mu_i b_i + \overline{\mu}_i a_i \tag{6}$$

with $\mathbf{r} := (r_i)_{i=1}^n$ and $\vec{\alpha} := (\alpha_i)_{i=1}^n$. To solve (6), calculate

$$\det \mathbf{A} = \prod_{i=1}^{n} \lambda_i - (-1)^n \prod_{j=1}^{n} \overline{\lambda}_j \begin{cases} > 0 & \text{for } n \text{ odd} \\ = 0 & \text{for } n \text{ even,} \end{cases} \tag{7}$$

the first case following from the positivity of λ_i and $\overline{\lambda}_i$, and the second from the fact that $\prod_{i=1}^n \lambda_i = \prod_{j=1}^n \overline{\lambda}_j$ for all integers $n \geq 3$. This last statement follows immediately from the fact that $\dfrac{\lambda_i}{\overline{\lambda}_i} = \dfrac{\text{area } \Delta v_0 v_i v_{i+1}}{\text{area } \Delta v_0 v_{i-1} v_i}$, by taking $\prod_{i=1}^n$ of both sides. The statement and its proof just given reduce to those of *Ceva's Theorem* when $n = 3$, a well known geometry theorem which states: *The three ratios into which a line through each of the vertices of a triangle divide the opposite sides have product 1 if (and only if) the three lines are concurrent.* From (7) we have

PROPOSITION 1. *The matrix* $\mathbf{A}$ *of the linear system (6) for the interior ordinates in a 2-disk is nonsingular for* n *odd, and singular for* n *even.*

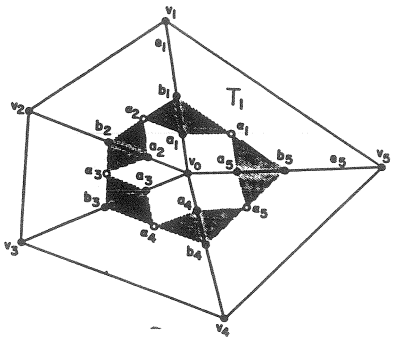

FIGURE 4. C^1 conditions around a vertex.

Hence, (6) has a unique solution for n odd, but further conditions need to be satisfied for there to be a solution for n even. (A similar result was obtained in a more special context by Chui and Lai [6].)

Before dealing with the case of even degree interior vertices, we remark that if we happened to have a triangulation with *all* odd degree interior vertices, all 2-disks are solvable and the interpolation problem is thus solved. One could pose the alternative problem with only the vertices fixed and not the actual triangulation. It is usually possible to triangulate a given set of vertices so that interior vertices are all of odd degree, but the formulation of precise conditions for when this can be done is an open problem.

Turning, now, to the case of even degree vertices, we must establish conditions to ensure that our linear system (6) has a solution. It will have a solution if and only if $\mathbf{r} \in \mathcal{R}(\mathbf{A})$, or equivalently, iff $\mathbf{r} \cdot \mathbf{y} = 0 \ \forall \mathbf{y} \in \mathcal{N}(\mathbf{A}^{\mathrm{T}})$, the left nullspace of $\mathbf{A}$. Now $\mathcal{N}(\mathbf{A}^{\mathrm{T}})$ is easily seen to be a one dimensional space, scalar multiples of a vector $\mathbf{s} := (s_i)_{i=1}^n$ with components

$$s_i = (-1)^{i+1}\Big(\prod_{j<i} \lambda_j\Big)\Big(\prod_{k>i} \overline{\lambda}_k\Big). \tag{8}$$

so that (6) has a solution if and only if

$$\mathbf{r} \cdot \mathbf{s} = 0. \tag{9}$$

Note that $\mathrm{rank}(\mathbf{A}) = n - 1$, so when (9) is satisfied, the solution of (6) will also have one degree of freedom. In (9), μ_i and a_i in r_i, as well as s_i are fixed by the geometry of the triangulation or the by interpolation data, so the only possible variables are the b_i, the midpoint ordinates on each edge. Thus (9) can be written as a linear equation for the b_i, in the form

$$\sum_{i=1}^{n} (\mu_i s_i) b_i = -\sum_{i=1}^{n} \overline{\mu}_i s_i a_i \ (\textit{constant}). \tag{10}$$

This equation involves exactly those b_i on edges e_i with $\mu_i \neq 0$. An edge e_i with $\mu_i = 0$ is said to be **degenerate** at its endpoint v_0, and by the definition of μ_i (see (4)) has the geometric property that the adjacent edges e_{i-1} and e_{i+1} are colinear.

A singular vertex has *all* incident edges degenerate, so there are no variables b_i in (10); the left hand side is 0. Fortunately, in this case the right hand side also turns out to be 0 , so that (10) is satisfied. Thus, there exists a solution to (6) for the case of singular vertices, and as noted

above, it has one degree of freedom. This accounts for the *third and last term of the expression* (2) for the number of extra degrees of freedom S_4^1 has to solve the interpolation problem.

For other even degree interior vertices there is a nontrivial equation (10) to be satisfied by the midpoint ordinates b_i on nondegenerate edges, in order for (6) to have a solution. Clearly, though, it is not possible to satisfy (10) with *all* the b_i already specified, as we had earlier tentatively done. Now we see that we must actually leave unspecified b_i on *one* of the nondegenerate edges incident at an even degree vertex. This one midpoint ordinate is then determined by the others around that vertex by (10). Then with (10) satisfied, there exists a solution to (6) for the interior ordinates α_i in the 2-disk around the vertex. Has one degree of freedom promised by the first term E of (2) been lost by not allowing one of the midpoint ordinates to be arbitrarily specified? No, this degree of freedom now appears in the solution $\vec{\alpha}$ for the interior ordinates in the 2-disk.

It would now seem that the problem is solved. All we have to do is to select one nondegenerate edge at each even degree interior vertex, and let its midpoint ordinate be determined from the others adjacent to the vertex by (10). However, this is not, in general, as straightforward as it appears: there are two consistency conditions to satisfy: (i) the two vertices at the endpoints of an edge cannot both pick that edge, and preferably, (ii) no "loops" of edges are allowed, i.e., given n vertices v_i, we cannot have each v_i select edge $\overline{v_i v_{i+1}}$. This consistency of edge selection leads naturally to *trees* on the edges of the triangulation, as was seen independently by the author [12] and Alfeld, Piper, and Schumaker [3], who used them for establishing the dimension and a basis for S_4^1. If vertex v_1 selects edge $\overline{v_1 v_2}$, then v_2 is the *parent* vertex of v_1. The tree continues back to its **root**, at which must be located one of the three types of vertices at which (10) does *not* have to be satisfied in order for there to be a solution to (6). These **terminating vertices** are: (i) odd degree vertices, (ii) singular vertices, and (iii) boundary vertices. In addition to having terminating vertices at their roots, these **proper trees** have the properties that (i) all vertices other than those at the roots are **non-terminating**, i.e., even degree interior vertices other than singular vertices), and (ii) every edge is nondegenerate at its "**leaf**-ward" vertex.

Thus, to solve the interpolation problem, one must construct a forest of such trees containing all the *non*-terminating vertices of the triangulation. For, if one has such trees, one can start at the leaves, satisfying (10) using the midpoint ordinates on the edges at these vertices, and work back to the roots, where *no* conditions need to be satisfied in order to solve the 2-disk. By an elementary graph theoretical argument (cf. Thm. 3 of [3]), it is possible to construct such a forest if there exists a **proper path**—a path only along edges nondegenerate at their "leaf-ward" vertices—*from each non-terminating vertex to a terminating one.* When there exists a proper path from a vertex v to a vertex w, we say that v can **reach** w, or w is **reachable** by v, or simply $v \rightarrow w$.

The condition that each non-terminating vertex can *reach* a terminating vertex is satisfied for almost all triangulations. For example, for a triangulation with *no* degenerate edges, the *boundary* is reachable by every non-terminating vertex since *every* path is proper. In fact it takes a situation much more special than the mere presence of degenerate edges to violate this condition; the simplest such situation is illustrated in Figure 5 (from [12]).

In the triangulation depicted in Figure 5, all 12 interior vertices are non-terminating, so the only type of terminating vertex is a boundary vertex. However, since all 12 edges shown in bold are degenerate at their interior endpoints, none of these non-terminating interior vertices can reach the boundary. This is a rather special geometrical situation: If any one of the 12 degenerate edges were non-degenerate, then *all* interior vertices could reach the boundary boundary via that edge, and the problem would be solved. Since it is apparent that this difficulty can arise only in very special cases, it is meaningful to state the following.

THEOREM 1. *For triangulations Δ in which every non-terminating vertex can reach a terminating vertex, there exists a Hermite interpolant in $S_4^1(\Delta)$.*

Let us summarize the construction of this interpolant.

1. Determine the Bézier ordinates in the 1-disk from the interpolation data.

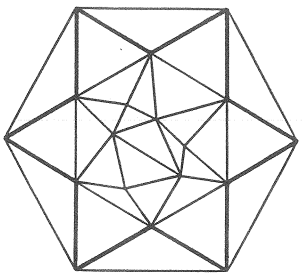

FIGURE 5. A triangulation for which the interpolation problem is not solvable by the tree method.

2. Using the assumption that each non-terminating vertex can reach a terminating vertex, construct a forest of proper trees containing all the non-terminating vertices of the triangulation.
3. Solve the 2-disks at each of the leaf vertices of the trees, by choosing arbitrarily (or, say, to make the interpolant cubic along the edges) all midpoint ordinates except the one on the edge linking to the parent vertex in the tree. This remaining midpoint ordinate is chosen to satisfy (10), guaranteeing that there exists a solution to (6) for the interior ordinates α_i of the 2-disk.
4. Similarly, solve the 2-disks at the parents of the leaves, where, now, the midpoint ordinates on edges linking from the child vertices have already been determined. Continue this process, working back to the roots, which, being terminating vertices, can be solved with all midpoint ordinates previously specified. Note that some terminating vertices may not have originally been roots of trees; these are handled are handled no differently than root vertices on trees which have already been solved all the way to their roots.

Since [12], we have made progress on the solution of **exceptional triangulations** not satisfying the hypotheses of Theorem 1, which will be described in the next section.

4. Proving interpolation for exceptional triangulations

Let us first formalize the notion of exceptional triangulations, which we define to be ones in which some non-terminating vertices cannot reach a terminating vertex. Following the notation of [3], let $\mathcal{V}_v$ be the set of all vertices reachable by v, and $\mathcal{E}_v$ be the set of all edges of Δ joining vertices in $\mathcal{V}_v$. It is evident that $\mathcal{E}_v$ is a subtriangulation of Δ. Also, there is a one-to-one correspondence between a set $\mathcal{V}_v$ and its associated set $\mathcal{E}_v$, so we can speak interchangably of a vertex being in these two sets.

Then an equivalent definition of an exceptional triangulation to the one above is *a triangulation which contains a non-terminating vertex v such that $\mathcal{V}_v$ contains no terminating vertices.* For a such a vertex v, we call the subtriangulation $\mathcal{E}_v$ an **isolated subtriangulation**, or **IST**.

In light of the correspondence between $\mathcal{V}_v$ and $\mathcal{E}_v$, an IST can more simply be defined as a *subtriangulation $\mathcal{E}_v$ containing no terminating vertices.* Clearly, no terminating vertex is reachable by a vertex $w \in \mathcal{E}_v$, because if w *could* reach a terminating vertex t, then, since v can reach w, it too could reach t, by the obvious transitivity property of reachability, for a contradiction.

In the exceptional triangulation depicted in Figure 5, the subtriangulation consisting of all edges joining the 12 interior vertices is an example of an IST.

By definition, an exceptional triangulation is one containing an IST. Moreover, there is no other "exceptional" situation possible in an exceptional triangulation, as any vertex *not* in an IST can reach a terminating vertex (for if it could not, it *would* be in an IST). Therefore, in the procedure for solving non-exceptional triangulations described at the end of the previous section,

once all non-terminating vertices which can reach terminating ones are placed in a forest of trees (so that the 2-disks of these vertices can be solved), *the only remaining vertices are those in ISTs*, and thus we have

PROPOSITION 2. *To prove the Conjecture that Hermite interpolation with S_4^1 can be achieved on any triangulation, it suffices to prove that the interpolation can be accomplished on an IST.*

We now derive some further properties of ISTs, leading to a more useful definition than our present one, i.e., a set $\mathcal{E}_v$ containing no terminating vertices. First, since an IST contains no terminating vertices, in particular, it contains no boundary vertices. Hence it consists entirely of interior triangles, ones with no vertices or edges on the boundary. Consider, then, a vertex on the boundary of the IST. Evidently, it must have an incident edge which is not part of the IST. Call such an edge, i.e., one with one vertex in the IST, but not itself in the IST, an **outgoing edge**.

PROPOSITION 3. *The outgoing edges from an IST are degenerate at their endpoint in the IST.*

LEMMA 1. *Let v be a vertex in an IST $\mathcal{E}_w$. Then $\mathcal{E}_v \subseteq \mathcal{E}_w$.*

PROOF: Let $u \in \mathcal{V}_v$, and it then suffices to show that $u \in \mathcal{V}_w$. Now $u \in \mathcal{V}_v$ means $v \rightarrow u$, and since $v \in \mathcal{E}_w$, we also have $w \rightarrow v$. Hence by transitivity, $w \rightarrow u$, i.e., $u \in \mathcal{V}_w$, as desired. ■

PROOF OF PROPOSITION 3: Let v be a vertex on the boundary of an IST $\tilde{\Delta}$, and $e := \overline{vw}$ be an outgoing edge, so by definition of the latter, $w \notin \tilde{\Delta}$. If e were *not* degenerate at v, then $v \rightarrow w$, so that $w \in \mathcal{V}_v$, a contradiction, since by the Lemma 1, $\mathcal{E}_v \subseteq \tilde{\Delta}$. ■

Now consider the boundary polygon $\tilde{v}_1 \cdots \tilde{v}_n$ of an IST. We know that all the vertices $\tilde{v}_i$ have outgoing edges, which we have just seen to be degenerate. It follows that the polygon $\tilde{v}_1 \cdots \tilde{v}_n$ is convex, for its exterior angles $\angle \tilde{v}_{i-1}\tilde{v}_i\tilde{v}_{i+1}$, being angles between edges including at least one degenerate edge, are $\geq \pi$. Equality is obtained when there is exactly one degenerate edge. Furthermore, there can be no more than *two* outgoing edges at a vertex $\tilde{v}_i$, since *three* adjacent degenerate edges any vertex necessarily implies that the vertex is *singular*, i.e., terminating.

Thus, an IST is a subtriangulation $\tilde{\Delta}$ of Δ with the properties (among others) that: (i) all of its vertices are *non-terminating*, and (ii) all outgoing edges are *degenerate* at their endpoint vertex in $\tilde{\Delta}$, with every vertex on the boundary of $\tilde{\Delta}$ possessing 1 or 2 such edges.

The above is actually equivalent to the definition of an IST, and will serve as our working definition. To see this, given a subtriangulation $\tilde{\Delta}$ with the above properties, show it contains a vertex v such that $\tilde{\Delta} = \mathcal{E}_v$. It can be shown that some v on the boundary of $\tilde{\Delta}$ will work.

Now, we begin to consider how we can augment our approach for solving non-exceptional triangulations, as described in the previous section, to solving ISTs. The reason our previous approach will not work on ISTs is that they contain no terminating vertices, nor can any be reached; the paths are "bottled up" in an IST. If we want to retain a similar approach, we are forced to reconsider *loops* of vertices. Let us then consider the simplest loop, that of three vertices, i.e., a triangle, and ask under what circumstances can the linear equations (10) at the three vertices simultaneously be solved. We now establish a geometric condition on the triangle so that this can be done, thus enabling solution of the 2-disks a the vertices of the triangle.

Consider an interior triangle with vertices v_1, v_2, v_3 of even degrees d_1, d_2, d_3, with adjacent triangles $\Delta w_1 v_2 v_3$, $\Delta w_2 v_1 v_3$, $\Delta w_3 v_1 v_2$. At each vertex $v_j, j = 1,2,3$, let $e_i^j, b_i^j, \lambda_i^j, \mu_i^j, i = 1, \ldots, d_j$ denote the incident edges , midpoint ordinates, and geometric parameters, respectively, analogous to the earlier definitions of $e_i, b_i, \lambda_i, \mu_i$ at a single vertex, with the labelling such that $i = 1$ corresponds to the edge $\overline{v_j v_{j+1}}$, where here and throughout this discussion, indices minus 1 associated with the three vertices are taken modulo 3, so that the indices have values in $\{1,2,3\}$. See Figure 6. Also, let $c_j := b_1^{j+1} \equiv b_2^{j+2}$, $j = 1,2,3$, the midpoint ordinates on the edges of $\Delta v_1 v_2 v_3$.

THEOREM 2. *Let interior triangle $\Delta v_1 v_2 v_3$ with associated Bézier ordinates b_i^j be as defined above. Assume all b_i^j, $i \neq 1,2$ are fixed, i.e., all Bézier ordinates b_i^j except the ones on the edges*

is easy to prove that "straight" degree 4 IST boundary vertices have an adjacent non-concurrent triangle in the IST. Note that by the *degree* of a vertex on the boundary of a subtriangulation we mean its degree on the *whole* triangulation, i.e., including outgoing edges.

Finally, we mention another result concerning degree 4 vertices, the first half of which enables us to solve the exceptional triangulation depicted in Figure 5. Its proof is simple geometry. Note that 6 is the most common degree of vertices in a triangulation, and in particular of vertices on the boundary of an IST.

LEMMA 3. *If an IST has a degree 6 convex boundary vertex connected by an edge to an interior degree 4 vertex, then one of the two triangles of the IST which share that edge must be non-concurrent. Also, if an IST has a degree 6 straight boundary vertex connected by an edge to an interior degree 4 vertex not connected to another boundary vertex, then, again, one of the triangles sharing that edge must be non-concurrent.*

Thus, such an IST can be solved by using the non-concurrent triangle as a terminator.

The highly constrained geometry of concurrent triangulations in the presence of degree 4 vertices is incompatible with that in the presence of the degenerate outgoing edges. It seems possible, in cases where the degree 4 vertices are *not* adjacent to the boundary of the IST, to extend Lemma 3 to provide some kind of link to the boundary which exploits such an incompatibility, to prove the impossibility of having a concurrent IST, thus proving the Conjecture.

References

[1] Alfeld, P. (1986), On the dimension of multivariate piecewise polynomials, in: Proceedings of the Biennial Dundee Conference on Numerical Analysis, June 25–28, 1985, Pitman Publishers.

[2] Alfeld, P. and Schumaker, L. L. (1986), The dimension of bivariate spline spaces of smoothness r for degree $d \geq 4r + 1$, Constructive Approximation, **3**, 189–197.

[3] Alfeld, P., Piper, B. and Schumaker, L. L. (1987), An explicit basis for C^1 quartic bivariate splines, SIAM J. Numer. Analysis **24**, 891–911.

[4] Barnhill, R. E. and Farin, G. (1981), C^1 quintic interpolation over triangles: Two explicit representations, Internat. J. Numer. Methods Eng. **17**, 1763–1778.

[5] Billera, Louis J. (1986), Homology of Smooth Splines: Generic Triangulations and a Conjecture of Strang, Trans. AMS **310**, 325–340.

[6] Chui, C. K. and Lai, M. J. (1985), On bivariate vertex splines, in: Schempp, W. and Zeller, K., eds., *Multivariate Approximation Theory III* , Birkhäuser Verlag, Basel, 84-115.

[7] Diener, D. (1988), Notes on Hermite interpolation in $S_4^1(\Delta)$, manuscript.

[8] Dong, H. (1988), Spaces of multivariate spline functions on triangulations, Masters Ths., Zheziang U.

[9] Farin, G. (1980), Bézier polynomials over triangles and the construction of piecewise C^r polynomials, TR/91, Dept. of Mathematics, Brunel University, Uxbridge, England.

[10] Morgan, J. and Scott, R. (1975), A nodal basis for C^1 piecewise polynomials of degree $n \geq 5$, Math. Comp. **29**, 736-740.

[11] Nadler, E. (1986), Hermite interpolation by smooth piecewise polynomials on triangulations, Paper presented at Constructive Function Theory Conference, July 1986, University of Alberta.

[12] Nadler, E. (1987), Hermite interpolation by C^1 piecewise polynomials on triangulations, IBM Research Report RC 12507, submitted for publication.

[13] Schumaker, L. L. (1979), On the dimension of spaces of piecewise polynomials in two variables, in: Schempp, W. and Zeller, K., eds. *Multivariate Approximation Theory* , Birkhäuser, Basel, 396-412.

[14] Schumaker, L. L. (1984), Bounds on the dimension of spaces of multivariate piecewise polynomials, Rocky Mountain J. Math. **14**, 251-264.

[15] Strang, G. (1974), The dimension of piecewise polynomial spaces, and one-sided approximation, in: Watson, G. A., ed., *Conference on the Numerical Solution of Differential Equations*, Dundee 1973, Lecture Notes No. 363, Springer-Verlag, Berlin, 144-152.

BEST PARAMETER INTERPOLATION IN L_p - NORMS

Christine Rademacher, Karl Scherer
Institut für Angewandte Mathematik, Universität Bonn
53 Bonn 1, Wegelerstr. 6, FRG

Abstract: Best parametric interpolation is the extension of the classic problem of best interpolation to vector - valued data. In addition the underlying minimization principle includes variation with respect to the nodes. This yields a choice of a "best parametrization" which is of importance for the geometric properties of the interpolating curve.

The functionals to be minimized are chosen here as L_p - norms of the $k-th$ derivative. We prove existence and characterization theorems which extend those of Scherer - Smith [6] in the case $p = 2$ and of Pinkus [5] in the case of scalar data. In case $k = 3$ we sharpen the existence result of [6] and exhibit an example where no solution exists.

1. Introduction. Given data $\{\underline{y}_i\}_{i=1}^n$ with $\underline{y}_i \in \mathbb{R}^d$ and a sequence of nodes of the form

$$\underline{t} : a = t_1 < t_2 < \cdots < t_n = b \quad , \tag{1.1}$$

one considers the following classes of interpolating curves

$$U(\{\underline{y}_i\}_{i=1}^n; \underline{t}) := \{\underline{f} \in (L_p^k(a,b))^d : \underline{f}(t_i) = \underline{y}_i, 1 \le i \le n\} \quad . \tag{1.2}$$

Here $L_p^k(a,b)$ is the usual Sobolev space for $1 \le p \le \infty$ and $k = 1, 2, \ldots$ and $(L_p^k(a,b))^d$ the d -fold product of these spaces.

In the sequel we denote by $|\cdot|$ the absolute value of a number in $\mathbb{R}$ and by $\|\cdot\|$ any norm on $\mathbb{R}^d$ (it will be clear from the context which of these equivalent norms is meant) . Then we set for $g \in L_p(a,b)$

$$A_p(g) := \begin{cases} \int_a^b |g(t)|^p dt \quad , & 1 \le p < \infty \\ \operatorname{ess\,sup}_{a \le t \le b} |g(t)| \quad , & p = \infty \quad . \end{cases} \tag{1.3}$$

Finally we introduce a continous functional $\emptyset$ on $\mathbb{R}_+^d$ with the following properties.

$$\emptyset(x_1, \ldots, x_d) \ge 0 \quad \text{for} \quad x_1, \ldots, x_d \ge 0 \quad , \tag{1.4i}$$

$$\emptyset \quad \text{is strictly increasing in} \quad x = (x_1, \ldots, x_d) \quad , i.e. \tag{1.4ii}$$

$$\emptyset(x_1, \ldots x_d) \le \emptyset(\tilde{x}_1, \ldots, \tilde{x}_d) \quad \text{for} \quad x_i \le \tilde{x}_i \quad , 1 \le i \le d$$

$$\text{and strict inequality if} \quad x \ne \tilde{x} \quad ,$$

$$\emptyset \quad \text{is coercive on} \quad \mathbb{R}^d, \quad i.e. \quad . \tag{1.4iii}$$

$$\emptyset(x_1,\dots,x_d)\to\infty,\quad \text{if}\quad \|x\|\to\infty\quad .$$

We are then able to formulate our problem: determine a sequence $\underline{t}$ of the form (1.1) and a $\underline{f}=(f_1,\dots f_d)\in(L_p^k(a,b))^d$ such that

$$I_p=\inf_{\underline{t}}\inf\{\emptyset(A_p(f_1^{(k)}),\dots,A_p(f_d^{(k)})):\underline{f}\in U(\{\underline{y}_i\}_{i=1}^n;\underline{t})\} \tag{1.5}$$

is attained. Of course we assume $n>k$ to avoid trivialities. A special choice of $\emptyset$ is given by

$$\emptyset(x_1,\dots,x_d):=\sum_{i=1}^d|x_i|^\rho\quad,\rho>0\quad . \tag{1.6}$$

For $p=2,\rho=1$ this problem was considered in [6] and earlier by Töpfer [7] , Marin [5] for $k=2$. Pinkus [5] considered general $p,1\le p\le\infty$, and k , however only in the scalar case $d=1$ where the choice (1.6) is irrelevant.

2. Existence. We start with the investigation of a simpler form of problem (1.5). To this end we consider the functionals

$$\lambda_j(\underline{f}):=\underline{f}^{(j)}(t_{v_0})/j!\quad,0\le j\le k-1 \tag{2.1}$$

where t_{v_0} is an element of $\underline{t}$ and then for fixed $M>0$ the problem of finding a solution of

(2.2)

$$I_{M,p}=\inf_{\underline{t}}\inf\{\emptyset(A_p(f_1^{(k)}),\dots,A_p(f_d^{(k)})):\underline{f}\in U(\{\underline{y}_i\}_{i=1}^n;\underline{t}),\lambda_j(\underline{f})=\underline{s}^j,\max_{1\le j\le k-1}\|s^{(j)}\|\le M\}$$

Theorem: Problem (2.2) has a solution for $1<p\le\infty$ under the above conditions on $\emptyset$.

Proof: To each feasible $\underline{f}$ in (2.2) we associate the vector-valued polynomial

$$\underline{p}(t)=\underline{f}(t_{v_0})+\sum_{j=1}^{k-1}\lambda_j(\underline{f})(t-t_{v_o})^j=\underline{y}_{v_0}+\sum_{j=1}^{k-1}\underline{s}^{(j)}(t-t_{v_o})^j \tag{2.3}$$

We then write

$$\underline{f}(t)=\underline{p}(t)+\tilde{\underline{f}}(t)\quad ,$$

and have by Peano's theorem (= Taylor expansion applied to $\tilde{\underline{f}}(t),\lambda_j(\tilde{\underline{f}})$)

$$\tilde{\underline{f}}(t)=\int_a^b\underline{f}^{(k)}(\tau)G(t,\tau;\{\lambda_j\})d\tau \tag{2.4}$$

with Peano - kernel

$$G(t,\tau;\{\lambda_j\})=\frac{(t-\tau)_+^{k-1}}{(k-1)!}-\sum_{j=0}^{k-1}(t-t_{v_0})^j\lambda_j((\cdot-\tau)_+^{k-1}) \tag{2.5}$$

Now we consider a minimizing sequence for problem (2.2), thus a sequence of $\underline{t}^{(N)}$ of form (1.1), a sequence $\underline{f}_N \in (L_p^k(a,b))^d$ and a sequence of vectors $\{\underline{s}_N^{(j)}\}_{j=1}^{k-1}$ such that

$$I_{M,p} = \lim_{N\to\infty} \emptyset(A_p(f_{1,N}^{(k)}),\ldots,A_p(f_{d,N}^{(k)})) \quad , \tag{2.6}$$

and such that $\underline{f}_N(t_i^{(N)}) = \underline{y}_i, 1 \le i \le n$, and $\lambda_j(\underline{f}_N) = \underline{s}_N^{(j)}$ for $1 \le j \le k-1$.
By the coerciveness condition (1.4iii) there exists a constant $C > 0$ independent of N such that

$$\sum_{\nu=1}^{d} A_p(f_{\nu,N}^{(k)}) \le C \quad . \tag{2.7}$$

Now we use the weak compactness of the unit ball of $L_p(a,b)$ for $1 < p < \infty$ and the weak $*$ compactness in case $p = \infty$. Then there exists in all cases a $\underline{g}^* \in (L_p(a,b))^d$ such that for any $\psi \in L_{p'}(a,b), 1/p + 1/p' = 1$, there holds

$$\lim_{N\to\infty} \int_a^b \underline{f}_N^{(k)}(\tau)\psi(t)d\tau = \int_a^b g^*(\tau)\psi(\tau)d\tau \quad . \tag{2.8}$$

Also we have by a well known result in functional analysis that

$$A_p(g_\nu^*) \le \frac{\lim}{N\to\infty} A_p(f_{\nu,N}^{(k)}) \quad , \qquad 1 \le \nu \le d. \tag{2.9}$$

Furthermore we can assume, eventually by passing to a subsequence, that

$$\lim_{N\to\infty} t_i^{(N)} = t_i^*, 1 \le i \le n \quad . \tag{2.10}$$

and that

$$\lim_{N\to\infty} \underline{s}_N^{(j)} = s_j^* \quad .$$

Using this in the representation (2.3) for the polynomial $\underline{p}_N$ corresponding to $\underline{f}_N$ we easily conclude that

$$\lim_{N\to\infty} \underline{p}_N(t) = \underline{p}^*(t) \equiv \underline{y}_{\nu_0} + \sum_{j=1}^{k-1} \underline{s}_j^*(t - t_{\nu_0}^*)^j/j! \quad ,$$

and this convergence is uniform on $[a,b]$. We define then

$$\underline{f}^*(t) := \underline{p}^*(t) + \int_a^b g^*(\tau)G(t,\tau;\{\lambda_j^*\})d\tau \quad .$$

Here we denote by $G(t,\tau;\{\lambda_j^*\})$ and $G(t,\tau;\{\lambda_{j,N}\})$, respectively, functions defined by (2.5) but with t_{ν_0} replaced by $t_{\nu_0}^*$ and $t_{\nu_0,N}$ respectively. In view of (2.7), (2.8) and

$$|\underline{f}_N(t) - \int_a^b \underline{g}^*(\tau)G(t,\tau;\{\lambda_j^*\})d\tau| \le \tag{2.11}$$

$$|\int_a^b \underline{f}_N^{(k)}(\tau)[G(t,\tau;\{\lambda_{j,N}\}) - G(t,\tau;\{\lambda_j^*\})]d\tau| + |\int_a^b [\underline{f}_N^{(k)}(\tau) - \underline{g}^*(\tau)]G(t,\tau;\{\lambda_j^*\})d\tau|$$

it follows then that $\underline{f}_N(t) \equiv \tilde{\underline{f}}_N(t) + \underline{p}_N(t)$ converges pointwise to $\underline{f}^*(t)$. In particular $\underline{f}^*(t)$ is a feasible function for the infimum (2.2). Furthermore we have $\underline{f}^{*(k)}(t) = \underline{g}^*(t)$ and by (2.6) , (2.9), (1.4ii)

$$\emptyset(A_p(f_1^{*(k)}),\ldots,A_p(f_d^{*(k)})) \leq \lim_{N\to\infty} \emptyset(A_p(f_{1,N}^{(k)}),\ldots,A_p(f_{d,N}^{(k)})) = I_{M,p} \quad ,$$

which shows that $\underline{f}^*$ is the desired solution of (2.2).

Remark 1: Instead of (2.1) we can choose actually boundary conditions of the form

$$\lambda_j(f) = \begin{cases} f^{(j)}(a) & , \quad 1 \leq j \leq k_1 \\ f^{(j-k_1)}(b) & , \quad k_1 < j \leq k-1 \end{cases} ,$$

with some integer k_1. We can then consider problem (2.2) with these functionals λ_j and fixed s_j as additional data at the boundary. By the same proof as in Theorem 1 this standard problem of best interpolation has always a solution.

Remark 2: The method of theorem 1 allows one also to treat the case of closed curves or the periodic problem (for convenience take $(a,b) = (0,1)$)

$$(2.12)\quad \hat{I}_p = \inf_{\underline{t}} \inf\{\emptyset(A_p(f_1^{(k)}),\ldots,A_p(f_d^{(k)})) : f \in U(\{\underline{y}_i\}_{i=1}^n;\underline{t}), f^{(\nu)}(1) = f^{(\nu)}(0), 1 \leq \nu \leq k-1\}$$

We can write this in the form (2.2) with $s_j = 0$, if we take

$$(2.13)\qquad \lambda_j(f) := [f^{(j-1)}(1) - f^{(j-1)}(0)]/j! \quad , 1 \leq j \leq k \quad .$$

For the corresponding polynomial in (2.3) we write

$$\underline{p}(t) \equiv Q(f)(t) = a_0 + \sum_{j=1}^{k} a_j \varphi_j(t)$$

In order to obtain the representation (2.4) with appropriate kernel one has to choose the polynomials φ_j such that the map $\underline{f} \to Q(f)$ becomes a projector onto the space π_{k-1} of polynomials of degree $k-1$. This achieved by taking $\varphi_j \in \pi_k$ such that

$$\lambda_i(\varphi_j) = \delta_{ij} \quad , 1 \leq i,j \leq k \quad .$$

One can easily check that this is the case if $\varphi_j(t)$ is the $j-th$ Bernoulli polynomial $B_j(t)$ defined by

$$B_1(t) = t - 1/2 \quad , \quad 0 < t < 1$$

$$B_r(t) = rB_{r-1}(t) \quad , \quad \int_0^1 B_r(t)dt = 0 \quad .$$

The corresponding Peano-kernel is then given by (2.5) where the second term is replaced by application of the projector Q to $(\cdot - \tau)_+^{k-1}/(k-1)!$, and Q is defined by determing the coefficients a_j via

$$\lambda_j(Q(f)) = \lambda_j(f), \quad 1 \leq j \leq k; \sum_{j=1}^{k} a_j = 0$$

Now the argument of Theorem 1 applies and we conclude that the periodic problem (2.12) does have always a solution.

Next we modify and extend the above considerations so as to give an existence proof for the initial problem (1.6).

Theorem 2: Let be $1 < p \leq \infty$ and $\emptyset$ as above. Either problem (1.6) has a solution or the data $\{\underline{y}_i\}_{i=1}^n$ are asymptotically of order k, i.e. there exists a sequence of vector - valued polynomials $\underline{q}_N(t) \in \pi_k$ and a sequence $\{t_i^{(N)}\}_{i=1}^n$ of nodes of the form (1.1) such that

$$\underline{y}_i = \lim_{N\to\infty} \underline{q}_N(t_i^{(N)}) \qquad ,1 \leq i \leq n \quad . \tag{2.14}$$

Proof: We consider a minimizing sequence for problem (1.6), thus a sequence $\underline{t}^{(N)}$ satisfying (2.10) and a sequence of corresponding interpolants $\underline{f}_N \in (L_p^k(a,b))^d$. More specifically, let the limiting sequence $\underline{t}^*$ in (2.10) be of the form

$$a = t_1^* = \cdots = t_{j_2-1}^* < t_{j_2}^* = \cdots < \cdots < t_{j_r}^* = \cdots = b \quad ,j_1 = 1 \quad . \tag{2.15}$$

Now we assume first that $r \geq k$ so that the nodes $t_{j\mu}, 1 \leq \mu \leq k$, are simple. Then we split $\underline{f}_N$ into

$$\underline{f}_N(t) = \underline{p}_N(t) + \tilde{\underline{f}}_N(t)$$

as before but with

$$\underline{p}_N(t) = \sum_{\nu=1}^{k} f(t_{j\nu}^{(N)}) l_{\nu,N}(t) = \sum_{\nu=1}^{k} \underline{y}_{j_\nu} l_{\nu,N}(t) \quad , \tag{2.16}$$

where $l_{\nu,N}$ are the Lagrangian fundamental polynomials according to

$$\lambda_{\mu,N}(l_{\nu,N}) = \delta_{\mu,\nu} \quad \text{for} \quad 1 \leq \mu,\nu \leq k \quad ,\lambda_{\mu,N}(f) := f(t_{j_\mu}^{(N)}) \quad . \tag{2.17}$$

For $\tilde{f}_N(t)$ we have then the representation (2.4) with kernel function

$$G(t,\tau;\{\lambda_{j,N}\}) = \frac{(t-\tau)_+^{k-1}}{(k-1)!} - \sum_{\mu=1}^{k} \lambda_{\mu,N}((\cdot-\tau)_+^{k-1}) l_{\mu,N}(t)/(k-1)! \quad . \tag{2.18}$$

It is easy to see that these functions converge for each fixed t uniformly in τ to a kernel $G(t,\tau;\{\lambda_j^*\})$ where the λ_μ^* and l_μ are formed as in (2.17) but with $t_{j\mu}^*$ replacing $t_{j\mu}^{(N)}$. Now the same argument as in Theorem 1 applies, in particular, the estimate (2.11) remains true, so that existence of a solution of (1.6) follows.

Assume now on the contrary that $r < k$ in (2.15) holds. Then we complete the sequence $\{t_{j\nu}^{(N)}\}_{\nu=1}^r$ with j_ν as in (2.15) to a sequence $\{t_{j\nu}^{(N)}\}_{\nu=1}^k$ by adding any further $r-k$ points of $\underline{t}^{(N)}$. Then we form as before $\tilde{f}_N$ with $\underline{p}_N$ as in (2.16) and $G(t,\tau;\{\lambda_{j,N}\})$ as in (2.18). In view of $r \geq 2$ in (2.15) the limiting points $\{t_{j\nu}^*\}_{\nu=1}^k$ have at most multiplicity $k-1$. The limit of the functions $G(t,\tau;\{\lambda_{j,N}\})$ is well defined since it involves at most $(k-2)$ fold differentiation of truncated power $(t-\tau)_+^{k-1}$ (take Newton's representation in (2.18)). Furthermore the convergence is uniform so that an estimate of the form (2.11) for $t = t_i^{(N)}$ implies that

$$\lim_{N\to\infty} \tilde{f}_N(t_i^{(N)}) = \int_a^b g^*(\tau) G(t_i^*,\tau;\{\lambda_j^*\}) d\tau \equiv \underline{w}_i \tag{2.19}$$

for $1 \le i \le n$. Also we see that by (2.15) $\underline{w}_i = \text{const.}$ must hold for $j_\nu \le i < j_{\nu+1}$. It follows that $\lim_{N\to\infty} \underline{p}_N(t_i^{(N)}) = \underline{q}_i$ exists for $1 \le i \le n$ and that

$$\underline{q}_i - y_i = \underline{w}_{j\nu} \qquad , j_\nu \le i < j_{\nu+1} \quad , \quad 1 \le \nu < r \quad .$$

Now let $\underline{q}^*(t)$ be that polynomial of degree $r-1 < k-1$ which interpolates the data $\underline{w}_{j\nu}$ for $1 \le \nu \le r$ at the nodes $t^*_{j\nu}$. Then there holds for $j_\nu \le i < j_{\nu+1}$

$$\lim_{N\to\infty} [\underline{p}_N(t_i^{(N)}) - \underline{q}^*(t_i^{(N)})] = \underline{q}_i - \underline{q}^*(t_i^*) = \underline{q}_i - \underline{w}_{j\nu} = y_i$$

Thus $q_N(t) \equiv \underline{p}_N(t) - \underline{q}^*(t)$ is the sequence as described in (2.14) .

Remark 3: The argument leading to (2.19) shows also that for "rough" data satisfying $\underline{y}_{i+1} \neq \underline{y}_i$ the optimal knots must be simple if a solution exists.

In some cases it is easy to determine whether the data $\{\underline{y}_i\}_{i=1}^n, n > k$, are asymptotically polynomial of order k. We formulate the following lemma whose proof we omit since it can be found essentially in [6].

LEMMA: In the cases $d = 1$, any k , and $k = 2$, any d , asymptotically polynomial data $\{\underline{y}_i\}_{i=1}^n, n > k$, of order k lie on a polynomial curve of order k.

As an immediate consequence we have the

Corollary: In the cases $d = 1$, any k , and $k = 2$, any d, there exists always a solution of problem (1.5) for $1 < p \le \infty$.

3. The case k = 3 . We first improve the result of Theorem 2.

Theorem 3: For $k = 3, 1 < p \le \infty$, problem (1.5) has always a solution or the data $\{y_i\}_{i=1}^n$ have the form

$$\underline{y}_l = \begin{cases} \underline{y}_1 + \alpha_l \underline{q} & , \quad 1 \le l \le m \\ \underline{y}_n + \alpha_l \underline{q} & , m < l \le n \end{cases} .$$

Here $\underline{q}$ is a fixed vector and m an integer, $1 \le m < n$. The α_l are nonnegative numbers which are increasing for $l \le m$ and decreasing for $l > m$.

Proof: We carry on the argument of Theorem 2. Hence we consider a minimizing sequence $t^{(N)}, \underline{f}_N$ such that (2.15) holds with $r = 2$ and $j_2 - 1 \equiv m$. In this case there exists further a sequence $\{\underline{q}_N(t)\}$ of polynomial curves in π_3 such that (2.14) holds. We write these polynomials in their Lagrangian form, thus

$$\underline{q}_N(t) = q_N(t_l^{(N)}) \frac{(t-a)(t-b)}{(t_l^{(N)}-a)(t_l^{(N)}-b)} + q_N(a) \frac{(t-t_l^{(N)})(t-b)}{(a-t_l^{(N)})(a-b)} + q_N(b) \frac{(t-a)(t-t_l^{(N)})}{(b-a)(b-t_l^{(N)})} \quad .$$

In the case $1 \le l \le m$ we multiply this relation by $(t_l^{(N)} - a)$ and get by (2.14), (2.15)

$$\lim_{N\to\infty} \underline{q}_N(t)(t_l^{(N)} - a) = \underline{y}_l \frac{(t-a)(t-b)}{a-b} - \underline{y}_1 \frac{(t-a)(t-b)}{a-b} \quad ,$$

whereas in case $m < l < n$ we multiply by $(b - t_l^{(N)})$ and get

$$\lim_{N\to\infty} \underline{q}_N(t)(b - t_l^{(N)}) = -\underline{y}_l \frac{(t-a)(t-b)}{b-a} + \underline{y}_n \frac{(t-a)(t-b)}{b-a} \quad .$$

Introducing the function $\varphi(t) \equiv (t-a)(b-t)/(b-a) \geq 0$ for $t \in [a,b]$ one has

$$\lim_{N\to} \underline{q}_N(t)(t_l^{(N)} - a) = (\underline{y}_l - \underline{y}_1)\varphi(t) \qquad , 1 \leq l \leq m \quad ,$$

$$\lim_{N\to\infty} \underline{q}_N(t)(b - t_l^{(N)}) = (\underline{y}_l - \underline{y}_n)\varphi(t) \qquad , m < l < n \quad .$$

Now by passing to a subsequence if necessary the limit of $\underline{q}_N(t)/||q_N(t)||$ exists for $N \to \infty$. If we denote it by $\underline{q}(t)$ we conclude now the existence of numbers $\beta_l \equiv \beta_l(t) \geq 0$ such that for $a < t < b$

$$\underline{q}(t)\beta_l = \begin{cases} \underline{y}_l - \underline{y}_1 & , \quad 1 \leq l \leq m \quad , \\ \underline{y}_l - \underline{y}_n & , \quad m < l < n \quad . \end{cases}$$

In the cases $m = 1$ or $m = n$ only one of these formulae holds. This proves the theorem.

The result of this theorem can be considered as a concretization of the notion "asymptotically polynomial data of order 3". In particular it shows that such data are (up to rotation) two dimensional. An example of just this type has been given already in [6]. We will show now that it gives actually a counterexample for existence of a solution (1.5).

We consider the four - point problem (1.5) in case $p = 2$ and $\rho = 1$ in (1.6), assuming that the data have the form

(2.18)
$$\underline{y}_2 = y_1 + \alpha_2 \underline{q} \quad , \alpha_2 > 0 \equiv \alpha_1 \quad ,$$

$$\underline{y}_3 = y_4 + \alpha_3 \underline{q} \quad , \alpha_3 > 0 \equiv \alpha_4 \quad .$$

For a fixed knot sequence $\underline{t} = \{t_i\}_{i=1}^4$ of the form (1.1) the solution $\underline{f}^*$ of problem (1.6) for $k = 3, p = 2$ has the form (cf [1])

$$\underline{f}^{*(3)}(x) = \beta N(x|a, t_2, t_3, b) \quad ,$$

where $N(x|a,t_2,t_3,b)$ denotes the L_∞-normalized B - spline of order 3 with respect to the knots a, t_2, t_3, and b_0 . The coefficient β is determined by

$$\beta \int_a^b N(x|a,t_2,t_3,b)^2 dx = \frac{(b-a)}{12}[t_1,\ldots,t_4]\underline{y} \quad ,$$

where $[t_1,\ldots,t_4]\underline{y}$ denotes the divided difference of order 3 with respect to the $\{\underline{y}_i\}_{i=1}^4$. It follows that I_2 has the value

(2.19)
$$(I_2)^2 = \inf_{a<t_2<t_3<b} \left(\frac{(b-a)}{12}|||[t_1,\ldots,t_4]\underline{y}|||\right)^2 / \int_a^b N(x|a,t_2,t_3,b)^2 dx$$

Here $\|\ \ \|$ denotes the Eucledean norm. By (2.18) we compute

$$(2.20)\quad (b-a)[t_1,\ldots,t_4]\underline{y} = \|\underline{q}[\frac{-\alpha_3}{(b-t_3)(b-t_2)} + \frac{\alpha_2}{(t_3-a)(t_2-a)}] - \frac{\underline{y}_3-\underline{y}_2}{t_3-t_2}(\frac{1}{b-t_2}+\frac{1}{t_3-a})\| \quad .$$

Now suppose that the infimum in (2.19) is attained for some knot sequence $a < t_2^* < t_3^* < b$. If we denote by $N^*(x)$ the corresponding B - spline this yields

$$(2.21)\qquad 144(I_2)^2 = \frac{1}{(t_3^*-t_2^*)^2}(\frac{1}{b-t_2^*}+\frac{1}{t_3^*-a})^2\|\rho\underline{q} - [\underline{y}_3-\underline{y}_2]\|^2 / \int_a^b N^*(x)^2dx \quad ,$$

where ρ is a certain number.

Then we consider knot sequences $\{t_2^{(N)}, t_3^{(N)}\}$ with $\lim_{N\to\infty} t_2^{(N)} = a$ and $t_3^{(N)}$ determined by

$$(2.22)\qquad \frac{\alpha_3}{(b-t_2^{(N)})(b-t_3^{(N)})} := \frac{\alpha_2}{(t_2^{(N)}-a)(b-a)} + \frac{\alpha_3-2\rho}{(b-a)^2} \quad .$$

This implies that $t_3^{(N)}$ tends from below to b for any value of ρ. Hence $t_3^{(N)}$ is feasible knot for N sufficiently large. It follows that $(t_1^{(N)} = a, t_4^{(N)} = b)$

$$I_2^2 \le \lim_{N\to\infty} \|\frac{b-a}{12}[t_1^{(N)},\ldots,t_4^{(N)}]\underline{y}\|^2 / \int_a^b N_N(x)^2dx$$

where $N_N(x)$ is the B-Spline with respect to $a, t_2^{(N)}, t_3^{(N)}$ and b. Next some calculation shows that $t_3^{(N)}$ has been chosen such that

$$\lim_{N\to\infty}[\frac{\alpha_2}{(t_3^{(N)}-a)(t_2^{(N)}-a)} - \frac{\alpha_3}{(b-t_3^{(N)})(b-t_2^{(N)})}] = \frac{2\rho}{(b-a)^2}$$

holds. Using this in (2.20) and observing $\lim_{N\to\infty} N_N(x) = N(x|a,a,b,b)$ we arrive at

$$(2.23)\qquad 144I_2^2 \le \frac{4}{(b-a)^4}\|\rho\underline{q} - [\underline{y}_3-\underline{y}_2]\|^2 / \int_a^b N(x|a,a,b,b)^2dx \quad .$$

Then we need the inequality

$$(2.24)\qquad (t_3-t_2)^2\int N(x|a,t_2,t_3,b)^2dx \le (b-a)^2\int N(x|a,a,b,b)^2dx \quad .$$

In order to prove this we use the recurrence relation for B-splines. This yields

$$\int N(x|a,t_2,t_3,b)^2dx = \int[(x-a)N(x|a,t_2,t_3)/(t_3-a) + (b-x)N(x|t_2,t_3,b)/(b-t_2)]^2dx$$

$$= \int_a^{t_2}[(x-a)^2/(t_3-a)(t_2-a)]^2dx + \int_{t_2}^b[(b-x)^2/(b-t_3)(b-t_2)]^2dx$$

$$+\int_{t_2}^{t_3}[(x-a)(t_3-x)/(t_3-a)(t_3-t_2)+(b-x)(x-t_2)/(b-t_2)(t_3-t_2)]^2dx \quad .$$

Then we estimate the last integral from above by the inequalities

$$(t_3-x)/(t_3-a) \le (b-x)/(b-a) \qquad ,x \ge a \quad ,$$

$$(x-t_2)/(b-t_2) \le (x-a)/(b-a) \qquad ,x \le b \quad .$$

For the first and second integral we use the inequalities

$$(x-a)/(t_3-a)(t_2-a) \le (b-x)/(b-a)(t_3-t_2) \qquad ,x \in [a,t_2] \quad ,$$

$$(b-x)/(b-t_3)(b-t_2) \le (x-a)/(b-a)(t_3-t_2) \qquad ,x \in [t_3,b] \quad ,$$

which follow from the two previous inequalities. Furthermore one observes that

$$N(x|a,a,b,b) = 4(x-a)(b-x)/(b-a)^2 \qquad ,x \in [a,b] \quad ,$$

and the desired inequality (2.24) easily follows.

Now we insert (2.24) in (2.21) and the resulting inequality into (2.23). This implies after cancellation of common factors (assuming that $\underline{q}$ and $\underline{y}_4 - \underline{y}_1$ are linearly independent) that

$$(\frac{1}{b-t_2^*}+\frac{1}{t_3^*-a})^2 \overset{!}{\le} \frac{4}{(b-a)^2}$$

must hold. But this is a contradiction unless $t_2^* = a, t_3^* = b$. Hence we conclude that problem (1.5) has no solution in the case of data of the form (2.18), where $\underline{q}$ and $\underline{y}_4 - \underline{y}_1$ are linearly independent.

Geometrically this phenomenon means that for the knot sequence $\{\underline{t}^{(N)}\}$ of the form (2.22) the corresponding spline curves $\underline{f}_N$ (of degree 5) have arc - lengths tending to infinity for $N \to \infty$. This makes it possible to interpolate the data (2.18) while the values $\int_a^b ||f_N'''(t)||^2 dt$ are decreasing. A similar observation has been made in the problem of minimizing curvature with free arc length (cf. [3]), with non-existence of a solution as a consequence. This should be expected too if $k > 3$ in (1.5), (1.6) for $p = 2, \rho = 1$. In this respect it would be interesting to see how "asymptotically data of order k " do look like for such k , i.e. to prove a theorem like Theorem 3.

4. **Characterization.** It is well known (cf. de Boor [1]) that for a fixed knot sequence $\underline{t}$ of form (1.1) the solution f^* of the scalar problem

$$\inf\{(\int_a^b |f^{(k)}(t)|^p dt))^{1/p} : f \in L_p^k(a,b), f(t_i) = y_i \quad \text{for} \quad 1 \le i \le n\} \tag{4.1}$$

has for $1 < p < \infty$ the representation

$$f^{*(k)}(x) = |\varphi(x)|^{p'-1} sgn\varphi(x) \qquad ,1/p + 1/p' = 1 \quad , \tag{4.2}$$

where

$$\varphi(x) = \sum_{j=1}^{n-k} c_j M_{j,k}(x) \quad , \tag{4.3}$$

The $M_{j,k}(x)$ are the L_1 normalized B - splines defined via

$$M_{j,k}(x) = k[t_j, \ldots, t_{j+k}](\cdot - x)_+^{k-1}$$

and the coefficients c_j are determined via the non-linear equations

$$\int_a^b f^{*(k)}(x) M_{i,k}(x) dx = k![t_i, \ldots, t_{i+k}]y \qquad , 1 \leq i \leq n-k \quad . \tag{4.4}$$

The solution of these equations is unique for $1 < p < \infty$ since problem (4.1) has a unique solution in this case by general approximation theoretic reasons (see e.g. Jerome - Fisher [2]). In case $p = \infty$ the representation (4.2) makes still formally sense but determines $f^{*(k)}$ only outside the zero set of $\varphi(x)$ (see [1]). As a result the solution is not unique if this set has positive measure.

In view of our assumptions on the function $\emptyset$ in (1.4 ii) we can apply these results immediately to the solution of the inner infimum in (1.5). It is thus a generalized spline curve in the sense that its components are functions of the form (4.2). In order to obtain a characterization for the optimal sequence $\underline{t}$ in (1.5) we have to be more specific about $\emptyset$. Thus we assume that it has the form (1.6). We then proceed by combining the "duality approach" described in [1] with variational techniques and extend the characterizations previously given [4], [5] and [6].

This duality approach consists in writing problem (1.6), (1.7) equivalently as

$$I_p = \inf_{\underline{t}} \sum_{l=1}^{d} \inf_{f_l \in L_p^k(a,b)} \sup_{r_l \in L_{p'}(a,b)} \{ | \int_a^b f_l^{(k)} r_l |^{p\rho} : \int_a^b |r_l|^{p'} = 1, y_i^{(l)} = f_l(t_i), 1 \leq i \leq n \} \quad . \tag{4.5}$$

Here we consider $1 < p \leq \infty$ or $1 \leq p' < \infty$. For the variational approach we introduce the Lagrangian - function

$$\emptyset(\underline{t}, \underline{f}, \underline{r}) = \sum_{l=1}^{d} \{ | \int_a^b f_l^{(k)} r_l |^{p\rho} + \mu_l [\int_a^b |r_l|^{p'} - 1] \} + \sum_{i=1}^{n} (\underline{\lambda}_i, \underline{f}(t_i) - \underline{y}_i)$$

with Lagrangian parameters $\mu_l \in I\!R, \underline{\lambda}_i \in I\!R^d$. We assume now that a feasible stationary point $\underline{t}^*, \underline{f}^*, \underline{r}^*$ exists and consider first the cases $1 < p < \infty$. Then the variation of f_l in direction h_l (in the sense of Gateaux) yields

$$0 = \frac{\partial \emptyset(h_l)}{\partial f_l} = p\rho | \int_a^b f_l^{*(k)} r_l^* |^{p\rho - 1} (sgn \int_a^b f_l^{*(k)} r_l^*) \int_a^b h_l^{(k)} r_l^* + \sum_{i=1}^{n} \lambda_i^{(l)} h_l(t_i) \quad .$$

If we consider now arbitrary $g \in L_p(a,b)$ and determine h_l via $h_l^{(k)} = g, h_l^{(\nu)}(a) = 0$ for $0 \leq \nu < k$, we have by Taylor's formula

$$h_l(t_i) = \int_a^b G_i(\tau) h_l^{(k)}(\tau) d\tau \qquad , G_i(\tau) \equiv (t_i - \tau)_+^{k-1}/(k-1)! \quad .$$

Inserting this in the above conditions we conclude that for $1 \leq l \leq d$

$$\sigma_l r_l^*(x) = -\sum_{i=1}^{n} \lambda_i^{(l)} G_i(x) \qquad , \sigma_l \equiv p\rho |\int_a^b f_l^{*(k)} r_l^{*} |^{p\rho-1} sgn \int_a^b f_l^{*(k)} r_l^* \quad . \tag{4.6}$$

Next we consider the variation of $\underline{\tau}^*$ in the (feasible) direction $\underline{v} \in L_p(a,b)$. This yields

$$0 = \frac{\partial \emptyset}{\partial r_l}(v_l) = \sigma_l \int_a^b f_l^{*(k)} v_l + \mu_l \int_a^b (|r_l^*|^{p'-1} sgn r_l^*) v_l \quad . \tag{4.7}$$

From this we derive

$$\sigma_l f_l^{*(k)}(x) = -p' \mu_l |r_l^*(x)|^{p'-1} sgn r_l^*(x) \quad . \tag{4.8}$$

Finally we consider the variations of the knots t_j^* giving

$$0 = \frac{\partial \emptyset}{\partial t_j} = (\underline{y}_j, \underline{f}^{*'}(t_j)) \equiv \sum_{l=1}^{d} \lambda_j^{(l)} f_l^{*'}(t_j) \qquad , 2 \leq j \leq n-1 \quad .$$

This condition can be brought into a more intuitive form by observing that (4.6) implies easily that

$$\sigma_l [r_l^{*(k-1)}(t_j+) - r_l^{*(k-1)}(t_j-)] = -\lambda_j^{(l)} \qquad , 2 \leq j \leq n \quad .$$

Since we may asume $\sigma_l \neq 0$ in (4.5) we obtain

$$0 = \sum_{l=1}^{d} \sigma_l [r_l^{*(k-1)}(t_j+) - r_l^{*(k-1)}(t_j-)] f_l^{*'}(t_j) \qquad , 2 \leq j \leq n-1 \quad . \tag{4.9}$$

The solution $\underline{f}^*, \underline{t}^*$ can now be computed by inserting (4.6) into (4.8), where the unknowns $\{\mu_l\}_{l=1}^d$ and $\{t_j\}_{j=2}^{n-1}$ can be computed by the constraints in (4.5) and (4.9) . We know from the results mentioned above for fixed $\underline{t}$ that the first system of (for $p \neq 2$ non-linear) equations has a unique solution . However for the system (4.9) there may exist several solutions. Below we will discuss some cases where unicity holds.

In the case $p = \infty$ the situation is a bit more complicated. Here we have to replace both p and p' by 1 in the bracket term of (4.5). Then the argument leading to (4.6) remains still true whereas the variation of $\underline{\tau}^*$ has to be done in a more subtle way since its Gateaux derivative does not exist anymore in the usual sense. Equation (4.7) has to be replaced by

$$0 = \sigma_l \int_a^b f_l^{*(k-1)} v_l + \mu_l [\int_{E_r} v_l sgn r_l + \int_{[a,b]/E_r} v_l] \quad . \tag{4.7a}$$

Here E_r denotes the set $\{x \in [a,b] : r_l(x) \neq 0\}$. Hence equation (4.8) holds in this case only on the set E_r. Therefore $f_l^{*(k)}$ is not uniquely determined (for fixed $\underline{t}$) if the zero set of r_l^* has positive measure. This is in agreement to what has been said above about the representation (4.2). But no matter how the form of $f_l^{*(k)}$ may be the general existence theory of section 2 guarentees that, at

least if the data are not asynptotically polynomial of order k, there exists always a solution pair f^*, t^* for which equations (4.6), (4.8), (4.9) and constraints in (4.5) are satisfied.

In the scalar case $d = 1$ the equations (4.9) have a particular simple meaning: either τ^* does not have knot at t_j, i.e. the jump of its $(k-1)$ th derivative vanishes, or f^* has an extremum there. This result was derived previously by Marin [4] for $p = 2 = k$ and by Pinkus [5] for $1 \leq p \leq \infty$, any k , by different arguments. In the latter paper uniqueness of the solution is shown for $p = \infty$ and general k , if the data have "alternating structure".We take the opportunity here to show that Marin's argument can extended to all $p \in (1, \infty]$, in particular we give an explit formula for the optimal knot sequence $\underline{t}^*$.

THEOREM 4: In the case $d = 1, k = 2$ there exists a unique solution of problem (1.5) for $1 \leq p < \infty$. If the data are alternating, i.e. have the property $(y_{i+1} - y_i)(y_i - y_{i-1}) < 0$ for $2 \leq i \leq n-1$, the optimal knots t_i^* are computed by

$$t_{i+1}^* - t_i^* := h_i^* \quad , \quad h_i^*/h_{i+1}^* = \epsilon_i |y_{i+1} - y_i|^{1/2} / \epsilon_{i+1} |y_{i+2} - y_{i+1}|^{1/2}$$

with

$$\epsilon_i = \sqrt{2} \quad \text{for} \quad 2 \leq i \leq n-2 \quad \text{and} \quad \epsilon_1 = \epsilon_{n-1} = 1 \quad .$$

Remark: The exact value of the h_i^*'s is easily computed via the constrained $\sum_{i=1}^{n-1} h_i^* = 1$. Note further that the h_i^* are independent of p.

Proof: We consider first the case of alternating data. By (4.2), (4.3) any solution pair $\underline{t}, \underline{s}(x)$ has the form $(1/p + 1/p' = 1)$

$$s''(x) = |\varphi(x)|^{p'-1} sgn\varphi(x), \quad \varphi(x) = \sum_{j=1}^{n-2} c_j N_{j,2}(x) \quad . \tag{4.10}$$

The $N_{j,2}(x)$ are here L_∞ normalized B-Splines of degree 1 so that $\varphi(x)$ is piecewise linear and $\varphi(t_{j+1}) = c_j$ for $1 \leq j \leq n-2$. In view of the interpolating property of $s(x)$ its derivative changes its sign at least $(n-2)$ times in the interior of (a, b). Hence $s''(x)$ has at least $n-1$ zero in $[a, b]$ including its boundary conditions. Then, in view of (4.10), $\varphi(x)$ has exactly one zero ξ_i in each segment $(t_i, t_{i+1}), 2 \leq i \leq n-2$ and the coefficients c_j must alternate in sign.

Now $\varphi(x)$ has for $x \in (t_i, t_{i+1}), 1 \leq i \leq n-1$, the representation $(c_o \equiv c_{n-1} \equiv 0)$

$$\varphi(x) = \varphi(t_i) + [\varphi(t_{i+1}) - \varphi(t_i)](x - t_i)/h_i = c_{i-1} + (c_i - c_{i-1})(x - t_i)/h_i$$

By integration $s'(x)$ has the representation

$$s'(x) = \frac{h_i |\varphi(x)|^{p'}}{p'(c_i - c_{i-1})} + \alpha_i \qquad , x \in (t_i, t_{i+1}) \quad . \tag{4.11}$$

Now we observe that the sign of $\varphi'(t_j+) - \varphi'(t_j) = (c_j - c_{j-1})/h_j - (c_{j-1} - c_{j-2})/h_{j-1}$ does not vanish since the c_j alternate in sign. Then (4.9) implies by using (4.11) that

$$\alpha_j + \frac{h_j |c_j|^{p'}}{p'(c_j - c_{j-1})} = s'(t_{j+1}-) = 0 = s'(t_j+) = \frac{h_j |c_{j-1}|^{p'}}{p'(c_j - c_{j-1})} + \alpha_j$$

Therefore we conclude that $c_j = \gamma sgn\varphi(t_{j+1})$ for $1 \le j \le n-2$ and some $\gamma > 0, i.e. \varphi(x)$ and $s''(x)$ are equi - oscillating. With this information in (4.11) the conditions $\varphi'(t_j \pm) = 0, 2 \le j \le n-1$ determine the α_i up to γ , namely

$$\alpha_i = \begin{cases} (sgn\varphi(t_i))h_i\gamma^{p'-1}/2p' & , \quad 2 \le i \le n-2 \\ (-sgn\varphi(t_2))h_1\gamma^{p'-1}/p' & , \quad i = 1 \\ (sgn\varphi(t_{n-1}))h_{n-1}\gamma^{p'-1}/p' & , \quad i = n-1 \end{cases} .$$

By a further integration of (4.11) we can determine the h_i up to γ. For $2 \le i \le n-2$ we have

$$y_{i+1} - y_i = s(t_{i+1}) - s(t_i) = \frac{h_i^2(sgn\varphi(t_{i+1}))}{(p'+1)p'|c_i - c_{i-1}|^2}(|\varphi(t_{i+1})|^{p'+1} + |\varphi(t_i)|^{p'+1}) + \alpha_i h_i$$

$$= h_i^2(sgn\varphi(t_i))\gamma^{p'-1}[1 - 1/(p'+1)]/2p' = (sgn\varphi(t_i))h_i^2\gamma^{p'-1}/(2p'+2)$$

In the cases $i = 1$ and $i = n-1$ a similar computation gives

$$|y_2 - y_1| = h_1^2\gamma^{p'-1}/(p'+1) \qquad , |y_n - y_{n-1}| = h_{n-1}^2\gamma^{p'-1}/(p'+1) \quad .$$

From this the formulae of the theorem follow directly.

Of course the preceding demonstrates uniqueness in the case of alternating data. In the general case we consider at first the reduced data set consisting of the turning points of the data. This problem has a unique solution which is the cubic spline interpolating these turning points and with knots exactly there. The remaining nodes for interpolation are uniquely determined since this spline is strictly oscillating between its knots. Any other solution must be a cubic spline too. If it would have more knots than the turning points it would have at each such knot a strict extremum. The data structure would then imply that there is still another extremum between the knots which yields a contradiction. ∎

5. Final remarks. It is interesting to consider the case $k = 1$ of problem (1.5), (1.6) which can be solved easily for $1 < p < \infty$. Relations (4.6), (4.8) show that $\underline{f}^{*'}$ is a piecewise constant curve since so are the functions $G_i(\tau)$ in this case. Hence $\underline{f}^*$ must be the polygon interpolating the data. In particular we have

$$\underline{f}^{*'}|_{(t_i,t_{i+1})} = \underline{c}_i \qquad , \underline{y}_{i+1} - \underline{y}_i = c_i h_i \qquad , 1 \le i \le n-1 \quad .$$

With the help of this we can compute the functional in (1.5), (1.6) to be minimized with respect to $\underline{t}$. We do this only for the choice $\rho = 1$ in (1.7), the result for general ρ is essentially the same. This leads to the problem

$$\inf\{\sum_{l=1}^{d}\sum_{i=1}^{n-1} h_i^{1-p}|y_{i+1}^{(l)} - y_i^{(l)}|^p : \sum_{i=1}^{n-1} h_i = 1\} \quad .$$

With the help of a Lagrangian - multiplier it is then easily verified that the infimum is attained for

$$0 = \sum_{l=1}^{d}(1-p)|y_{i+1}^{(l)} - y_i^{(l)}|^p h_i^{-p} + \lambda \qquad 1 \le i \le n-1 \quad .$$

This is equivalent to the condition

$$h_i/h_{i+1} = ||\underline{y}_{i+1} - y_i||_p / ||\underline{y}_{i+2} - \underline{y}_{i+1}||_p \qquad , 1 \le i \le n-2$$

where $||\ \ ||_p$ enotes the l_p -norm for $\mathbb{R}^d$. But this is just the rule for the well known chord-length parametrization which is recognized therefore as being optimal with respect to a variational principle as well.

It is possible to consider further variational problems concerning best parametrization. One could first think of the case $p = 1$ in problem (1.5). However the infimum for fixed $\underline{t}$ may not have a solution in this case. Therefore one has to change the problem a little bit and replace the L_1 - norm of the k - th derivative by the BV - norm of the $(k-1)$ the derivative (cf. [2], [5]). Pinkus [5] has studied problem (1.5) in this form for the scalar case.

Another possible generalization of problem (1.5) would be to use a (regular) linear differential - operator of $k-th$ order instead of the $k-th$ derivative. The existence theory of section 2 carries over to this case without much difference. The characterization theory would lead to so - called L - spline - curves as solutions (cf. [2]). Finally we mention the variational problem

$$\inf_{\underline{t}} \inf\{(\int_a^b ||\underline{f}^{(k)}(t)||^p dt)^{1/p} : \underline{f} \in (L_p(a,b))^d, \underline{f}(t_i) = \underline{y}_i, 1 \le i \le n\} \quad ,$$

where $||\ \ ||$ denotes the Euclidean Norm and $1 < p < \infty$ (with obvious modification for $p = \infty$). Because of this choice it seems to be a natural problem but does not fit into the previous framework unless $p = 2$.

References

[1] C. de Boor, Splines as linear combinations of B - splines. A survey. In "Approximation Theor II" (G.G.Lorentz - C.K.Chui - L.L.Schumaker eds), Academic Press, New York 1976.

[2] S.Fisher - J.W.Jerome, Minimum norm extremals in function spaces, Lecture Notes in Math. 479, Springer, New York 1975.

[3] J.W.Jerome, Smooth interpolating curves of prescribed length and minimum curvature, Proc. Amer. Math. Soc. 51 (1975), p. 62 - 66.

[4] S.Marin, An approach to data parametrization in parametric cubic spline - interpolation problems. J. Approx. Theory 41 (1984) , 64 - 86

[5] A.Pinkus, On smoothest interplation, Preprint 1986

[6] K. Scherer - P.W. Smith: Existence of best parametric interpolation by curves. To appear in SIAM J.Math. Anal.

[7] H.J. Töpfer: Models for smooth curve fitting. In: Numer. Methoden der Approximationstheorie 6 (L. Collaty ed.), ISNM 59. Birkhäuser, Basel 1981

SOME RESULTS ON INTERPOLATION IN TWO VARIABLES

V.RAMIREZ, J.LORENTE & F.J.MUÑOZ
Departamento de Matemática Aplicada.
Facultad de Ciencias
18071 Granada
Spain

ABSTRACT: Interpolation systems, as a technique for solving interpolation problems, are used in this paper for solving interpolation problems in R^2 by polynomial spaces which contain as particular cases $\Pi_n(x,y) = \langle x^i y^j \rangle$ with $0 \leq i+j \leq n$, and $Q_{n,m}(x,y) = \langle x^i y^j \rangle$, $0 \leq i \leq n$; $0 \leq j \leq m$.

1. Introduction

In [1,2] M.Gasca, J.I.Maeztu and V.Ramirez introduced an interpolation technique that they called "Interpolation Systems".

In this paper, by using interpolation systems, we prove the unisolvency of certain interpolation problems from a different point of view. So, we will start with a data L_i, $i=1,\ldots,n$ which are unisolvent in an n-dimensional vector space V, and then we will try to find other n different data which also are unisolvent in the same vector space V. We shall start with some easy problems, for example the interpolation (in $\Pi_n(x,y)$) of lagrangian data on a simplex or the interpolation (in $Q_{n,m}(x,y)$) with the data on a rectangular grid, and find other problems whose data could be of lagrangian type, Hermite type, etc...

2. Definitions, notation and previous results.

First, we introduce some notations that we will need, in a similar way as we did in [4,1,3].

Let I be a set of indices as follows:

$$I = \{ (0,0),\ldots,(0,m(0)),(1,0),\ldots,(n,m(n)) \} .$$

We define an interpolation system in R^2 as a set S given by

$$S = \{ (f_i, f_{ij}),\ (i,j) \in I \} ,$$

where f_i and f_{ij} are functions of the following form:

• $f_i = a_i x + b_i y + c_i$, $i=0,\ldots,n$; $f_{ij} = a_{ij} x + b_{ij} y + c_{ij}$, $(i,j) \in I$

with $a_i b_{ij} \neq a_{ij} b_i$, for every $(i,j) \in I$.

Some other notations that we need are the following:

For a fixed index $(i,j) \in I$:

• u_{ij} is the unique point in R^2 such that $f_i(u_{ij}) = f_{ij}(u_{ij}) = 0$.

• $\rho_i = (-b_i, a_i)$; $\rho_{ij} = (-b_{ij}, a_{ij})$, $(i,j) \in I$.

• t is the number of functions from

$$(f_0, \ldots, f_{i-1}, f_{i0}, \ldots, f_{ij-1}), \qquad (1)$$

vanishing at u_{ij} and such that their graph coincides with the graph of the function f_i.

• s is the number of functions from (1) vanishing in u_{ij} and whose graph do not coincide with the graph of f_i .

• ϕ_{ij}, $(i,j) \in I$, is the function given by:

$$\phi_{ij}(x,y) = f_0 \cdots f_{i-1} f_{i,0} \cdots f_{i,j-1} .$$

E(S) will be the space generated by the functions ϕ_{ij} . On the other hand,

$$L_{ij}(f) = \frac{\delta^{s+t}}{\delta \rho_{ij}^{t} \, \delta \rho_i^{s}} f \Big|_{u_{ij}} , \quad (i,j) \in I.$$

The set of functionals L_{ij} operates on the space of polynomials in two variables. It will be denoted by $\mathcal{L}(S)$ and we will call it the Associated Data with the interpolation system. Similarly, E(S) is the interpolation space associated with S.

• Now, we have the following result:

$$\det(L_{ij}(\phi_{hk}))_{(i,j),(h,k) \in I} \neq 0$$

Moreover, if the functions ϕ_{hk} and the linear forms L_{ij} are lexicographically ordered, then the determinant is lower triangular.

• On the other hand, it is proved that $E(S)=\Pi_n(x,y)$ if and only if $m(i)=n-i$, $i=0,..,n$. When a system satisfies this property it is said to be a system of order n.

3. Lagrangian-stepped interpolation systems

We will call S a lagrangian-stepped interpolation system (l.s.i.s.) if

$$m(0) \geq m(1) \geq \ldots \geq m(n) \text{ and}$$

$$f_i(x,y) = y - a_i;\ f_{ij}(x,y) = x - b_j\ , \quad (i,j) \in I$$

assuming, without any loss of generality, that

$$a_0 < a_1 < \ldots < a_n\ ;\ \ b_0 < \ldots < b_{m(0)}.$$

If $e(0)$, $e(1)$,.., $e(r)$, are r+1 non-negative integer numbers, we denote

$$V(e(0),\ldots,e(r))=\langle 1,x,..,x^{e(0)},y,yx,\ldots,yx^{e(1)},\ldots\ldots,y^r x^{e(r)}\rangle\ .$$

Then $V(n,n-1,\ldots,1,0) \equiv \Pi_n(x,y)$; $\quad V(n,\overset{m+1)}{\ldots\ldots},n) \equiv Q_{n,m}(x,y)$

are two of the most usual spaces in the interpolation of bivariate functions.

The main goal in this work is centered in looking for interpolation problems which are unisolvent in a space as those defined before.

It is easy to prove the following result:

Theorem 1. If S is a l.s.i.s. then the interpolation space associated with S, denoted by E(S), is given by $E(S)=V(m(0),\ldots,m(n))$.

Now, we want to find other interpolation systems which are not stepped but they are equivalent to a stepped one in the sense that they have the same associated interpolation space.

Stepped subsystem. Let S_0 be a l.s.i.s. and let S' be a subset of S_0 obtained by taking out from S_0 either the function:

f_0, (and therefore taking also out the functions $f_{00}, f_{01}, \cdots$ $\ldots\ldots$, $f_{0m(0)}$, and the common zero of each one of these functions with f_0).

or the function

$f_{00} = f_{10} = .. = f_{n0}$, (and therefore taking also out those funtions f_i such that m(i) = 0)

In this case, we will call S' a subsystem of S_0 and we will write S' c S_0.

If S'=Ø, it will be denoted by S(Ø). Otherwise, it will be denoted by S_1, and then S_1 is a new l.s.i.s. .

Properties.

Any l.s.i.s. having more than one associated datum admit two different subsystems and at least one of them is non-empty.

On the other hand, if S_0 is a system of order n, then any subsystem of S_0 is of order n-1.

If S_0 is a subsystem of S_1 and $S_1 \neq \emptyset$, then we have that

$$\mathcal{L}(S_1) \subset \mathcal{L}(S_0) \text{ and } E(S_1) \subset E(S_0).$$

Sequence of subsystems of a stepped system.

Given a stepped system S_0, we will call a sequence of subsystems of S_0 to any set of systems $(S_0, S_1, \ldots, S_k, S_{k+1})$ such that:

$$S(\emptyset)=S_{k+1} \subset S_k \subset \ldots \subset S_1 \subset S_0$$

(all the inclusions are strict).

Decomposition of a l.s.i.s.

Given a sequence of subsystems associated to a l.s.i.s. S_0, we will call a decomposition of S_0 to the set

$$((l_i(x,y), h(i)) , i=0,1,..,k)$$

where $l_i(x,y)$ is the function taken out from S_i to obtain S_{i+1} as a subsystem of S_i, and $h(i)+1 = card(I_i) - card(I_{i+1})$.

4. Stepped interpolation systems

Let SE be an interpolation system given by

$$SE = \{ (r_i, r_{ij}),\ i=0,\ldots,k;\ j=0,\ldots,h(i) \}$$

We will say that SE is a stepped interpolation system (of dimension $(m(0), \ldots, m(n))$, if there exists a l.s.i.s. (with the same indices) and a decomposition of it such that, if S_i is not a system of order $h(i)$, then the following conditons hold:

a) $r_i(x,y) - l_i(x,y) = \text{constant}$

b) The graphs of r_i and r_{ij} are orthogonal, $j=0,\ldots,h(i)$

The stepped interpolation system SE is also called an interpolation system equivalent to S_0.

We have the following result:

Theorem 2. If SE is an interpolation system equivalent to a l.s.i.s. S_0 of indeces $(m(0),\ldots,m(n))$, then $E(SE)\equiv V(m(0),\ldots,m(n))$.

EXAMPLES:

Next we are going to show several examples. The following notations will be used.

• Lagrangian data → directional derivative ◯ second derivatives

In the space $V(3,3,1,1) = \langle 1, x, x^2, x^3, y, yx, yx^2, yx^3, y^2, y^2x, y^3, y^3x \rangle$ the problem of interpolation with lagrangian data over a rectangular grid is unisolvent.

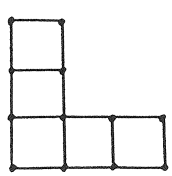

Let us see that, in the same space, the problem of interpolation with lagrangian data and first order derivatives over the vertices of a square is also unisolvent. This is the problem

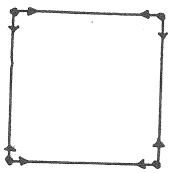

The descomposition of first system l.s.i.s. and the construction of the second one (which is equivalent to the first l.s.i.s.) is, given step by step,

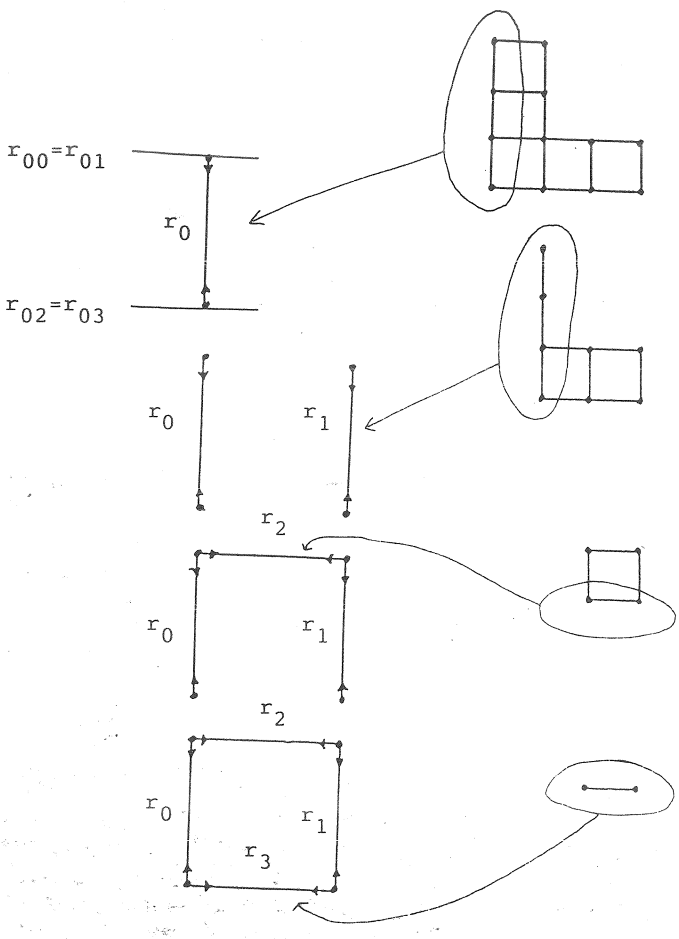

Here, $k=3$, $h(0)=3$, $h(1)=3$, $h(2)=1$, $h(3)=1$.

In the space $V(2,1)=\langle 1, x, x^2, y, xy\rangle$

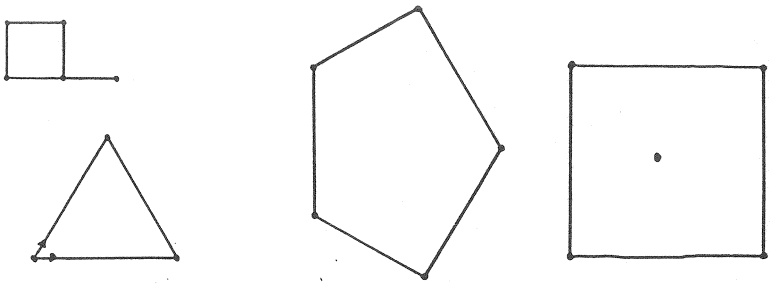

In the space $V(3,3)\equiv Q_{3,1}(x,y)=\langle 1, x, x^2, x^3, y, xy, x^2y, x^3y\rangle$

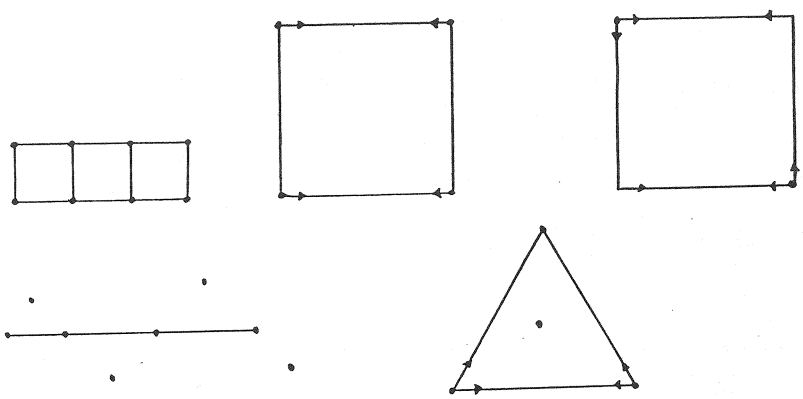

In the space $V(2,2,2)\equiv Q_{2,2}(x,y)=\langle 1, x, x^2, y, xy, x^2y, y^2, xy^2, x^2y^2\rangle$

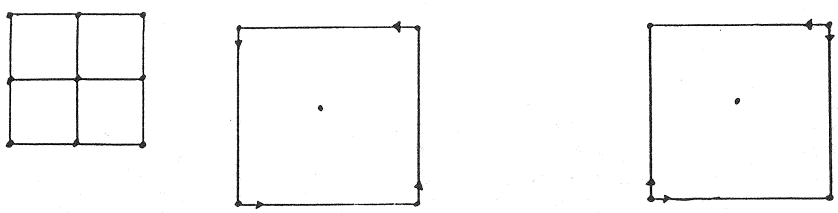

In the space $V(3,2,1,0)=W_3(x,y)$

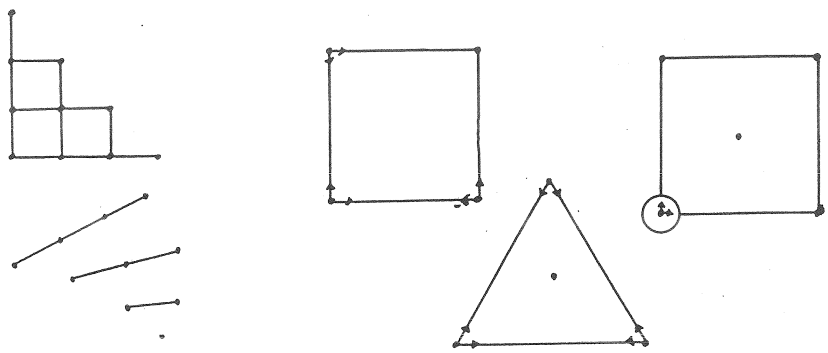

In the space $V(3,2,2,1)=\langle 1,x,x^2,x^3,y,xy,x^2y,y^2,y^2x,y^2x^2,y^3,y^3x\rangle$

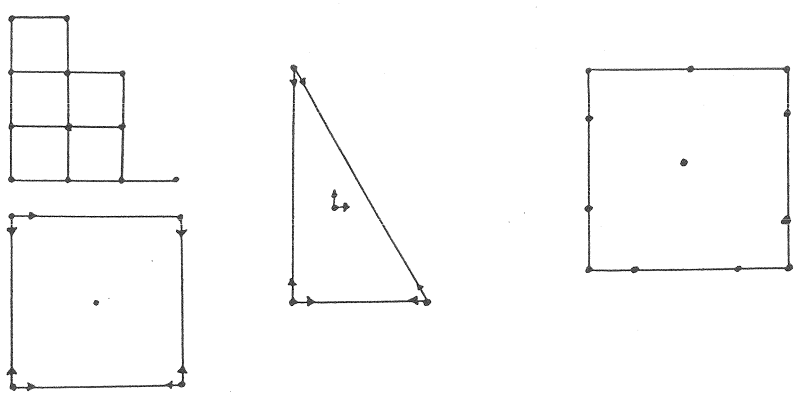

In the space $V(3,3,1,1)=\langle 1,x,x^2,x^3,y,yx,yx^2,yx^3,y^2,y^2x,y^3,y^3x\rangle$

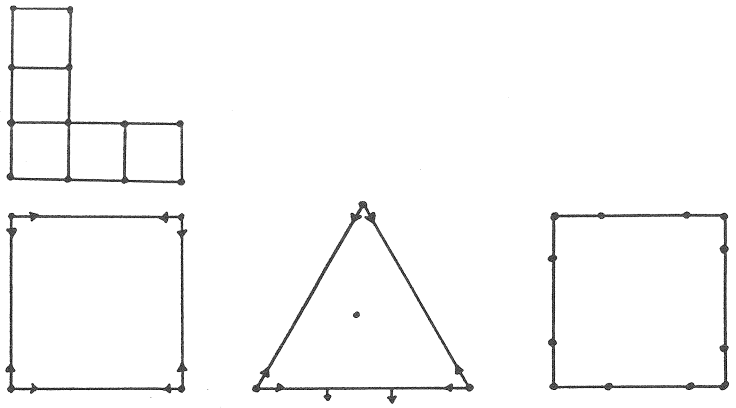

5. References

(1) Gasca, M. and Maeztu, J. I. (1982) 'On Lagrange and Hermite interpolation in R^k' Num. Math. 39, pp.1-14.

(2) Gasca, M. and Ramírez, V. (1984) 'Interpolation Systems in R^k'. Journal of Approximation Theory 42, pp.36-52.

(3) Lorente, J. and Ramírez, V. (1987) 'On Interpolation System and H-Reducible Interpolation Problems'. In "Topics in Multivariate Approximation" Edited by C.K.Chui, L.Schumaker & F.I.Utreras. pp.153-164 Academic Press.

(4) Maeztu, J. I. (1982) 'Divided differences associated with reversible systems in R^2, SIAM Num. Anal. 19, pp.1032-1040.

(5) Ramírez, V. (1980) 'Interpolación de Hermite en varias variables' doctoral dissertation, University of Granada, Spain.

(6) Ramírez, V. (1985) 'Problemes $P_{p,q,r}$- Unisolvents' publ.ANO nº 149. Université de Lille I, U.E.R. I.E.E.A. France.

Algunos aspectos de la triangulación de Delaunay en el Plano

Leonardo Traversoni Domínguez

Universidad Autónoma Metropolitana
División de Ciencias Básicas e Ingeniería
Departamento de Ingeniería de Procesos e Hidráulica
Ingeniería Hidrológica
Av. Michoacán y la Purísima
Col. Vicentina Apartado Postal 55-534
Código Postal 09340
México, D.F.
México.

Resumen

Se propone el uso de los círculos de cobertura para la construcción de triangulaciones de Delaunay.

1 Idea General y algunos hechos notables

Dado un conjunto de puntos en el plano no superpuestos, existen algunas interesantes figuras asociadas al mismo cualesquiera que este sea:

1.1 Polígonos de Thiessen o teselización de Voronoi

Son el lugar geométrico de los puntos del plano cuya distancia a uno dado del conjunto original es menor que a cualquier otro del citado conjunto.

Estos conjuntos de puntos son abiertos y cubren todo el plano.

Existen sin embargo, algunos puntos que no entran en la clasificación anterior y son aquellos que son equidistantes de dos puntos del conjunto (los de la mediatriz del segmento que determinan).

Otros, equidistan de tres o más puntos del conjunto y son los que se obtienen al cortar las mediatrices antes citadas.

Las mediatrices son los lados de los polígonos y los puntos citados al final sus vértices.

1.2 La idea de que los vértices de los polígonos de Thiessen equidistan de tres o más puntos del conjunto original sugiere el concepto de los círculos de cobertura

La circunferencia perímetro de estos círculos está determinada por los puntos equidistantes del vértice del polígono y tienen algunas propiedades interesantes:

En primer lugar no contienen a ningún punto del conjunto (estos están sobre la circunferencia pero no en el interior).

En segundo lugar cubren al polígono totalmente y en general a todo el conjunto de puntos y en particular cubren a su cerradura convexa.

Por último es importante destacar que esta construcción es realmente dual de los polígonos de Thiessen y siempre se puede realizar, no importa lo caprichosa que pueda ser la disposición de los puntos del conjunto original.

1.3 Triángulos de Delaunay

En la mayor parte de la literatura, el respecto se considera exclusivamente el caso de que sólo tres puntos equidisten de cada vértice y ellos forman un triángulo de Delaunay.

Asimismo, estos triángulos son considerados los duales de los polígonos de Thiessen.

Los casos en los que más de tres puntos equidistan de uno de los vértices, son considerados raros, de casi imposible ocurrencia y por lo tanto desechados

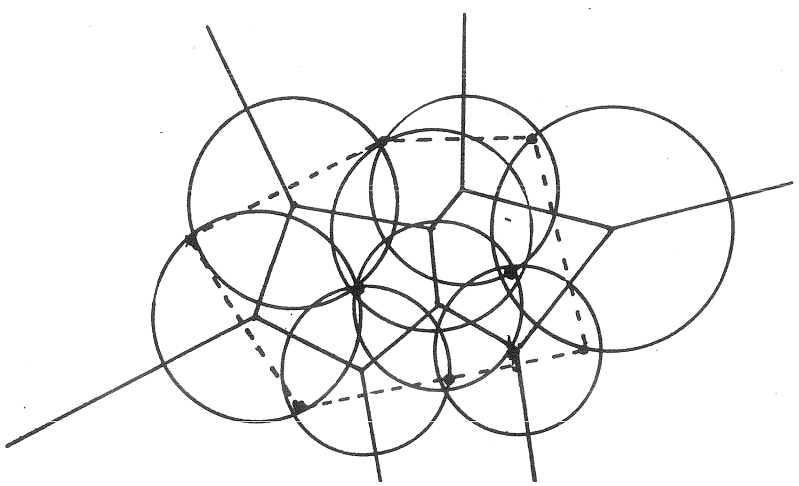

Figura 1: *En el ejemplo se vé cómo los polígonos de Thiessen (líneas contínuas) son cubiertos por los Círculos de Cobertura, (a excepción de los exteriores que no son cerrados). Asimismo, se vé que cubren la cerradura convexa (línea punteada).*

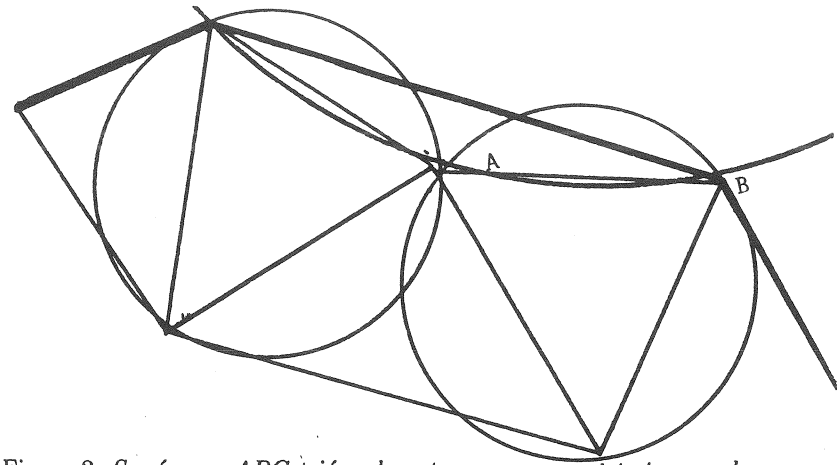

Figura 2: *Supóngase ABC triángulo exterior que completa la cerradura convexa no cubierto por los círculos de cobertura, entonces el círculo que contiene a ABC es también de Cobertura ya que ningún cículo está contenido en él, ya que de estarlo cubriría a ABC.*

de la teoría.

Es curioso destacar que el artículo original de B. Delaunay, escrito en homenaje a Voronoi, no se refiere a esta dualidad, es más se titula "*Las esferas vacías*".

2 Algoritmo de Construcción de Círculos de Cobertura

Los problemas de generar polígonos de Thiessen, Triángulos de Delaunay ó círculos de Cobertura, al igual que el problema de localizar un punto en el plano dividido en polígonos de Thiessen o el de hallar la cerradura convexa de un conjunto de puntos en el plano, son todos problemas relacionados entre si y aún más, en algunos casos son equivalentes. Con cualquiera de ellos resuelto, con pocos pasos se puede construir cualquiera de los otros.

Se ha optado en este caso por construir un algoritmo que genere círculos de cobertura, y no alguna de las otras construcciones.

El tipo de algoritmo elegido es incremental e implica el mismo número de operaciones que otro tipo de algoritmos destinados a construir triángulos de Delaunay como por ejemplo el algoritmo de Watson.

Se presenta a continuación el caso general en el *ene-ésimo* incremento.

Sean entonces dados n puntos del conjunto no superpuestos y todos ellos agrupados en sus respectivos círculos de cobertura.

Considérese un nuevo punto, el $n + 1$ que se agrega al conjunto original de n puntos, diferente de cualquiera de ellos.

Este puede caer dentro de alguno de los círculos de cobertura (figura 3) o fuera de cualquiera (figura 4).

En el primer caso, es aplicable un razonamiento muy similar al usado en el algoritmo de Watson:

Al considerar el nuevo conjunto de $n+1$ puntos, los círculos de cobertura dentro de los que cae el $n+1$ punto dejen de serlo justamente por tenerlo dentro.

El problema pasa a ser entonces, construir el nuevo conjunto de círculos de cobertura que deberá estar constituido por el conjunto anterior menos los inhabilitados por tener el punto $n+1$ dentro más los c´ irculos que contienen el punto $n+1$.

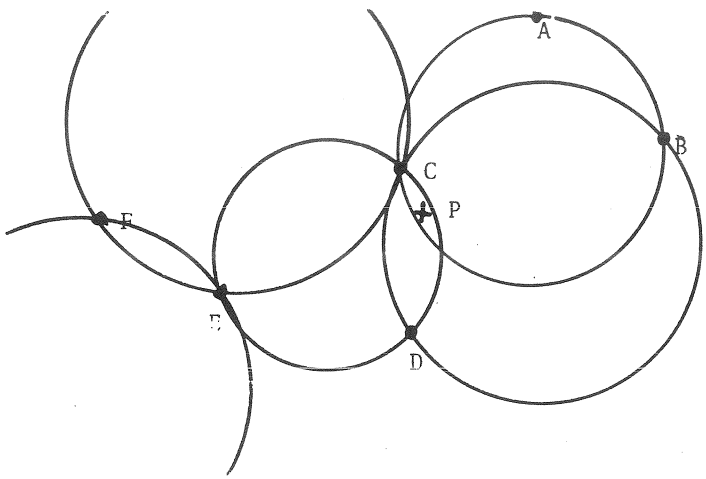

Figura 3: *El punto cae en los círculos ABC, BCD y CDE;estos ya no son de cobertura en el conjunto de $n+1$ puntos.*

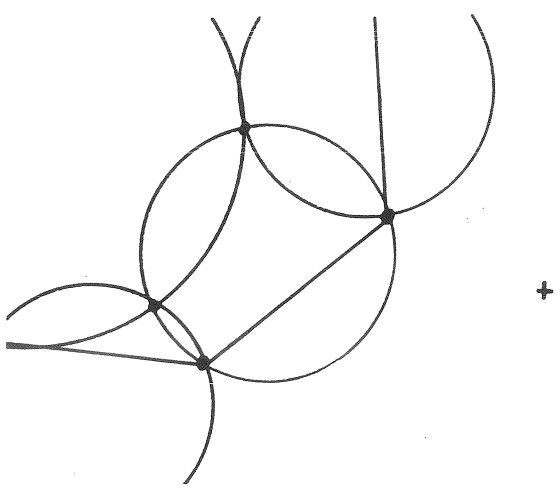

Figura 4: *El punto cae fuera de todos los círculos (eso implica que también fuera de la cerradura).*

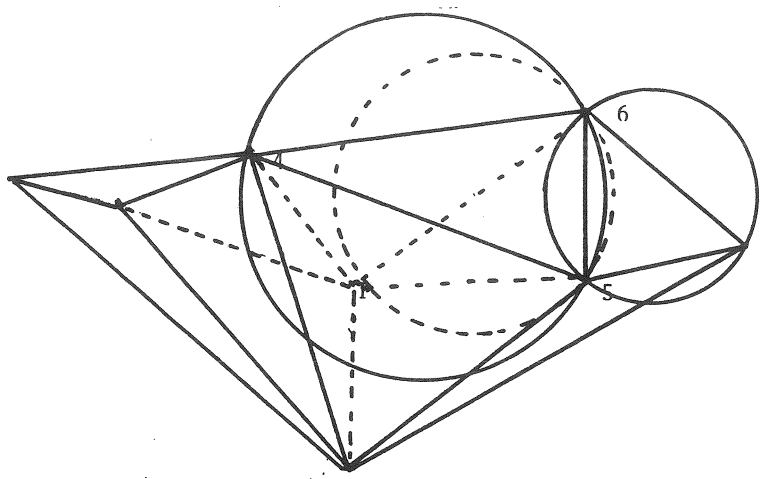

Figura 5: *Tómese uno, cualquiera de los círculos nuevos (sea el punteado), se puede demostrar que está totalmente cubierto por dos círculos del conjunto anterior. Nótese que el punto P ve el segmento 5, 6 con un ángulo mayor que el correspondiente cambiando P por 4, entonces el lugar geométrico de los puntos que ven al segmento 5, 6 con el mismo ángulo que P es una circunferencia con radio menor que la correspondiente al punto 4. Aplicando un razonamiento similar con el punto 7 y por el ángulo suplementario al que pasa por el punto P, se puede mostrar que el resto del círculo que no había sido considerado, está contenido en el círculo que pasa por 5, 6, y 7.*

Se trata entonces de determinar los nuevos círculos, para determinarlos se requieren al menos 3 puntos, uno de ellos es el punto $n+1$ los otros dos serán las parejas de puntos tomados en forma ordenada en la radiación de centro $n+1$ del conjunto de puntos que determinaban a los círculos inhabilitados con la excepción de las parejas de puntos que fueran comunes al mismo tiempo a dos circunferencias.

Se demuestra (figura 5) que los círculos así formados son de cobertura.

El otro caso a considerar, es que el punto $n+1$ no caiga dentro de ningún círculo de cobertura de los que formaban el conjunto de círculos que cubrían a los n primeros puntos.

De ser así es menester encontrar los nuevos círculos que tienen en su circunferencia al punto $n+1$.

Aprovechando el método que se usa para localizar al punto $n+1$ (que será explicado más adelante) se conoce el círculo más cercano al punto $n+1$.

Comenzando con ese círculo y continuando por los adyacentes al mismo, se procede en forma similar al caso anterior, es decir, la terna de puntos que generan la circunferencia del nuevo círculo son, el punto $n+1$ y parejas de puntos tales que no sean comunes (ambos) a dos circunferencias al mismo tiempo.

Se demuestra que este proceso da origen a círculos de cobertura y que tiene final.

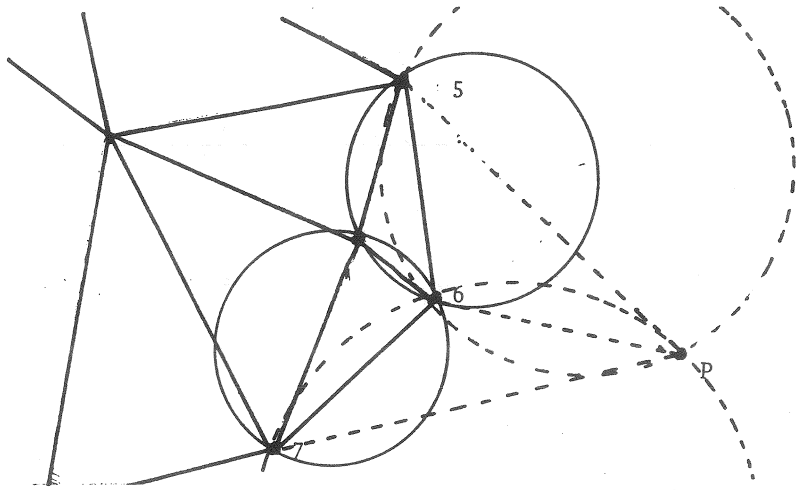

Figura 6: *Dado el punto P se van analizando de dos en dos, los puntos que generan las cjas comenzando por la más cercana (y el punto de ella más cercano), probando contra el punto inmediato anterior analizado, si no está dentro de la nueva cja. Los círculos así obtenidos son de cobertura, ya que si se los divide en dos arcos por ejemplo en la figura el 5P6 y el otro, justamente este último está inscrito en el círculo 645 por ser arco capaz de un ángulo mayor que el 4 y el resto (el arco 5P6 está fuera de la cerradura convexa).*

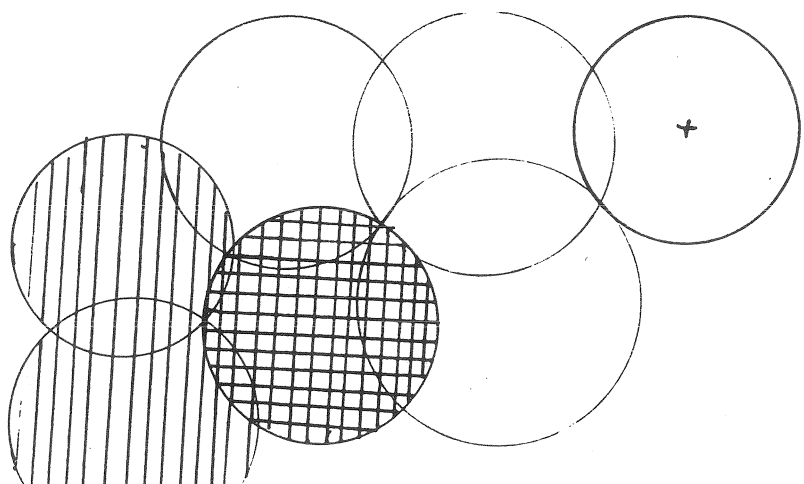

Figura 7: *Dado el punto $P(n+1)$ se comienza con las circunferencias que pasan por un punto cualquiera (el x) y se halla la de menor potencia (rayada doble).*

3 Ubicación del Punto

Para ubicar el punto $n+1$, paso previo e indispensable para realizar cada paso del algoritmo anterior, se busca no tener que probar una a una con todos los círculos del conjunto.

Para ello, se toma un punto cualquiera y se evalúa la potencia de $n+1$ respecto a las circunferencias que pasan por él. De ser todas positivas, se ordenan en forma decreciente y se repite el proceso con todas las circunferencias que cortan en puntos del conjunto a la de menor potencia.

El proceso termina cuando al menos una de ellas tiene potencia negativa o cero, o bien cuando todas las vecinas de la que tiene menor potencia, ya han sido evaluadas previamente, o cuando la potencia crece en vez de disminuir (las potencias mínimas deben ser una sucesión decreciente), en este último caso el punto $n+1$ está fuera de todos los círculos.

Este proceso, si bien requiere el mismo número de operaciones que estos procesos de localización, estos son mucho más sencillos.

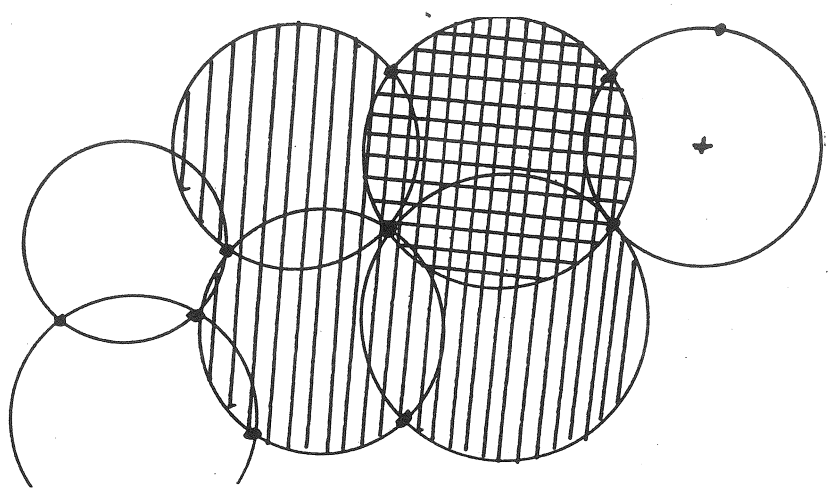

Figura 8: *Se toman para su análisis los círculos que tienen puntos comunes con la de menor potencia y se repite el proceso*

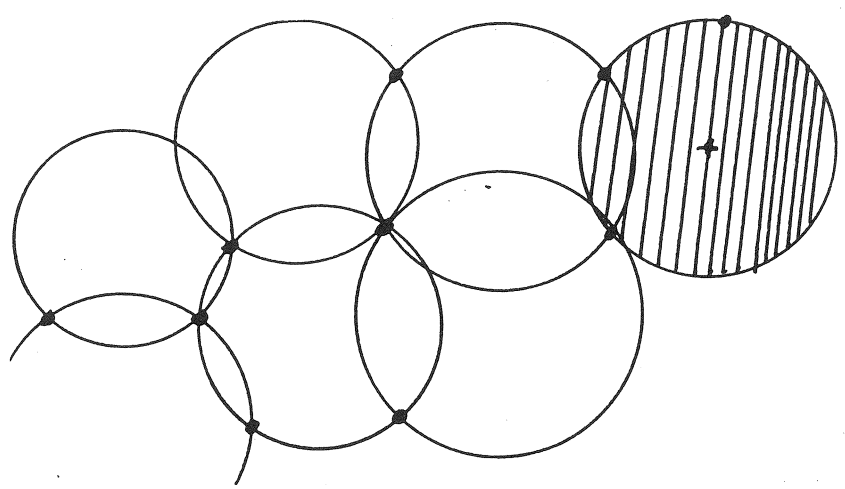

Figura 9: *El proceso culmina al encontrar las cfas respecto a las que el punto P tiene potencia negativa.*

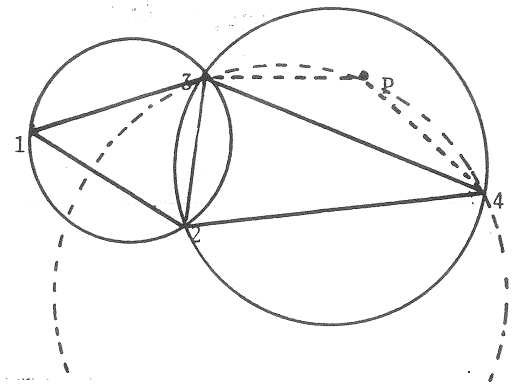

Figura 10: *Localmente, considerando solo el cuadrilátero 1342 los círculos en raya continua son de cobertura, no es así si se considera el punto P, esto requiere un paso extra de corrección.*

4 Equivalencias y ventajas con otros métodos

Como el lector ya habrá notado, la figura que forman los puntos que generan las circunferencias de los círculos de cobertura son muchas veces triángulos de Delaunay.

Cuando existen más de tres puntos, sin embargo no hay que hacer ninguna modificación a la teoría ni existe la posibilidad de que como en el algoritmo de Lawson (figuras 10 y 11) haya ambiguedades de costosa (en tiempo y sencillez) resolución.

Comparando el algoritmo presentado con los que utilizan un super triángulo inicial para que el nuevo punto $(n+1)$ quede siempre dentro de la cerradura convexa tiene la ventaja de que a diferencia de ellos siempre da todos los triángulos (figura 12).

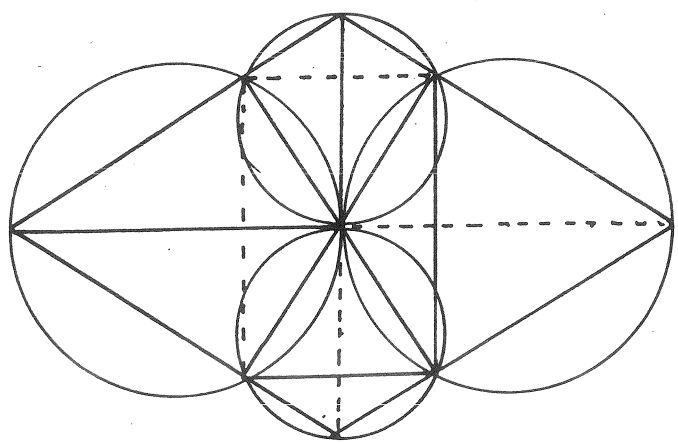

Figura 11: *Hay miles de ejemplos en los que el algoritmo de Lawson nos puede llevar a un loop infinito o al menos hacernos hacer muchas operaciones innecesarias antes de parar. Estos casos no son tan artificiales cuando el número de puntos aumenta y con la regularidad (más en aplicaciones ingenieriles).*

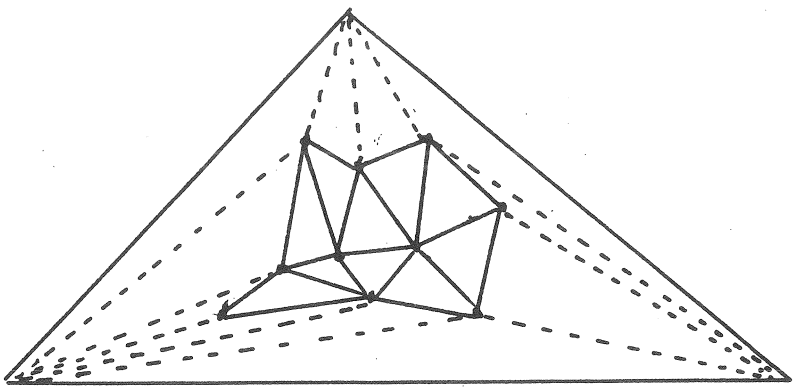

Figura 12: *Al eliminar los triángulos auxiliares, los que quedan no completan la cerradura convexa y hay que ralizar muchas operaciones para completarla todas ellas fuera del algoritmo original.*

Referencias

[1] . Delaunay ; Sur les spheres vides, Academia de Ciencias de la URSS, 1929.

[2] . Line A. K. and Renka R. J.; A storage efficient method for construction of a Thiessen triangulation, Rocky Mountain. J. Math. 14.1 (Winter 1984) 119-139.

[3] .T. Lee and A.K. Lin; Generalized Delaunay triangulation for planar Graphs, Discrete & Computational Geometry 1: 201-217, 1986.

[4] . Correc E. Chapuis; Fast Computation of Delaunay triangulations, Adv. Eng. Software, 1987, Vol. 9 No. 2.

[5] ex A. Dwyer; A faster Divide and Conquer Algorithm for Constructing Delaunay triangulations, Algorithmica, 1987, 2: 137-151.

Interpolación de superficies paramétricas no regulares mediante elementos finitos

J.J. Torrens[1], F.J. Serón[1], M.C. López de Silanes[1]
R. Arcangéli[2], D. Apprato[2]

Resumen. Se estudia el problema de interpolación de una superficie paramétrica no regular a partir de datos de tipo Lagrange de tal superficie situados sobre una malla curvilínea. Para compensar la ausencia de una parametrización natural de los puntos dados, se introduce una parametrización uniforme y se construye un interpolante de tipo "elementos finitos"de la superficie. Se estudia asimismo el error de aproximación de este método.

1. Introducción

El objeto de este trabajo es el estudio de la interpolación de una superficie paramétrica no regular a partir de puntos situados en los vértices de una malla curvilínea.

En las secciones 1.1 y 1.2, se introducen algunas notaciones y definiciones. En el párrafo 2 se realiza un estudio preliminar del problema de interpolación de funciones vectoriales no regulares utilizando elementos finitos rectangulares de tipo Hermite.

Por último, el párrafo 3 está dedicado a la interpolación de superficies paramétricas no regulares. En la sección 3.1 se modeliza el problema, mientras que en la sección 3.2 se desarrolla el procedimiento de construcción del interpolante y se dan algunos resultados relativos al error de aproximación.-

1.1. Notaciones

Dado un conjunto E de $\mathbb{R}^2$, se indica con $\overline{E}$, E° y ∂E la clausura, el interior y la frontera de E, respectivamente.

Para todo $\alpha = (\alpha_1, \alpha_2) \in \mathbb{N}^2$, se definen $|\alpha| = \alpha_1 + \alpha_2$ y $|\alpha|_\infty = \max(\alpha_1, \alpha_2)$, y se denota por ∂^α el operador de derivación parcial de orden $|\alpha|$ en $\mathbb{R}^2$:

$$\partial^\alpha = \frac{\partial^{|\alpha|}}{\partial x_1^{\alpha_1} \partial x_2^{\alpha_2}}$$

Dados un conjunto conexo E de $\mathbb{R}^2$ y $m \in \mathbb{N}$, se denota por $Q_m(E)$ el espacio de restricciones a E de los polinomios de grado menor o igual que m respecto a cada variable.

Para todo abierto ω no vacío de $\mathbb{R}^2$ y para todo $m, n \in \mathbb{N}$, $n \geq 1$, se designa por $H^m(\omega, \mathbb{R}^n)$ el espacio de Sobolev de orden m de (las clases de) funciones ψ con valores en $\mathbb{R}^n$ tales que, para $i = 1, \ldots, n$, y para todo $\alpha \in \mathbb{N}^2$ tal que $|\alpha| \leq m$, $\partial^\alpha(p_i \circ \psi) \in L^2(\omega)$, donde p_i, $i = 1, \ldots, n$, son las proyecciones canónicas. Se dota a este espacio de las seminormas :

[1] Departamento de Matemática Aplicada, E.T.S.I.I., calle María de Luna 3, E-50015 Zaragoza, España

[2] Département de Mathématiques, Université de Pau, Avenue de l'Université, F-64000 Pau, France

$$\psi \longrightarrow |\psi|_{l,\omega,\mathbb{R}^n} = \left(\sum_{i=1}^{n} \sum_{|\alpha|=l} \int_{\omega} |\partial^\alpha (p_i \circ \psi)|^2 dx \right)^{\frac{1}{2}} , \; l \in \mathbb{N}, \; l \leq m$$

y de la norma :

$$\psi \longrightarrow \|\psi\|_{m,\omega,\mathbb{R}^n} = \left(\sum_{l=0}^{m} |\psi|^2_{l,\omega,\mathbb{R}^n} \right)^{\frac{1}{2}}$$

Asimismo, si $s = m + \sigma$, con $m \in \mathbb{N}$ y $\sigma \in]0,1[$, se denota por $H^s(\omega, \mathbb{R}^n)$ el espacio de Sobolev de orden no entero s (cf. R.A. Adams[1] o J.L. Lions-E.Magenes[7]) cuyos elementos son funciones con valores en $\mathbb{R}^n$.

Dados un abierto ω no vacío de $\mathbb{R}^2$ y $m, n \in \mathbb{N}$, $n \geq 1$, se designa por $C^m(\omega, \mathbb{R}^n)$ el espacio de funciones ψ con valores en $\mathbb{R}^n$ tales que, para $i = 1, \ldots, n$, y para todo $\alpha \in \mathbb{N}^2$ tal que $|\alpha| \leq m$, $\partial^\alpha (p_i \circ \psi)$ es continua en ω. Análogamente, se denota por $C^m(\overline{\omega}, \mathbb{R}^n)$ el espacio de funciones $\psi \in C^m(\omega, \mathbb{R}^n)$ tales que, para $i = 1, \ldots, n$, y para todo $\alpha \in \mathbb{N}^2$ tal que $|\alpha| \leq m$, $\partial^\alpha (p_i \circ \psi)$ admite una extensión continua a $\overline{\omega}$, la cual se indicará igualmente por $\partial^\alpha (p_i \circ \psi)$. Este espacio está dotado de la norma :

$$\psi \longrightarrow \|\psi\|_{C^m(\overline{\omega},\mathbb{R}^n)} = \max_{1 \leq i \leq n} \; \max_{0 \leq |\alpha| \leq m} \; \max_{x \in \overline{\omega}} |\partial^\alpha (p_i \circ \psi)(x)|$$

Por último, la misma letra C designará diversas constantes positivas.

1.2. El espacio $C^m_\tau(\omega', \mathbb{R}^3)$

Sea ω un abierto conexo, acotado y no vacío de $\mathbb{R}^2$, cuya frontera es lipschitziana. Sea τ un subconjunto no vacío y cerrado de $\overline{\omega}$. Sea $\omega' = \omega \setminus \tau$.

Se dice que una familia finita $\{\omega_1, \ldots, \omega_l\}$ de subconjuntos de ω' representa a τ en ω si :

(i) Para $i = 1, \ldots, l$, ω_i es abierto, conexo, acotado, no vacío y de frontera lipschitziana

(ii) $\overline{\omega} = \bigcup_{i=1}^{l} \overline{\omega}_i$ y, para $i \neq j$, $\omega_i \cap \omega_j = \emptyset$

(iii) $\tau \subset \bigcup_{i=1}^{l} \partial\omega_i$

En cuanto sigue se supondrá que la familia $\{\omega_1, \ldots, \omega_l\}$ representa a τ en ω.

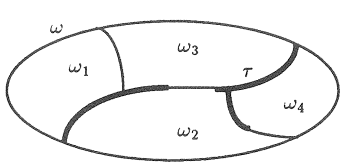

Fig. 1

Dado $m \in \mathbb{N}$, se define el espacio $C^m_\tau(\omega', \mathbb{R}^3)$ de funciones $\psi \in C^m(\omega', \mathbb{R}^3)$ tales que, para $i = 1, \ldots, l$, $\psi_{|_{\omega_i}} \in C^m(\overline{\omega}_i, \mathbb{R}^3)$.

Se demuestran los siguientes resultados :

Lema 1.1. *Sea E un subconjunto abierto de ω' con frontera lipschitziana. Entonces, para toda $\psi \in C^m_\tau(\omega', \mathbb{R}^3)$, $\psi_{|_E} \in C^m(\overline{E}, \mathbb{R}^3)$.* ∎

Teorema 1.1. *$C^m_\tau(\omega', \mathbb{R}^3)$ es un espacio de Banach con la norma :*

$$\psi \longrightarrow \|\psi\|_{C^m_\tau(\omega', \mathbb{R}^3)} = \max_{1 \le i \le l} \|\psi|_{\omega_i}\|_{C^m(\overline{\omega}_i, \mathbb{R}^3)}$$

Además, el espacio $C^m_\tau(\omega', \mathbb{R}^3)$ y la norma $\| \cdot \|_{C^m_\tau(\omega', \mathbb{R}^3)}$ son independientes de la elección de la familia $\{\omega_1, \ldots, \omega_l\}$ que representa a τ en ω. ∎

Teorema 1.2.
(i) *Si $s > m + 1$, entonces $H^s(\omega', \mathbb{R}^3)$ se inyecta continuamente en $C^m_\tau(\omega', \mathbb{R}^3)$.*
(ii) *Si $\psi \in C^m_\tau(\omega', \mathbb{R}^3)$ y, para $i = 1, \ldots, l$, $\psi_{|_{\omega_i}} \in H^{m+1}(\omega_i, \mathbb{R}^3)$, entonces :*

$\psi \in H^{m+1}(\omega', \mathbb{R}^3)$. ∎

Finalmente, para todo $E \subset \overline{\omega}$ y para toda $\psi \in C^m_\tau(\omega', \mathbb{R}^3)$ se define el conjunto

$$\psi(E) = \bigcup_{i=1}^{l} \psi_{|_{\omega_i}}(E \cap \overline{\omega}_i).$$

2. Interpolación de funciones vectoriales no regulares sobre mallas uniformes

Sea Ω un abierto conexo, acotado y no vacío de $\mathbb{R}^2$, cuya frontera es lipschitziana y está formada por segmentos paralelos a los ejes de coordenadas.

Sea H un subconjunto acotado de $\mathbb{R}^*_+$ tal que $0 \in \overline{H}$.

Se supone que, para todo $h \in H$, existe una triangulación $\mathcal{T}_h$ de $\overline{\Omega}$ mediante cuadrados iguales de lados de longitud h. Se designa por B_h el conjunto de vértices de $\mathcal{T}_h$.

Sea Φ un subconjunto cerrado y no vacío de $\overline{\Omega}$ tal que, para todo $h \in H$, Φ es unión de lados de cuadrados de $\mathcal{T}_h$. Sea $\Omega' = \Omega \setminus \Phi$. Se comprueba fácilmente que existe una familia que representa a Φ en Ω. Asimismo, para todo $m \in \mathbb{N}$, se define el espacio $C^m_\Phi(\Omega', \mathbb{R}^3)$ al igual que en la sección 1.2.

En todo cuanto sigue, k será un entero fijo mayor o igual que 1.

Para todo $h \in H$, sea V_h un espacio de tipo "elementos finitos"construido sobre $\mathcal{T}_h$ a partir del elemento finito genérico de Bogner-Fox-Schmit de clase C^k. Recordemos que tal elemento se puede definir como una terna (K, P_K, Σ_K) (cf. P.G. Ciarlet [5]) donde K designa un cuadrado cualquiera de $\mathcal{T}_h$, $P_K = Q_{2k+1}(K)$ y $\Sigma_K = \{ v \to \partial^\alpha v(b) \mid b \in K \cap B_h \ , \alpha \in J_k \}$, siendo $J_k = \{ \alpha \in \mathbb{N}^2 \mid |\alpha|_\infty \le k \}$.

Se introducen las siguientes notaciones :

- $\forall b \in B_h$, $\forall \alpha \in J_k$, w^α_b es la función de base de V_h asociada al nodo b y al grado de libertad $v \to \partial^\alpha v(b)$
- $\forall b \in B_h$, $S_b = \cup\{ K \in \mathcal{T}_h \mid b \in K \}$
- $\forall b \in B_h$, γ_b es el número de componentes conexas de $S_b \setminus \Phi$, cada una de las cuales se denota por S^j_b , $j = 1, \ldots, \gamma_b$
- $\forall b \in B_h$, $\forall j = 1, \ldots, \gamma_b$, $\forall \alpha \in J_k$, $w^{(\alpha,j)}_b = w^\alpha_b \cdot \chi_{\overline{S}^j_b}$, donde $\chi_{\overline{S}^j_b}$ es la función característica de $\overline{S}^j_b$

- V_h' es el espacio vectorial generado por la familia :

$$\{\ w_b^{(\alpha,j)}\ \mid\ b \in B_h,\ j = 1, \ldots, \gamma_b,\ \alpha \in J_k\ \}$$

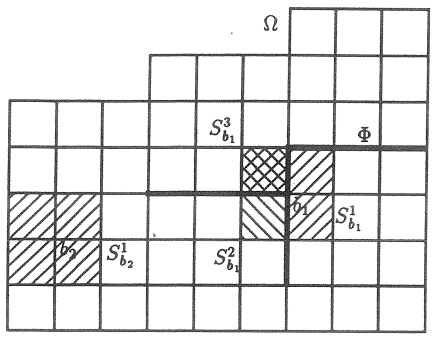

Fig. 2.1

Del teorema 1.2 se deduce que :

(2.1) $(V_h')^3$ es un subespacio de dimension finita de $H^{k+1}(\Omega', \mathbb{R}^3) \cap C^k_\Phi(\Omega', \mathbb{R}^3)$

En esta situación, para cada $h \in H$, se define un operador A_h de interpolación de Lagrange, mediante funciones de $(V_h')^3$, de la forma siguiente :

(2.2)
$$\left|\begin{array}{l}
\forall v \in C^0_\Phi(\Omega', \mathbb{R}^3),\ A_h v = \displaystyle\sum_{b \in B_h} \sum_{j=1}^{\gamma_b} \sum_{\alpha \in J_k} v_b^{\alpha,j}\ w_b^{(\alpha,j)} \\
\text{donde : } \forall b \in B_h,\ \forall j = 1, \ldots, \gamma_b,\ \forall \alpha \in J_k,\ v_b^{\alpha,j} = \partial^\alpha \Pi_{K_b^j} v(b), \\
\text{siendo } K_b^j \text{ un subconjunto cerrado de } \overline{\Omega} \text{ que verifica :} \\
\quad \text{(i) } K_b^j \text{ es un cuadrado de lados de longitud } (2k+1)h \text{, unión de} \\
\quad\quad \text{cuadrados de } \mathcal{T}_h ; \\
\quad \text{(ii) } (K_b^j)^\circ \cap \Phi = \emptyset\ ; \\
\quad \text{(iii) } (K_b^j)^\circ \cap (S_b^j)^\circ \neq \emptyset \text{ y } b \in K_b^j ; \\
\text{y donde además } \Pi_{K_b^j} v \in (Q_{2k+1}(K_b^j))^3 \text{ es el interpolante de La-} \\
\text{grange de } v_{|(K_b^j)^\circ} \text{ en los nodos de } B_h \cap K_b^j
\end{array}\right.$$

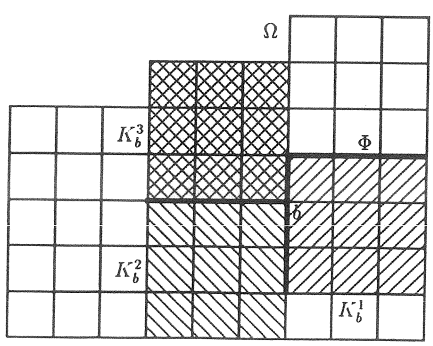

Fig. 2.2. Dominios K_b^j para $b \in \Phi$ y $k = 1$

Observación 2.1. Con las notaciones introducidas anteriormente, se tiene que, para toda $\psi \in C^0_\Phi(\Omega', \mathbb{R}^3)$, $A_h v(B_h) = v(B_h)$. Además, de (2.1) se sigue que $A_h v$ es una función de clase C^k en Ω'. ∎

Observación 2.2. Para definir el interpolante $A_h v$ de una función v del espacio $C^0_\Phi(\Omega', \mathbb{R}^3)$, no se utilizan más que datos de tipo Lagrange. Los coeficientes $v_b^{\alpha,j}$, para $\alpha \in J_k \setminus \{(0,0)\}$, están asociados a los grados de libertad correspondientes a las derivadas parciales. Sin embargo, no se necesita conocer el valor de éstas, pues las expresiones introducidas en (2.2) para definir tales coeficientes no son otra cosa que fórmulas en diferencias finitas construidas sobre ciertos subdominios para aproximar las derivadas. ∎

Observación 2.3. El operador A_h depende de la elección de los dominios K_b^j, la cual, a priori, puede ser arbitraria. ∎

Dado $h \in H$, para todo $K \in \mathcal{T}_h$, sean $\mathcal{K}^* = \cup\{ K_b^j \mid b \in K \cap B_h, j \in \{1, \ldots, \gamma_b\}, K^\circ \subset S_b^j \}$ y $\mathcal{K} = (\mathcal{K}^* \setminus \Phi)^\circ$. Se tiene el siguiente resultado :

Teorema 2.1. *Sea $m \in \mathbb{N}$, $m \geq 2$. Se supone que, para todo $h \in H$ y para todo $K \in \mathcal{T}_h$, $\mathcal{K}$ es conexo y $K^\circ \subset \mathcal{K}$. Entonces, existe una constante $C > 0$ tal que :*

$\forall h \in H$, $\forall l = 0, \ldots, m'$, $\forall v \in H^m(\Omega', \mathbb{R}^3)$, $|v - A_h v|_{l,\Omega',\mathbb{R}^3} \leq C\, h^{m^*-l}\, |v|_{m^*,\Omega',\mathbb{R}^3}$

donde $m' = \min(m, k+1)$ y $m^* = \min(m, 2k+2)$. ∎

Observación 2.4. Cuando $m \geq 2k+2$, se deduce del teorema 2.1. que, para las funciones de $H^m(\Omega', \mathbb{R}^3)$, la estimación del error de interpolación correspondiente al operador A_h es del mismo orden en h que la correspondiente al operador de Hermite exacto. ∎

Aplicando el teorema 2.1. se prueba la siguiente :

Proposición 2.1. *Sea $m \in \mathbb{N}$, $m \geq 2$. Sea $l \in \mathbb{N}$ tal que $l \leq \min(m-1, k+1)$. Sea $(v_h)_{h \in H}$ una familia de $H^m(\Omega', \mathbb{R}^3)$ que verifica :*

(i) $\exists C > 0$, $\forall h \in H$, $\|v_h\|_{m^*,\Omega',\mathbb{R}^3} < C$, *donde* $m^* = \min(m, 2k+2)$

(ii) $\exists v \in H^l(\Omega', \mathbb{R}^3)$, $\lim_{h \to 0} \|v_h - v\|_{l,\Omega',\mathbb{R}^3} = 0$

Entonces, $\lim_{h \to 0} \|A_h v_h - v\|_{l,\Omega',\mathbb{R}^3} = 0$. ∎

3. Interpolación de superficies paramétricas no regulares

3.1. Modelización del problema

Sea H un subconjunto acotado de $\mathbb{R}_+^*$ tal que $0 \in \overline{H}$.

Se considera una superficie S de $\mathbb{R}^3$ y, para todo $h \in H$, se supone dado un conjunto finito G_h constituido por todos los vértices de una malla curvilínea de S.

Se supone también que S es una superficie paramétrica no regular en el siguiente sentido :

(3.1)

Existen :
- un abierto D de $\mathbb{R}^2$, conexo, acotado, no vacío y de frontera lipschitziana;
- un conjunto $F \subset \overline{D}$ cerrado y no vacío;
- una familia $\{D_1, \ldots, D_l\}$ que representa a F en D;
- una función $f \in C^k_F(D', \mathbb{R}^3)$, donde $D' = D \setminus F$ y $k \in \mathbb{N}$, $k \geq 1$;

tales que :
- f no admite una extensión continua a F (salvo a lo sumo en un número finito de puntos de F);
- $S = f(\overline{D})$.

Se supone además que :

(3.2)

(i) la frontera de D está formada por un número finito de segmentos paralelos a los ejes de coordenadas;

(ii) existe una familia $(\mathcal{Q}_h)_{h\in H}$ de triangulaciones de $\overline{D}$ mediante rectángulos de modo que :

- para todo $h \in H$, F es unión de lados de rectángulos de $\mathcal{Q}_h$;
- para todo $h \in H$, $f(D_h) = G_h$, siendo D_h el conjunto de vértices de $\mathcal{Q}_h$.

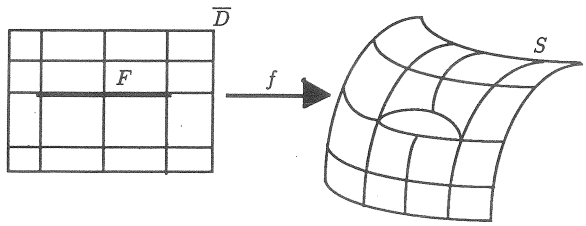

Fig. 3.1

En esta situación, se considera el problema de construir, para todo $h \in H$, una superficie que interpole a S en los puntos de G_h.

Se modeliza tal problema mediante la introducción de una familia de cambios de parámetro, para lo cual se supone que :

(3.3)

Existen :

- un abierto Ω de $\mathbb{R}^2$, conexo, acotado, no vacío y de frontera lipschitziana formada por segmentos paralelos a los ejes de coordenadas;
- para todo $h \in H$, una triangulación $\mathcal{T}_h$ de $\overline{\Omega}$ mediante cuadrados iguales de lados de longitud h;
- para todo $h \in H$, un homeomorfismo $\varphi_h : \overline{\Omega} \to \overline{D}$ de clase C^k;

de modo que :

- $\varphi_h(B_h) = D_h$, siendo B_h el conjunto de vértices de $\mathcal{T}_h$;
- $\varphi_h^{-1}(F)$ es unión de lados de cuadrados de $\mathcal{T}_h$.

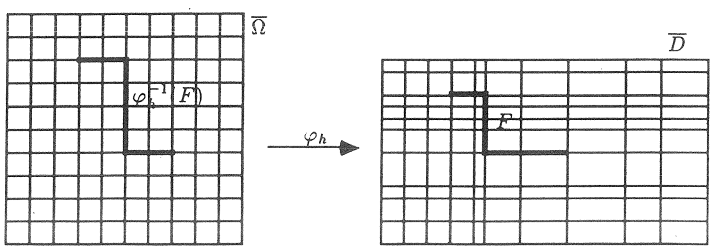

Fig. 3.2

Para todo $h \in H$, se define :

$$g_h = f \circ \varphi_h \tag{3.4}$$

La función g_h es una parametrización de S que verifica :

$$\begin{cases} \text{(i) } g_h(B_h) = G_h \\ \text{(ii)} g_h \in C^k_{\Phi_h}(\Omega'_h, \mathbb{R}^3) \end{cases} \tag{3.5}$$

donde $\Phi_h = \varphi_h^{-1}(F)$ y $\Omega'_h = \Omega \setminus \Phi_h$.

En la próxima sección se construirá una aproximación de la superficie S según el criterio siguiente : para interpolar S, interpólese la parametrización g_h de S.

3.2. Construcción de un interpolante de Lagrange de clase C^k. Estudio del error

Bajo ciertas hipótesis de monotonía de la familia $(G_h)_{h\in H}$ (cf. D. Apprato [2]), se demuestra que :

$$\exists \Phi \subset \overline{\Omega},\ \forall h \in H,\ \Phi_h = \Phi \tag{3.6}$$

es decir, el conjunto $\varphi_h^{-1}(F)$ de discontinuidad de g_h no depende de h.

Gracias a (3.3) y (3.6), nos situamos en las condiciones descritas en el párrafo 2. Entonces, a partir de (3.5), se define, para todo $h \in H$, un interpolante $A_h g_h$ de la parametrización g_h de S dada en (3.4), siendo A_h el operador introducido en (2.2). Nótese que la función $A_h g_h$ pertenece al espacio $C^k_\Phi(\Omega', \mathbb{R}^3)$ y que, además, $A_h g_h(B_h) = G_h$.

El estudio del error muestra que, bajo determinadas hipótesis suplementarias sobre f y sobre la familia $(\varphi_h)_{h\in H}$, este procedimiento de interpolación es convergente. En efecto, utilizando el teorema 2.1, se prueba el siguiente resultado de estimación del error :

Teorema 3.1. *Se supone que :*

$$f \in H^m(D', \mathbb{R}^3), \text{ donde } m \in \mathbb{N},\ m \geq 2 \tag{3.7}$$

$$\begin{cases} \text{(i) } \forall h \in H,\ \varphi_h \in C^m(\overline{\Omega}, \mathbb{R}^2),\ \varphi_h^{-1} \in C^1(\overline{D}, \mathbb{R}^2) \\ \text{(ii) } \exists C > 0,\ \forall h \in H,\ \|\varphi_h\|_{C^m(\overline{\Omega},\mathbb{R}^2)} \leq C,\ \|\varphi_h^{-1}\|_{C^1(\overline{D},\mathbb{R}^2)} \leq C \end{cases} \tag{3.8}$$

Entonces, existe una constante $C > 0$ tal que :

$$\forall h \in H,\ \forall l = 0, \ldots, m',\ |g_h - A_h g_h|_{l,\Omega',\mathbb{R}^3} \leq C\ h^{m^*-l}\ \|f\|_{m^*,D',\mathbb{R}^3}$$

donde $m' = \min(m, k+1)$ y $m^* = \min(m, 2k+2)$. ∎

Observación 3.1. Se demuestra (cf. D. Apprato [2]) que se satisfacen las hipótesis (3.3), (3.6) y (3.8) bajo ciertas condiciones de monotonía de la familia $(G_h)_{h\in H}$ y de regularidad de los nodos de las triangulaciones $(\mathcal{Q}_h)_{h\in H}$. Es más, se prueba que existe una parametrización g de S que pertenece a $H^m(\Omega', \mathbb{R}^3)$ y tal que g_h converge fuertemente a g en $H^{m-\theta}(\Omega', \mathbb{R}^3)$, para todo $\theta \in]0, r-1[$. Aplicando la proposición 2.1 y el teorema 3.1, se concluye que $A_h g_h$ converge fuertemente a g en $H^l(\Omega', \mathbb{R}^3)$, donde $l = \min(m-1, k+1)$. Teniendo en cuenta el teorema 1.2, esta convergencia es uniforme cuando $m \geq 3$. ∎

Bibliografía

[1] R.A. Adams : *Sobolev Spaces*, Academic Press, Nueva York (1975)

[2] D. Apprato : *Approximation de surfaces paramétrées par éléments finis*, Tesis doctoral, Universidad de Pau (Francia) (1987)

[3] D. Apprato - R. Arcangéli : *Approximation de surfaces paramétrées régulières par éléments finis. Partie I : Modélisation du problème*, U.A. 1204 C.N.R.S., publicación 1989/6

[4] R. Arcangéli - C. Rabut : *Sur l'erreur d'interpolation par fonctions splines*, RAIRO M^2AN vol. 20, n 2, pp. 191 - 201 (1986)

[5] P.G. Ciarlet : *The Finite Element Method for Elliptic Problems*, North-Holland, Amsterdam (1978)

[6] P.G. Ciarlet - P.A. Raviart : *Interpolation theory over curved elements, with applications to the finite element method*, Comput. Methods Appl. Mech. Engrg. vol. 1, pp. 217 - 249 (1972)

[7] J.L. Lions - E. Magenes : *Problèmes aux limites non homogènes et applications*, vol. 1, Dunod, Paris (1968)

[8] R. Manzanilla : *Sur l'approximation de surfaces définies par une équation explicite*, Tesis doctoral, Universidad de Pau (Francia) (1986)

MULTI-GRID AND B(OX)-SPLINES

RUUD VAN DAMME
Dept. of Applied Mathematics
University of Twente
P.O.Box 217
7500AE Enschede
The Netherlands

Abstract. The multi-grid algorithm is investigated for approximation problems, Laplace equations and biharmonic equations, when B-splines and box-splines (in one resp. two dimensions) are being used. It turns out that for approximation problems the algorithm cannot compete with standard iterative procedures. The multi-grid algorithm works fine for elliptic boundary value problems for all B-splines and a large class of box-splines. In particular it is *not* suited for box-splines on a 4-direction mesh. Theoretical predictions on convergence are made and compared with experiment: there is a good agreement between the two.

1. Introduction

If we want to solve a (least squares) approximation problem, or a differential equation with the aid of splines we are led to solve a system of (not necessarily linear) equations, Lu=f. The number of equations, N, in general becomes large. Conventional iterative procedures will need order N matrix multiplications; in practice this number can be reduced by preconditioning, but still the number of matrix multiplication can be obstructively time consuming [6]. Direct methods, even those incorporating the sparseness of the system, have this same failure.

Solving differential equations (boundary value problems) with Finite Difference Methods (FDM) leads to the same problem. In that field multi-grid algorithms were developed. If optimally implemented, they have the pleasant property that they converge with a number of matrix multiplications which is roughly independent of N. [7 and references therein].

We wish to examine whether multi-grid can be used in spline calculations; which problems are suited and especially which splines are the best to use. We concentrate on B-splines (one dimension) and box-splines (two dimensions). We do not wish to make an extensive comparison with other iterative procedures, but we wish to decide whether the multi-grid algorithm performs at least better than algorithms like e.g., conjugated gradient: As this is an algorithm

which is fairly easy to implement, the multi-grid algorithm should at least be better than this algorithm when one decides to use it: multi-grid methods are in general not easy to implement.

A multi-grid algorithm is an algorithm which solves equations by using the same problem repeatedly on different grids (section 2). It needs transformation rules for results from one grid to another. How to choose those transformation rules will be a matter of investigation in section 3. Another essential ingredient of multi-grid is the use of a 'conventional' iterative solver, which is called the 'smoother'. In the literature many of such smoothers exist; however, as we are primarily interested for which problems, and for which types of splines the multi-grid algorithm can work, we will use the most convenient one with respect to the theoretical analysis. This will be explained in section 4. The resulting convergence analysis of the two-grid algorithm will be sketched in the next section, whereas section 6. is devoted to numerical experiments using the algorithm for two and more grids, confirming indeed the theoretical predictions.

As we will restrict ourselves to the question of which problems and which splines are suited for multi-grid, we will not discuss here the applicability to nonlinear problems, the use of nested iterations nor ways of optimizing the algorithm (i.e. finding a 'practical' smoother) [7].

2. The multi-grid algorithm

Suppose we wish to solve a set of linear equations, which arises from some differential equation by discretizing it, or applying a Galerkin method; but at this point it may also be an approximation problem. We write this set of equations (which depends on the specific partition and thus on the mesh size H) as:

$$L^H U^H = F^H \qquad (1)$$

Consider another partition, with mesh size h, leading to

$$L^h u^h = f^h \qquad (2)$$

This equation is a compact notation of the problem: it will also contain the necessary boundary conditions in case of a differential equation. Although not being strictly necessary we will assume that the grid of meshsize h is obtained by a subdivision technique of grid with meshsize H: it is advantageous to use the very quick subdivision algorithms which are available for splines [1,2,4].

The best way to explain the principle of multi-grid is to describe the two-grid algorithm [7]. In the sequel we use capitals for the coarsest grid (H), small letters for the finer grid (h). As we use standard subdivision we have H = 2 h.

We first assume that we have selected some procedure $ which in principle can solve (2) in an iterative way:

$$u^h_{n+1} = \$(u^h_n) \qquad (3)$$

$ is called the 'smoother' in all literature on multi-grid [7].
Now consider the following algorithm:

Multi-grid algorithm:

0) Initialize u_0^h; it is the best guess at hand, else $u_0^h=0$

1) Iterate the equation on the fine grid during ν steps:

$$\text{For } n=1 \text{ to } \nu \text{ do } u_n^h = \$(u_{n-1}^h). \tag{4}$$

ν is free, but usually taken small. Throughout this paper we take $\nu=1$.

2) Compute the defect:

$$d^h = L^h u_\nu^h - f^h \tag{5}$$

or in terms of the error $e^h = u^h - \underline{u}^h$, $\underline{u}^h$ being the exact solution of (2)

$$d^h = L^h e^h \tag{6}$$

Exit the algorithm if the norm of d is small enough.

3) Approximate this defect on the coarser grid:

$$D^H = R\, d^h \tag{7}$$

A choice for R(estriction) will be made later.

4) Solve dU^H from the equation

$$L^H dU^H = D^H \tag{8}$$

5) Transform dU^H found in step 4) back to the finer grid by some interpolation, usually referred to as P(rolongation)

$$du^h = P\, dU^H \tag{9}$$

6) Subtract it from u_ν^h

$$u_0^h = u_\nu^h - du^h \tag{10}$$

which serves as a new best guess. Go back to 1).

In the two-grid algorithm we assume that step 4) can be done exactly; in a multi-grid algorithm we can recursively repeat the same procedure for the equation found in step 4): equation (8) is exactly of the same form as (1). Of course this recursion has to stop somewhere; therefore we solve (8) exactly on some grid, which is the coarsest grid - in the two-grid algorithm this coarsest grid is just the grid with mesh H.

The main idea of multi-grid is that convergence of the iterative procedure used, is dominated by the convergence of the low frequency modes. So after some iterations with the smoother (step 1) the error is assumed to be a much smoother function than the one which one started with. Because of this property it can suitably be represented on a coarser grid (step 2 and 3), the resulting equation to be solved being (8). If this can be done exactly, resulting in dU^H, one can interpolate this back to the fine grid, see step 5 and 6.

We can suitably combine steps (2-6) for a two-grid algorithm into:

$$u_0^h = u_\nu^h - P\,(L^H)^{-1}\, R\,(L^h u_\nu^h - f^h) \tag{11}.$$

This expression will be used in the convergence analysis of sect. 5.

In the next section we will discuss our choice for the transformation of coefficients between two different grids, the restriction R from fine to coarse, and the prolongation P, which interpolates from the

coarse to the fine grid. As we only work on problems which stem from a minimization (Galerkin, approximation in least squares sence) there exist natural choices for R and P.

3. Transformation R and P

The first problem is to find suitable transformations R and P for the various spline coefficients. The transformation P is the most straightforward as it has to interpolate. It is immediately clear that if there exists a subdivision technique for the spline at hand this interpolation is straightforward (see for B-spline [1], box-spline [4], Bezier-Bernstein spline [2]). Indeed one can express each basis function on the coarse grid as a linear combination of the basis functions on the fine grid:

$$B^H = Q\, b^h \tag{12}$$

with Q some (known) matrix. Then any function F, which is represented by a coefficient vector U can be written as

$$F = (U^H)^T B = (U^H)^T Q\, b^h. \tag{13}$$

On the other hand, we want it to be equal to the prolongation of U on the fine grid:

$$F = (u^h)^T b^h = (P\, U^H)^T b^h \tag{14}$$

which yields as an obvious choice for the prolongation P:

$$P = Q^T. \tag{15}$$

When working on problems which can be formulated as a minimization problem, we can show that there exists a unique choice for the restriction R as well, namely the adjoint of P [8]:

$$R = P^T = Q \tag{16}$$

Note that for linear minimization problems we have

$$L^H = Q\, L^h\, Q^T, \quad F^H = Q^T f^h \tag{17}$$

and our objective was to solve (see eq.5):

$$L^h\, du^h - d^h = 0 \tag{18}$$

whereas this choice for R implies that we solve:

$$L^H\, dU^H - D^H = P^T (L^h\, du^h - f^h) = 0 \tag{19}$$

which follows from (7-9,16-18). So instead of (18) we solve (19), which is the best we can do.

Having chosen our transformation P and R(15,16), in the next section we will discuss the other main ingredient of multi-grid, the smoother.

4. The smoother

An important ingredient of multi-grid is the choice for the iteration step, the so called smoother. For theoretical purposes an ordinary Jacobi iteration is commonly used; in many practical situation a much better choice of the smoother is available (for example Gauss-Seidel of type: red-black; ZEBRA; alternating ZEBRA; Lexicographical GS and so-called ILU smoothers, to name a few [9 and references therein]).

These practical smoothers lead to convergence rates which usually are much higher than the rates obtained with a Jacobi smoother; moreover the algorithms becomes much more robust with these practical smoothers: convergence factors become better when the number of grids involved is increased. Besides they usually do not loose their efficiency when the problem differs much from the problems which one uses for theoretical investigations (the models, the idealized problems, which be discussed in the next section).

Here we will adopt the theoretically more transparent relaxed Jacobi iteration, as we are primarily interested in the questions in which cases a multi-grid algorithm can be expected to work when applied to minimization problems with the aid of B-splines or box-splines.

A relaxed Jacobi iteration step is given by [6]:

$$\$(u^h) = u^h - \omega D^h (L^h u^h - f^h) \qquad (20)$$

here $D^h = \mathrm{Diag}^{-1}(L^h)$, ω is called the relaxation parameter, which serves as optimization parameter of the multi-grid algorithm.

5 Convergence properties for two-grid with B(ox)-splines

A multi-grid algorithm consists of two different ingredients: the *smoothing step* (step 1 in the algorithm), which primarily has to eliminate the fast components in the error:

$$u_1^h = \$(u_0^h) \qquad (3)$$

in which we take $ as defined in (20), and the *coarse grid correction*, the correction due to solving the defect equation on the coarser grid (steps 2-6 in the algorithm) which can be combined into (11) for the two-grid algorithm.

When investigating the effectiveness of a two-grid algorithm one usually investigates *model problems*. These are problems which are an idealized version of the real problems which one may want to investigate: boundary conditions are chosen suitably, the differential operator is chosen to be homogeneous. In those cases the complete analysis can be performed using the symmetries of matrix L in eq(2). In this way we establish multi-grid algorithms, which in theory should work. In practice it proves that the algorithms, constructed in this way indeed have the desired properties, even for less ideal problems: different boundary conditions, inhomogeneous equations etc.

We have chosen three standard problems, all arising from the following minimization problem:

$$M = \int_\Omega \left(\frac{1}{2}(\nabla^n u(x))^2\right) - f(x)\, u(x)\, d\Omega \qquad (21)$$

$$u(x) = \sum_i c_i\, b_i(x) \qquad (22)$$

Ω is the domain $[0,1]$ in $\mathbb{R}$ ($[0,1]^2$ in $\mathbb{R}^2$), the trial function u(x) is a linear combination of B-splines, resp. box-splines. When n=0 (21) represents a least squares approximation problem of some function f, in case of abundant and homogeneous data. If n=1 it is a Poisson/Laplace equation, n=2 represent the so called biharmonic equation, which is a

problem related to thin plate bending problems [8]. Especially the last problem is of interest to us, as standard finite element methods sometimes fail in these cases. For the analysis we assume u to vanish on the boundary.

Details in our analysis will mostly be given for the one-dimensional case (B-splines) as the analysis for 2-D box-splines roughly follows the same line. Therefore we then will only indicate the differences.

We closely follow the analysis given in [9]: in (5.1) we will investigate the smoothing ability of the smoother, in (5.2) we will give the total error reduction for a complete two-grid step. It will prove that the smoothing property of step 1) in the multi-grid algorithm globally determines the convergence rates of the complete algorithm.

5.1. THE SMOOTHING PROPERTIES FOR HOMOGENEOUS B-SPLINES

The effectiveness of the smoothing step (20) is determined by the ability of the smoothing step (step 2 in the algorithm) to eliminate the fast components in the error. In practice it yields a good estimate of the error reduction in a complete two/multi-grid step, the so called convergence rate, which we denote as 'cr'. This agreement will be dealt with in the next subsection.

The smoothing step should kill the fast frequency modes; therefore we first should be able to distinguish between high and low frequency components. It will be helpful to use Fourier transforms, which is for these splines given by [5] (d is the degree):

$$b_m(x) = \int_{-\infty}^{\infty} Q(z)^{d+1} \exp(-2\pi i(x-x_m)z/h)dz \qquad (23)$$

$$Q(z) = \left(\frac{\sin(\pi z)}{\pi z}\right)^{2d+2} \qquad (24)$$

x_m is the location of the control point of the b_m, $x_m=(m+\frac{d+1}{2})h$.

For the minimization problem (21) one can easily derive, using standard Fourier transform techniques, that the matrix L is given by

$$L_{k,m} = \int_{-\infty}^{\infty} Q(z)^{2d+2} (\pi z)^{2n} \exp(2\pi i z(k-m))dz. \qquad (25)$$

In (25) we omitted an h-dependent factor, as this common factor drops out. We define D as the inverse of the diagonal part of L:

$$D^{-1} = \int_{-\infty}^{\infty} Q(z)^{2d+2} (\pi z)^{2n} dz. \qquad (26)$$

Now we can determine the eigenvectors of DL (see 20):

$$e^r_m = \exp(2\pi i m r + i\phi) \qquad (27)$$

where ϕ is some arbitrary phase. The corresponding eigenvalues λ_r are

$$\begin{aligned}\lambda_r &= D \sum_{m=-\infty}^{\infty} \int_{-\infty}^{\infty} Q(z)^{2d+2} (\pi z)^{2n} \exp(2\pi i(r-m)z)dz \\ &= D \sum_{m=-\infty}^{\infty} Q(r+m)^{2d+2} (\pi(r+m))^{2n} \\ &= \frac{1}{(2\alpha+1)!} D \left\{ \sin(\tau)^{2d+2} \frac{d^{2\alpha}}{d\tau^{2\alpha}} \sin(\tau)^{-2} \right\}\Big|_{\tau=\pi r}, \quad \alpha=d+1-n. \end{aligned} \qquad (28)$$

From the imposed boundary conditions (for n>0) we infer

$$r \in [\tfrac{1}{2}h, \tfrac{1}{2}(1-h)]. \tag{29}$$

As in [9] we define the fast components as those components with Fourier components r which satisfy:

$$r \in [\tfrac{1}{4}, \tfrac{1}{2}(1-h)] \tag{30}$$

and the smoothing factor μ^* of S

$$\mu^* = \sup_h \{\max_r (|1 - \omega \lambda_r|,\ r \in [\tfrac{1}{4}, \tfrac{1}{2}(1-h)])\} \tag{31}$$

i.e. we look for the largest absolute eigenvalue in the spectrum of the smoother whose components are 'fast'. Although this splitting up in high and low frequency modes(30) seems somewhat ad hoc, in practice it yields very good estimates on the reduction of errors by the algorithm (cr). We have to distinguish the cases, n=0 and n>0.

5.1.1. *Least squares problems (n=0).* One can easily show that the condition number of DL remains bounded. One can also find ω values for which multi-grid will work. However the gain with respect to, for example, a conjugated gradient (CG) method is not present. In table 1 (pessimistic) estimates from [6] for the error reduction of one CG-step, (the convergence rate cr of CG), are compared with those of multi-grid.

TABLE 1 Theoretical convergence rates for multi-grid and Conjugated Gradient (n=0).

d	ω_{opt}	μ^*	cr(CG)
1	1.33	0.33	0.06
2	1.65	0.60	0.25
3	2.00	0.78	0.38
4	2.41	0.87	0.52

It is clear that conjugated gradient performs better in all cases. This phenomenon persists for the full convergence rates, as well as for two-dimensional problems, so we omit the case n=0 from the rest of the analysis.

5.1.2. *Boundary value problems (n>0).* For boundary value problems, the situation is completely different. First we examine some limiting cases of the spectrum of S. For the lowest and fastest modes we find for the eigenvalues:

$$\lambda_{h/2} = \mathcal{O}(h^{2n}),\ \lambda_{1/2(1-h)} = \mathcal{O}(1) \tag{32}$$

We can immediately deduce that the condition number κ becomes obstructively large. CG will prove to be very slowly converging. (This can be circumvented by choosing a suitable preconditioner, but we did

not investigate this in detail). By the explicit formulas (28,31) one can simply deduce the optimal choice for ω for reasonable values of degree d, for n=1 and n=2, thereby establishing the smoothing properties of S. We performed the straightforward algebra and found (see table 2):

TABLE 2. Theoretical smoothing factors at optimal smoothing parameters for boundary value problems.

d	n=1 ω_{opt}	μ^*	n=2 ω_{opt}	μ^*
1	0.67	0.33	-	-
2	0.70	0.06	0.60	0.60
3	0.83	0.33	0.83	0.33
4	0.90	0.60	0.63	0.16

Observe the preference for d=2n, which is a phenomenon we cannot explain (for n=2, d=5 μ^* rises again). In the next subsection (5.2) we will extend the analysis for a complete two-grid step and show that the smoothing factors found here are fair estimates of the theoretical convergence rates.

5.2. CONVERGENCE RATES FOR THE TWO-GRID ALGORITHM FOR B-SPLINES

Until now we investigated the smoothing ability of the smoothing step and not the effectiveness of the complete algorithm. However a complete analysis shows that this does not alter much to the previous findings: indeed μ^* proves to be very sound approximation of the error reduction in one two-grid step.

Observe that a two-grid step is given by:

$$u_1^h = S(u_0^h) \tag{4}$$

$$u_0^h = u_1^h - P\,(L^H)^{-1}\,R\,(L^h u_1^h - f^h) \tag{11}$$

or in terms of the defect d^h after step (1) in the algorithm:

$$d^h = (1 - P\,(L^H)^{-1}\,R\,L^h)\,d^h \tag{33}$$

Denoting eigenfunctions e^r and E^r on the fine resp. coarse grid:

$$E_m^r = \exp(2\pi i m r + i\Phi) \tag{34}$$

we can derive, by using the subdivision techniques [1]:

$$R\,e^r = 2\cos(\pi r)^{d+1}\,E^r \tag{35}$$

$$P\,E^r = \cos^{d+1}(\pi r)\,e^r + (-1)^d \sin^{d+1}(\pi r)\,e^{1/2-r}. \tag{36}$$

Of course we can relate eigenvalues of L^{2h} and L^h, Ξ_r and ξ_r:

$$L^H\,E^r = \Xi_r\,E^r\,,\quad \Xi_r = 2^{1-2n}\xi_{2r}. \tag{37}$$

The fact that for fixed r only two modes mix (r,1/2-r) makes it possible to give a complete analysis of a two-grid step by solving a

2*2 eigenvalue problem. (35-37) yield:

$$e_r \rightarrow (1 - \omega D \lambda_r)^{\nu}\{(1-2^{2n-1}\cos^{2d+2}(\pi r))e^{r} + 2^{2n-1}(-1)^{d}(\sin(\pi r)\cos(\pi r))^{d+1}e^{1/2-r}\} \qquad (38)$$

with D and λ defined in (26) and (28).
(38) yields two eigenvalues for each r, ρ^1 and ρ^2: then ρ, defined as:

$$\rho = \max_r \{ \max(|\rho_r^1|, |\rho_r^2|)\} \qquad (39)$$

will represent the minimal error reduction of one two-grid step. Minimizing with respect to ω gives the optimal relaxation parameter ω and optimal convergence rate cr:

$$cr = \inf_{\omega} (\rho). \qquad (40)$$

Results for ν=1 are shown in table 3. Note that the convergence rates and optimal ω values do not differ much from the smoothing factor μ^* found earlier in subsection 5.1.2 (Table 2).

TABLE 3. Theoretical convergence rates at optimal smoothing parameters for boundary value problems.

d	n=1 ω_{opt}	cr	n=2 ω_{opt}	cr
1	0.66	.34	-	-
2	0.71	.06	0.60	0.60
3	0.83	.33	0.83	0.34
4	0.90	.60	0.63	0.16

This concludes the analysis of one-dimensional problems. In sect. 6. these predictions will be compared with experiment. In the next subsection 5.3 we will first give a rough sketch of the analysis in the case of two-dimensional box-splines, and give the results.

5.3. CONVERGENCE RATES FOR BOX-SPLINES

We proceed by repeating the analysis for two-dimensional box-splines. The theory on box-splines can be found in [5].

First one defines directions e with multiplicities m ($e \in \mathbb{Z}^2/(0,0)$, $m \in \mathbb{N}$) We take standard 4-direction meshes with

$$e_1=(1,0), \quad e_2=(1,1), \quad e_3=(0,1) \quad \text{and} \quad e_4=(-1,1) \qquad (41)$$

A box-spline is completely determined by (41) and m_k (k=1,..,4), which we will denote by: $[m_1,m_2,m_3,m_4]$. If one of the multiplicities equals zero, the situation degenerates to a 3-direction mesh; another special case is $m_2=m_4=0$: they reduce to tensor product B-splines.

The Fourier-transforms of box-splines are known [5], which gives, after some calculation analogous to the one dimensional case, eigenvectors e with eigenvalues λ of DL given by:

$$e_m^r = \exp(2\pi i m r + i\phi) \tag{42}$$

$$r \in [\tfrac{1}{2}h, \tfrac{1}{2}(1-h)]^2,\ m \in \mathbb{Z}^2 \tag{43}$$

$$\lambda_r = D \sum_{k\in\mathbb{Z}^2} \prod_{q=1}^{4} \left[\{Q((r+k)e_q)\}^{2m_q} \right] \{\pi^2 (r+k)^2\}^n. \tag{44}$$

As in the one-dimensional case we have to make a distinction between high and low frequency modes. As done in [9] we define the smoothing property of $ by

$$\mu^* = \max(|1 - \omega \lambda_r|,\ \tfrac{1}{4} \le |r| \le \tfrac{1}{2}(1-h)),\ |(r,s)| = \max(r,s). \tag{45}$$

In general, the expressions become somewhat cumbersome, but it is possible to say some things in general. Observe the limiting cases of the eigenvalues: For the low frequency one

$$\lambda_{h/2,h/2} = \mathcal{O}(h^{2\min(m_1,m_2,m_3,m_4,n)}) \tag{46a}$$

and the fast ones

$$\lambda_{h/2,1/2(1-h)} = \mathcal{O}(1),\ \lambda_{1/2(1-h),h/2} = \mathcal{O}(1) \tag{46b}$$

$$\lambda_{1/2(1-h),1/2(1-h)} = \mathcal{O}(h^{2\min(m_2,m_4)}) \tag{46c}$$

So we are immediately led to the conclusion that if $m_2 \neq 0 \neq m_4$ $\mu^* = 1$, no matter what we choose for ω: it follows directly from (46c). This conclusion also holds for the convergence rate cr: box-splines on a 4-direction mesh will always have very bad convergence properties. A zero eigenvalue in (46) indicates a linear dependence in the splines used. Of course one eliminates the linear dependent splines in an actual computation; e.g., see [3]. Still the almost zero eigenvalue in (46c) can be seen as a remnant of this (eliminated) linear dependence: it is the one closest to r=(1/2,1/2) and it can be identified with the linear dependence of translates M of any box-spline on the 4-direction mesh[3]:

$$\sum_{m,n\in\mathbb{Z}} (-1)^{n+m} M(x-mh, y-nh) = 0 \tag{47}$$

We performed the analysis as shown before for convenient splines; i.e. we demanded their support to be relatively small, but at the same time were at least once continuous differentiable: therefore we restricted ourselves to box-splines of the following types: [1111], [2120] and [3030]. This analysis of box-splines is essentially the same as for B-splines, discussed in subsections 5.1 and 5.2. The only difference comes in that we now have to solve a 4*4 eigenvalue problem. As expected this indeed leads to no convergence for the box-splines of type [1111]; table 4 shows rates for the other two:

TABLE 4. Convergence rates at optimal smoothing parameters for box-splines (boundary value problem).

	n=1 ω_{opt}	cr	n=2 ω_{opt}	cr
[2120]	0.98	0.20	0.8	0.65
[3030]	1.20	0.62	0.8	0.60

It is probably worth noting that, as in the one-dimensional case, there is a preferable spline ([2120]) for the Laplace equation. Somewhat disappointingly we did not find one for the biharmonic equation. Probably, if there exists a 'preferable' box-spline for this equation, its degree will be large, and hence also its support. Therefore we doubt that this 'preferable' box-spline will be effective.

6. Comparison with experiment

We solved both the Poisson and biharmonic equation in one and two dimensions, with varying boundary conditions. Using B-splines for d equal 2,3 and 4 for both equations we found for convergence rates (cr) for the two-grid algorithm:

TABLE 5. Experimental convergence rates at optimal smoothing parameters for B-splines (boundary value).

d	n=1 ω_{opt}	cr	n=2 ω_{opt}	cr
2	0.71	0.08	0.58	0.45
3	0.83	0.40	0.65	0.30
4	0.90	0.65	0.63	0.10

In two dimensions we did experiments with box-splines [1111], [2120] and [3030]. As expected there was no convergence when using a 4-direction mesh. The other results are in table 6.

TABLE 6. Experimental convergence rates and optimal smooting parameters for Box-splines (boundary value).

	n=1 ω_{opt}	cr	n=2 ω_{opt}	cr
[2120]	1.00	0.25	0.85	0.70
[3030]	1.10	0.65	0.85	0.54

There are some comments we want to make.

1) For multi-grid we repeated these experiments; the rates slightly increased as expected: the reason is that the Jacobi smoother is not a practical one. Indeed using an ordinary Gauss-Seidel improved but more importantly stabilized the rates from table 5 and 6.

2) The results are hardly sensitive to the choice of boundary conditions; the rates which are shown are the worst we observed.
3) The numbers coincide quite well with the theoretical predictions of the previous section. (Table 2,3 vs. 5 and table 4 vs. 6).

7. Conclusions

The multi-grid algorithm works fine for B-splines and box-splines. But the latter should not involve a 4-direction mesh, amongst others. It is closely related to the linear dependence of box-splines on such meshes: although this dependence is eliminated in actual computations[3], the differential operator L^h in equation (2) still has *high* frequency eigenvectors with *low* eigenvalues.

As it stands here, for boundary value problems the algorithm will be better than e.g., a conjugate gradient method. In this paper we did not compare the performance with preconditioned conjugate gradient methods.

Of course, having established the best splines d=2 for Laplace type equations and d=4 for the biharmonic equation, both in one dimension, and [2120] for the Laplace equation in two, the first thing which has to be done is to look for proper smoothers for these splines. The problem will always be to cope with large supports of the individual splines, which makes life hard constructing them, as surely will be the case for the biharmonic equation in two dimensions.

ACKNOWLEDGEMENT. This work was presented at the NATO A.S.I. on 'Computation of Curves and Surfaces', july 1989 in Tenerife, Spain. The author wishes to thank C.R. Traas for many fruitful discussions.

8. References

1. Böhm, W., (1980), 'Inserting new knots into B-spline curves', Computer Aided Design 12, 199-201.
2. Böhm, W., G. Farin and J. Kahmann, (1984), 'A survey of curve and surface methods in CAGD, Computer Aided Geometric Design 1, 1-60.
3. Chui, C.K. and R.H. Wang, (1984), 'On a bivariate B-spline basis', Scientia Sinica 27, 1129-1142.
4. Dahmen, W. and C.A. Micchelli, (1984), 'Subdivision algorithm for the generation of box-spline surfaces', CAGD 1, 115-129.
5. deBoor C. and K. Höllig, (1982), 'B-splines from parallelepipeds', Journal d'analyse math. 42, 99-115.
6. Golub G.H. and C.F. van Loan, (1983), Matrix computations, John Hopkins University Press, Baltimore.
7. Hackbusch W.H., (1985), Multi-grid methods and applications, Springer, Berlin.
8. Schwarz, H.R., (1980), Metode der Finiten Elemente, Teubner Studienbücher, Stuttgart.
9. Stüben K. and U. Trottenberg, (1982), in W.H. Hackbusch and U. Trottenberg (eds.), Lect. Notes on Math. 960, Springer, Berlin.

Several Notions of Geometric Continuity for Implicit Plane Curves

Joe Warren *
Department of Computer Science
Rice University

November 1989

Abstract

This paper discusses several different, but equivalent notions of geometric continuity for implicitly defined plane curves. To illustrate the power of one of these notions, Bezout's intersection multiplicity, we give a construction for generating a knot with a high order of continuity ($n^2 - 1$) between a pair of algebraic plane curves of relatively low degree (n). We conclude by describing a direct method for forming a piecewise G^k implicit spline using algebraic curves of degree $k + 1$.

1 Introduction

The ability to construct and manipulate geometric representations is fundamental to computer-aided geometric design (CAGD). One of the simplest problems in CAGD is that of creating a smooth curve that approximates some given polygonal curve. Methods using piecewise Bezier curves or B-splines have been developed to solve this problem. These curves have a parametric representation in which the coordinates of points on the curves are functions of a free variable t. This representation is ideally suited for generating points on the curves. However, tasks such as determining whether a point lies within a closed parametric curve (a common operation when performing Boolean set operations) are much more difficult.

Alternatively, a curve may be represented implicitly as the zero contour of a bivariate function.

$$f(x, y) = 0$$

*Supported in part by NSF grant IRI 88-10747 and CCR 89-03431

Note that under this representation it is simple to determine whether a point lies inside a closed implicitly defined curve. Unfortunately, techniques for creating sequence of implicit curves that meet with a high order of continuity and approximate some desired object are not as well developed as their parametric counterparts. In this paper, we will discuss some mathematical issues involved in creating implicit curves that meet with high orders of continuity. We will also give several practical constructions for creating curves that meet with high orders of continuity.

2 Continuity for Implicit Curves

We begin by considering the definition of continuity between a pair of implicitly defined plane curves. Let

$$f(x,y) = 0$$

$$g(x,y) = 0$$

be a pair of implicitly defined curves that pass through the origin and are smooth at the origin. For the purpose of this paper, we will restrict our attention to f and g that are polynomial functions. Implicitly defined curves arising from this restriction are called *algebraic* curves. Algebraic curves include most of the curves commonly used in CAGD.

We focus on necessary and sufficient conditions on f and g for their corresponding curves to meet with continuity of order k. Obviously, if all of the derivatives of f and g up to order k agree at the origin, the two curves should meet with order k continuity. Agreement of the derivatives means that we could form a composite curve using part of $f = 0$ and part of $g = 0$ having derivatives that are continuous up to order k. (See figure 1). Is agreement of the derivative necessary for order k continuity? No, consider a function $a(x,y)$ that is nonzero at the origin. Note that since $a = 0$ does not pass through the origin, the curves $f = 0$ and $af = 0$ are identical in the neighborhood of the origin.. However, the derivatives of f and af need not agree at the origin. For example, if $f \equiv y$ and $a \equiv x + 1$, then the curves $y = 0$ and $(x + 1)y = 0$ are identical in the neighborhood of the origin. However, the second order partial derivatives, y_{xy} and $((x + 1)y)_{xy}$, are discontinuous at the origin.

In accordance with this observation, we make the following definition. The curves $f = 0$ and $g = 0$ (both smooth at the origin) meet with order k *rescaling* continuity if there

exists polynomials $a(x,y)$ and $b(x,y)$, nonzero at the origin, such that all partial derivatives of af and bg up to order k agree at the origin. a and b can be thought of as functions that rescale the partial derivatives of f and g without affecting the geometry of $f = 0$ and $g = 0$. What is the relationship of this notion of continuity for implicit curves to other notions of continuity for parametric curves? It is not too difficult to show using the Implicit Function theorem [Fleming 77] that order k rescaling continuity is locally equivalent to order k reparameterization continuity for parametric curves. (For a proof, we refer the interested reader to [Garrity/Warren 89].) Reparameterization continuity is often referred to as *geometric* continuity. Since reparameterization continuity and rescaling continuity are equivalent, we will simply refer to these notion of continuity as order k geometric continuity (G^k continuity). (In fact, geometric continuity is simply a modern formulation of the classical notion of "order of contact" from differential geometry. [Brauner 81])

We can apply this implicit formulation of geometric continuity to the problem of testing whether two curves are G^k at the origin. Since the polynomial a has a nonzero constant term, it may be treated as power series in x and y and inverted. If $\alpha = a^{-1}b$, then order k

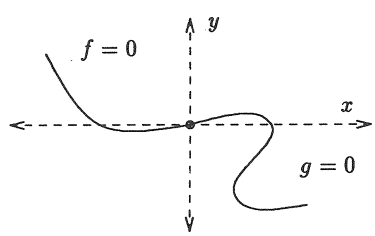

FIGURE 1: Two segments of implicit curves meeting at the origin

rescaling continuity implies that

$$f(x,y) = \alpha(x,y)g(x,y) \text{ modulo } (x,y)^{k+1} \tag{1}$$

where $(x,y)^{k+1}$ denotes the set of monomial in x and y of degree $k+1$ or greater. Given that we need only consider terms of degree k or less, α may be treated as a polynomial in x and y of degree $k-1$ whose coefficients are unknowns. Thus, equation 1 yields a system of linear equations in the symbolic coefficients of α.

If we write f and g in their Taylor series expansion

$$\begin{aligned} f(x,y) &= f_{10}x + f_{01}y + \frac{1}{2}f_{20}x^2 + f_{11}xy + \frac{1}{2}f_{02}y^2 + \ldots \\ g(x,y) &= g_{10}x + g_{01}y + \frac{1}{2}g_{20}x^2 + g_{11}xy + \frac{1}{2}g_{02}y^2 + \ldots \end{aligned}$$

then for G^1 continuity, α is simply the symbolic constant α_{00}. The resulting G^1 constraints are

$$\begin{aligned} f_{10} &= \alpha_{00}g_{10} \\ f_{01} &= \alpha_{00}g_{01}. \end{aligned}$$

These two equations exactly describe tangent line continuity. For G^2 continuity, α is a linear power series whose constant term α_{00} is nonzero.

$$\alpha(x,y) = \alpha_{00} + \alpha_{10}x + \alpha_{01}y$$

Equation 1 yields a set of five linear equations that characterize G^2 continuity.

$$\begin{aligned} f_{10} &= \alpha_{00}g_{10} \\ f_{01} &= \alpha_{00}g_{01} \\ f_{20} &= \alpha_{00}g_{20} + 2\alpha_{10}g_{10} \\ f_{11} &= \alpha_{00}g_{11} + \alpha_{10}g_{01} + \alpha_{01}g_{10} \\ f_{02} &= \alpha_{00}g_{02} + 2\alpha_{01}g_{01} \end{aligned}$$

The first two equations characterize G^1 continuity, while the last three equations characterize G^2 continuity.

These equations can also be used in the construction of geometrically continuous curves. For example, if $f = -2x + x^2 + y^2$, then the set of quadratic curves that meet the circle $f = 0$ at the origin with G^2 continuity is exactly

$$\begin{aligned} g(\alpha_{00}, \alpha_{10}, \alpha_{01}) &= \alpha_{00}(-2x + x^2 + y^2) \\ &\quad +\alpha_{10}(-2x^2) \\ &\quad +\alpha_{01}(-2xy) \end{aligned}$$

subject to $\alpha_{00} \neq 0$. A similar construction allows generation of constraints for higher degree curves intersecting at a point.

3 Bezout's Intersection Multiplicity

Another notion of continuity for algebraic curves arises as result of Bezout's Theorem [Hartshorne 77]. Roughly put, Bezout's theorem states that two algebraic plane curves of degrees m and n intersect in exactly mn points, subject to the constraint that the curves share no common curve. The theorem is stated to hold for curves in complex projective space subject to the caveat that certain intersection points may need to be counted more than once due conditions such as tangency. For example in figure 2 the line L is tangent to the circle C. This point of tangency must be counted twice to satisfy Bezout's theorem. Note that if we perturbed L slightly, the point of tangency splits into two points on C.

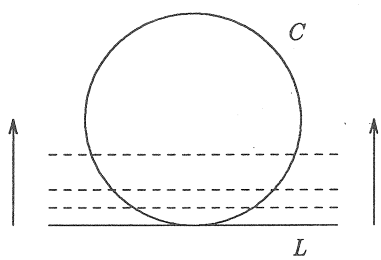

FIGURE 2: A circle and a line intersecting with multiplicity two

Let $f = 0$ and $g = 0$ be two algebraic curves intersecting at point p. The *intersection multpilicity* of $f = 0$ and $g = 0$ at p, denoted $I(f, g; p)$, corresponds to the number of points into which p splits if f and g are generically perturbed (see [Hartshorne 77] for a more formal definition). Under this definition, Bezout's theorem states that if $(f = 0) \cap (g = 0) = \cup p_i$ in complex projective space, then

$$\sum I(f, g; p_i) = mn.$$

If we restrict our attention to those cases in which $f = 0$ and $g = 0$ are smooth at p, then the order of continuity at p and the intersection multiplicity at p are related.

Theorem 1 *Let $f = 0$ and $g = 0$ be algebraic curves that are smooth at a common point p. $f = 0$ and $g = 0$ are G^k at p if and only if $I(f, g; p) = k + 1$.*

A proof of this theorem appears in [Garrity/Warren 89].

Why is this theorem particularly useful? It allows us to bring to bear some powerful results from algebraic geometry to the problem of creating geometrically continuous curves.

For example, [Fulton 69, pp. 74-75] gives an axiomatic characterization of intersection multiplicity for algebraic plane curves. Two of these axioms include:

- $I(f^n, g; p) = nI(f, g; p)$.
- $I(f, g; p) = I(f, g + \lambda f; p)\ \forall \lambda \in \mathbf{R}$.

To demonstrate the power of these axioms, let us consider the problem of creating two algebraic plane curves that meet with a high order of continuity. Let $f = y - x^3$. We wish to create a curve that meets $f = 0$ with G^8 continuity at the origin. First, note that $y = 0$ and $x = 0$ intersect with multiplicity one at the origin ($I(x, y; 0) = 1$). By the first axiom, $y = 0$ and $x^3 = 0$ must intersect with multiplicity three at the origin ($I(x^3, y; 0) = 3$). Therefore, by the second axiom, $y = 0$ and $y - x^3 = 0$ must intersect with multiplicity three at the origin ($I(y, y - x^3; 0) = 3$). This observation corresponds to the fact that $y - x^3 = 0$ has an inflection point at the origin. Applying the first axiom again, we note that $y^3 = 0$ and $y - x^3 = 0$ intersect with multiplicity nine at the origin ($I(y^3, y - x^3; 0) = 9$). Finally, applying the second axiom, we observe that $y - x^3 = 0$ and $y - x^3 + \lambda y^3 = 0$ intersect with multiplicity nine at the origin. To conclude, we note that $y - x^3 = 0$ and $y - x^3 + \lambda y^3 = 0$ are smooth at the origin for all $\lambda \neq 0$. Therefore, these curves must meet with G^8 continuity at the origin by the previous theorem.

This construction can be generalized to produce G^{n^2-1} knots between pairs of algebraic curves of degree n. The most practical application probably arises in the quadratic case. Given a quadratic curve $f = 0$, let $l = 0$ be the tangent line at the point p. The space of all quadratic curves that meet $f = 0$ with G^3 continuity is exactly $f + \lambda l^2 = 0$. Techniques of this sort could allow construction of quadratic splines that possess G^3 knots.

4 Implicit G^k Splines

To conclude, we will describe a method for constructing a piecewise G^k implicit spline curve using algebraic curves of degree $k + 1$. Each piece of the spline will be an algebraic curve $f = 0$ restricted to a triangular region. The polynomial f will be represented over this triangular domain using the bivariate Bernstein/Bézier representation (see [Farin 86] for a review). If we label the vertices of the triangle p, q and r, then we wish to construct a curve

$f = 0$ that meets the segments pq and pr with G^k continuity at the the vertices q and r respectively. (See figure 3).

In the bivariate Bernstein/Bézier representation, the vertices of the triangle pqr are

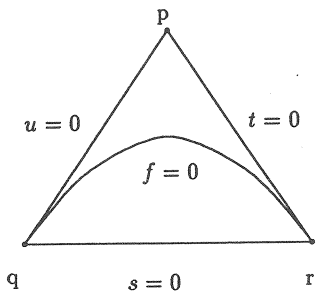

FIGURE 3: One segment of an implicit spline

assigned barycentric coordinates, s, t, and u, respectively. A point m interior to the triangle may be uniquely expressed as the convex combination

$$m = sp + tq + ur$$

where $s \geq 0, t \geq 0, u \geq 0, s + t + u = 1$. Now, any polynomial f of degree $k+1$ may be written uniquely as

$$f(s,t,u) = \sum_{h+i+j=k+1} b_{hij} \frac{(k+1)!}{h!i!j!} s^h t^i u^j$$

where $h \geq 0, i \geq 0, j \geq 0$. Each coefficient b_{hij}, often referred to as a *Bézier ordinate*, is associated with the *domain* point $(\frac{h}{k+1}, \frac{i}{k+1}, \frac{j}{k+1})$ on the triangle pqr. Note that each edge of the triangle pqr has $k+2$ domain points associated with it. If we force the ordinates of the first $k+1$ domain points along the edge from q to p to be zero (those ordinates b_{hi0} where $i \neq 0$), then $f = 0$ meets $u = 0$ (the equation of the edge pq) with G^k continuity. To prove this, we simply observe that f may be written in the form $au + bs^{k+1}$ where a and b are polynomials. Since $(u = 0) \cap (s = 0)$ is exactly q, $f = 0$ and $u = 0$ meet with order k rescaling continuity at q. Likewise, to force $f = 0$ to meet $t = 0$ with G^k continuity, we simply set the first $k+1$ ordinates along the edge from r to p to be zero (those ordinates b_{h0j} where $j \neq 0$). Finally, to ensure that $f = 0$ is smooth at q and r, we must guarantee that b_{0k1} and b_{01k} are nonzero.

Note that each for each curve segment of degree $k+1$, there remains $k(k-1)/2$ undetermined ordinates. These extra degrees of freedom may be used to force the curve to satisfy a variety of conditions. For example, if we set the ordinate associate with the point p to be one, then forcing the rest of the ordinates to be negative guarantees that the entire curve segment lies inside the triangle. The extra freedom can also be used to force the curve to have a rational parametrization by creating a singular point on the curve (see [Abhyankar/Bajaj 86] for details) or can be used to guarantee properties such as convexity.

Given such algebraic curve segments over individual triangles, we may create a spline by forming a connected sequence of triangles whose sides are collinear. Figure 4 shows two cubic polynomials over a pair of domain triangles. Each triangle is labeled with the Bèzier

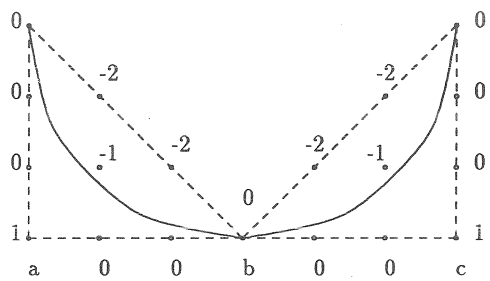

FIGURE 4: A pair of cubic curves with a G^2 knot

ordinates from its corresponding cubic polynomial. The solid curves are the algebraic curves corresponding to these polynomials. The cubic curves meet the segments ab and bc with G^2 continuity, respectively, since all of the ordinates along these edges are zero except at a and c. Since the line segments ab and bc are collinear, the two cubic curves must be G^2 with the same line and therefore must meet with G^2 continuity.

References

[Abhyankar/Bajaj 86] Abhyankar, S. and Bajaj, C. (1987), "Automatic Parameterization of Rational Curves and Surfaces III: Algebraic Plane Curves", *Computer Aided Geometric Design*, 5, 309 - 321.

[Brauner 81] Brauner, H. (1981), *Differentialgeometrie*, Vieweg, Weisbaden.

[DeRose 85] DeRose, T. (1985), *Geometric Continuity: A Parameterization Independent Measure of Continuity for Computer Aided Geometric Design*, Ph.D. thesis, Department of Computer Science, University of California at Berkeley.

[Farin 86] Farin, G. (1986) "Triangular Bernstein-Bezier patches," *Computer Aided Geometric Design*, Vol. 3, pp. 83-128.

[Fleming 77] Fleming, W. (1977) *Functions of Several Variables*, Springer-Verlag.

[Fulton 69] Fulton, W. (1978), *Algebraic Curves*, Benjamin/Cummings.

[Garrity/Warren 89] Garrity, T. and Warren, J. (1989), "Geometric Continuity", to appear in *Computer Aided Geometric Design.*

[Hartshorne 77] Hartshorne, R. (1977), *Algebraic Geometry*, Springer-Verlag.

[Herstein 75] Herstein, I. N. (1975) *Topics in Algebra*, second edition, Wiley.

[Kunz 85] Kunz, E. (1985) *Introduction to Commutative Algebra and Algebraic Geometry* Birkhauser, Boston.